Membrane Separations in Ionic Liquid Assisted Processing of Lignocellulosic Biomass

Von der Fakultät für Maschinenwesen
der Rheinisch-Westfälischen Technischen Hochschule Aachen
zur Erlangung des akademischen Grades
eines Doktors der Ingenieurwissenschaften genehmigte Dissertation

vorgelegt von

Christian Abels

Berichter: Universitätsprofessor Dr.-Ing. Matthias Wessling
Professor Benny Freeman

Tag der mündlichen Prüfung: 12. Dezember 2013

Acknowledgments

First of all I want to thank Matthias Wessling for giving me the right frame to write this thesis. His straight and ambitious way of making science work allowed me to finish my thesis. Moreover I want to thank him very much for his patience.

As well, I would like to express my special thanks to Thomas Melin for giving me the opportunity to experience the very different facettes of science and engineering. Working at his chair for about three years always implied fun and enthusiasm.

I would like to thank Professor Benny Freeman and Professor Heinz Pitsch for constituting the examination board.

I want to very kindly acknowledge the work of Antje Spiess, which was constantly present at TMFB and gave lot of input and additional advice to my thesis. As well, I want to thank her for the opportunity to share fundamental knowledge of enzyme technology.

I would like to acknowledge the contributions of Pablo Dominguez to this thesis by supporting me in the analysis of ionic liquid via HPLC.

I would like to thank all my colleagues which I worked with. Especially, I want to thank my various office mates Clemens Fritzmann, Stefanie Postel, Katharina Tarnacki and Burkhardt Ohs for charing office space with me. Furthermore, I want to thank Claudia Niewersch, Axel Moll, Frederike Carstensen and Helene Wulfhorst for working and publishing with me. Special thanks go to Jörn Viell for all the fruitful discussions about ionic liquids and to Sebastian Köster for borrowing his high performance vacuum pump.

A lot of students supported my work at the chair and I want to thank them all for their contributions which found their way into this thesis without special notification. I want to thank Björn Fischer for setting up my nanofiltration lab-plant, Axel Böcking and Andreas Elli for the lot of experimental work they carried out for me, Christian Redepenning for its outstanding diploma thesis and Kristof Thimm for a very precise and helpful bachelor thesis.

Last but not least, I want to thank my whole family for supporting me through all the years.

Für Maja und Emilia

Abstract

2nd generation biofuels currently hold a significant market share. With increasing impact of biofuel its production routes have to be optimized in terms of CO_2 emissions, competition with the food chain and utilization of the whole plant. The cluster of excellence "Tailor-made Fuels from Biomass" investigates processing of lignocellulosic biomass to next generation biofuels. Complete utilization of the raw material is achieved by initial separation of its constituents cellulose, hemicellulose and lignin under mild conditions. These three fractions can be chemically or biocatalytically converted under independently optimized conditions. This allows for the complete conversion of the plant material to valuable fuel compounds or side-products such as itaconic acid.

The fractionation of wooden biomass is performed with ionic liquid. Ionic liquid allows for the disintegration of the strong ligno-cellulose bonds, resulting in the dissolution of the raw material. A feasible fractionation of the constituents is part of the process design. Cellulose, for instance, is separated from the solution via precipitation with water. The cellulose fraction is than hydrolysed to glucose, which is fermented to itaconic acid. Itaconic acid serves as intermediate for the formation of 2-MTHF (2-methyltetrahydrofurane), a prospective fuel candidate.

In this thesis the conversion of cellulose to glucose downstream of the wood dissolution process in Ionic Liquid is discussed. This sub-process comprises the pretreatment of cellulose with ionic liquid to reduce its crystallinity. The amorphous cellulose is than enzymatically hydrolysed to glucose. The separation of the intermediate glucose from the reaction mixture is performed via multiple membrane seperation processes, namely ultrafiltration, nanofiltration and electrodialysis. The separation of glucose from residual saccharides in ionic liquid/water mixtures is carried out with nanofiltration. The mass transport of glucose across solvent-resistant nanofiltration membranes is modeled with the Maxwell-Stefan approach. The semi-empirical model, based on systematic experimental results, allows for the prediction of the glucose yield from the nanofiltration as a unit operation. The complete subprocess is economically evaluated with respect to a nearly complete recycle and dehydration of ionic liquid. In the outlook nanofiltration of highly concentrated ionic liquid solutions stemming directly from the wood dissolution process is discussed as well as the dissolution of wooden biomass with alternative solvent systems.

Zusammenfassung

Biokraftstoffe der 2. Generation haben heutzutage einen signifikanten Marktanteil erreicht. Aus diesem Erfolg resultiert die Verantwortung, Biokraftstoffe möglichst CO_2 neutral, mit geringem Einfluss auf die Nahrungsmittelkette und durch eine vollständige Verwertung der Rohbiomasse herzustellen. Im Exzellenz-Cluster der RWTH Aachen "Tailor-Made-Fuels from Biomass" wird deshalb die verfahrenstechnische Umsetzung von lignocellulose-haltiger Biomasse zu Biokraftstoffen und wirtschaftlich relevanten Nebenprodukten verfolgt. Grundlage zur vollständigen Verwertung der eingesetzten Biomasse ist die schonende Aufschlüsselung ihrer Bestandteile in eine Cellulose-, Hemicellulose- und Lignin-Fraktion. Aus dieser Fraktionierung ergibt sich die Möglichkeit, die gesamte Biomasse mit auf die Einzelkomponenten zugeschnittenen chemischen / biokatalytischen Umwandlungsprozessen zu relevanten Produkten wie etwa der Plattformchemikalie Itakonsäure zu verwerten.
Die verfahrenstechnische Umsetzung hölzerner Biomasse wird mit Ionischer Flüssigkeit durchgeführt. Die Ionische Flüssigkeit vermag es, die starken Lignocellulose-Bindungen des Rohstoffes zu zersetzen und die Biomasse zu lösen. In der Auslegung eines solchen Prozesses muss zunächst die selektive Abtrennung der einzelnen Fraktionen aus dem Lösungsmittel realisiert werden, z.B. durch die Ausfällung von Cellulose mit Wasser. Die Cellulose-Fraktion im Speziellen wird über eine Hydrolyse zu Glukose, Fermentation zu Itakonsäure und chemische Katalyse zu 2-MTHF (2-Methyltetrahydrofuran), einem Treibstoff-Kandidaten umgesetzt.
In dieser Doktorarbeit wird die Umsetzung von Cellulose zu Glukose nach der Holzauflösung in Ionischer Flüssigkeit betrachtet. Dieser Teilprozess umfasst die Vorbehandlung von Cellulose mit Ionischer Flüssigkeit zur Reduktion ihrer Kristallinität. Die nunmehr amorphe Cellulose wird enzymatisch zu Glukose umgewandelt. Die Abtrennung von Glukose aus dem Reaktionsgemisch erfolgt mit den Membranverfahren Ultrafiltration, Nanofiltration und Elektrodialyse. Die Abtrennung von Glukose von weiteren Sacchariden in Lösungsmittelgemischen aus Ionischer Flüssigkeit und Wasser mittels Nanofiltration wird mit dem Maxwell-Stefan-Ansatz modelliert. Die semi-empirische Modellierung, basierend auf systematischen experimentellen Untersuchungen, erlaubt die Auslegung der Nanofiltration als Trennverfahren bei festgelegter Glukose-Ausbeute. In einer abschließenden ökonomischen Analyse des vorgeschlagenen Teilprozesses wird ein nahezu vollständiges Recycling der Ionischen

Flüssigkeit und deren Trocknung berücksichtigt. Im Ausblick werden die Nanofiltration von hochkonzentrierten Ionischen Flüssigkeiten im Anschluss an den Holzauflösungsprozess betrachtet und weitere Prozess-Routen mit alternativen Lösungsmitteln vorgeschlagen.

Table of contents

CHAPTER 1

Introduction

1.1 The cluster of excellence "Tailor-Made Fuels from Biomass"

In the cluster of excellence "Tailor-Made Fuels from Biomass" processing of lignocellulosic raw materials to fuel compounds and valuable intermediates is investigated. Target is to preserve the diversity of biomolecules by selective conversion under mild conditions to allow for energy-efficient processes [1]. Therefore the viable route of wood gasification with subsequent reconstruction of macromolecules via Fischer-Tropsch synthesis - the Biomass to Liquid (BtL) process [2] is not taken into account within the TMFB research.

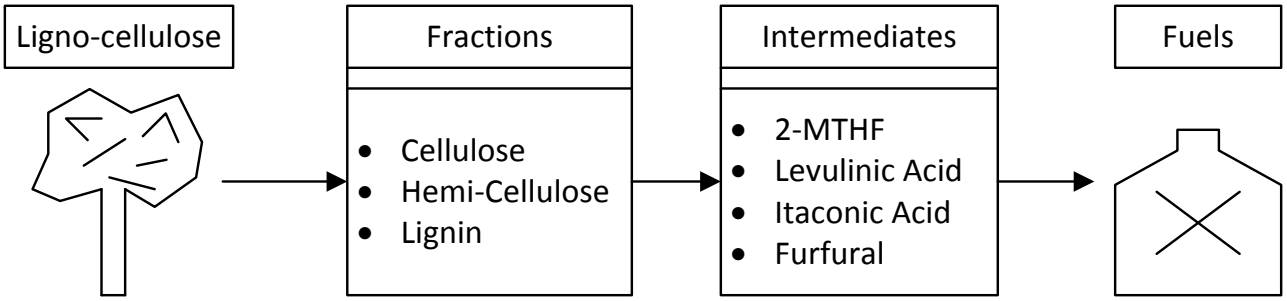

Figure 1.1: Concept of the excellence cluster "Tailor-Made Fuels from Biomass".

In Fig. 1.1 the basic concept of the TMFB research is schematically drawn. The focus is set on the conversion of lignocellulosic biomass to biofuel, therefore grass or wood are considered as starting materials. Initially, the biomass is pretreated to separate the main fractions cellulose, hemi-cellulose and lignin. The cellulose and hemi-cellulose fractions are than processed to the intermediates 2-MTHF, levulinic acid, itaconic acid and furfural. These intermediates offer the chance to produce far more products beside biofuel such as furans, esters or aromatic compounds. Implementing this intermediary level into the process scheme gives the opportunity to transform the biofuel refinery into a biorefinery which enables for complete replacement of fossil fuel based chemistry. Nevertheless, the production of a biofuel, in this case 3-MTHF, is the key issue of the cluster. In this thesis the conversion of wooden material to the respective intermediates is investigated in detail.

1.2 Ionic liquid assisted conversion of wood to fuel

In Fig. 1.2 the processing of wood to the fuel candidate 3-MTHF is schematically drawn. The conversion of wooden biomass to the respective intermediate has to comprise the pretreatment with a strong solvent which allows for the physico-chemical break-up of the strong lignocelluose bindings. In this case, the dissolution of wood is performed with ionic liquids. Within the TMFB cluster the solubility of wooden material in ionic liquids is investigated in detail in terms of disintegration and dissolution kinetics [3]. The dissolution process is followed by precipitation of the cellulose fraction with water or acetone [4].

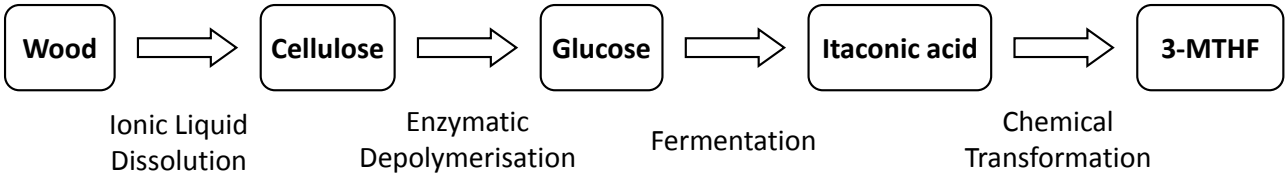

Figure 1.2: Transformation of wood to biofuel via ionic liquid pretreatment and chemical conversion.

Then the recovered cellulose is converted to glucose via enzymatic hydrolysis. In this subprocess traces of ionic liquid stemming from the pretreatment process can inhibit the enzymatic activity [5]. Then two routes can be followed to obtain a fuel candidate. A chemo-enzymatic route offers the chance to directly convert glucose to the respective fuel candidate [6]. Alternatively, the glucose can be fed to a fermentation broth producing itaconic acid or levulinic acid which are both considered as platform chemicals. The conversion of glucose to itaconic acid is performed by fermentation with the fungus Ustilago Maydis [7]. This process scheme with a platform chemical production prior the final conversion to a fuel candidate allows for a broad variety of products [8]. The efficiency of the entire process is examined as well and evaluated in detail in order to realistically assess chances and risks of proposed process concepts [9]. To complement the research by means of establishing a complete biorefinery, the utilization of cellulosic matter to other products beside fuels has already been revised [10].

1.3 Challenges in downstream processing

In Fig. 1.2 the basic scheme for the conversion of wood to glucose was shown. The underlying processes for each conversion are far more complex, particularly concerning the downstream processing. Separation of products, intermediates, wastes and solvents, respectively catalysts has to be performed after each conversion in order to establish an economic and ecological feasible process.

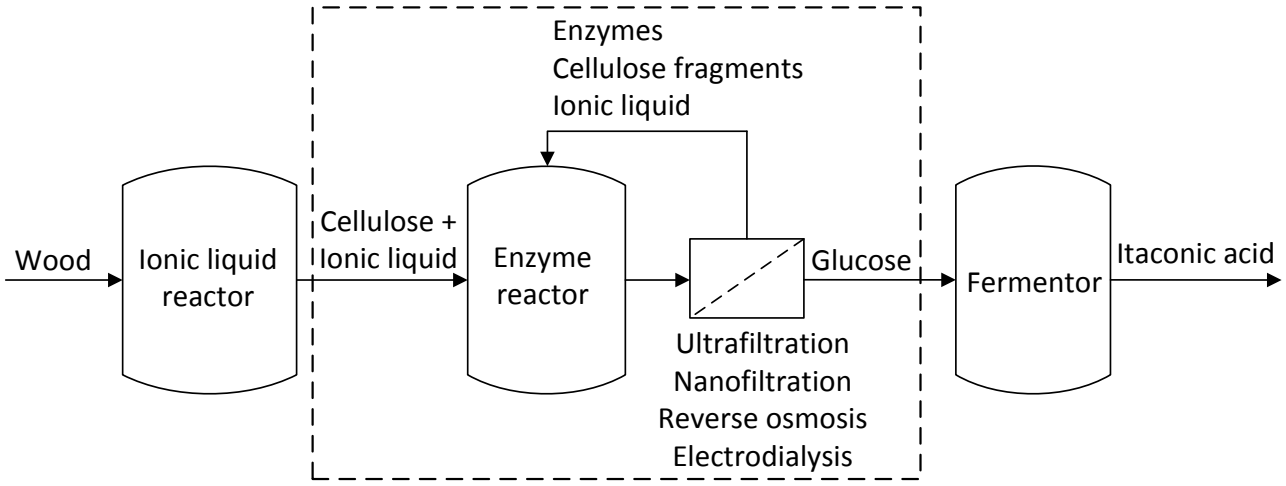

Figure 1.3: Processing of wood to itaconic acid. The frame is drawn around the subprocess which is investigated in detail within this thesis.

In Fig. 1.3 the downstream subprocess which is investigated in this thesis is shown. The incoming stream, which has to be processed, is supposed to consist of precipitated cellulose stemming from the wood dissolution process. Therefore the removal of ionic liquid from the final product stream of glucose has to be taken into account. As the enzymatic hydrolysis of cellulose to glucose may be incomplete, a detailed downstream process has to consider the removal or recycle of streams of cellulose residuals, enzymes and ionic liquid from the product glucose.

Focus is set on membrane unit operations because this technique allows for low-energy processing under mild conditions. The investigated membrane unit operations are ultrafiltration, nanofiltration, electrodialysis and reverse osmosis. Within this thesis these processes are experimentally examined on their reliability with special focus on the nanofiltration. In a concluding economic study of the subprocess the recovery of water from the glucose product stream via stripping is taken into account.

1.4 Scope of the thesis

Scope of the thesis is to set up a process for the recovery of glucose from ionic liquid assisted degradation of cellulose. The downstream processing comprises several unit operations such as ultrafiltration, nanofiltration or electrodialysis. Fig. 1.4 depicts the general approach of converting a physical phenomenon into a technical process.

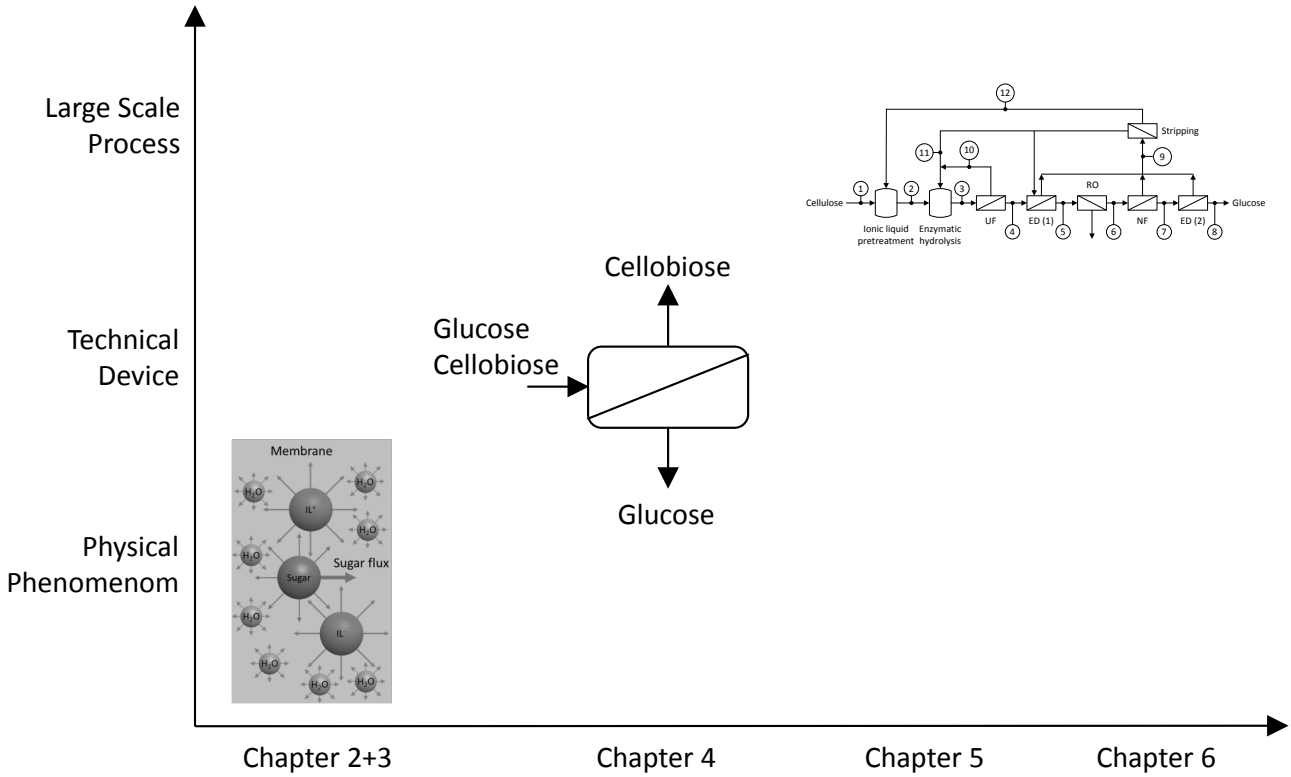

Figure 1.4: Scope of the thesis. Initially, the relevant physical phenomena of the membrane separation process are identified. Then the application for the respective unit operation within the TMFB cluster is found. Finally, an economic evaluation of the specified subprocess is undertaken.

First solvent-resistant nanofiltration membranes were examined for their separation performance regarding mixtures of ionic liquid, water and saccharides. It was found, that for low ionic liquid contents of up to about 40 wt.%, it is possible to obtain a reasonable permeate flux. A model based on the Maxwell-Stefan approach was set up and fitted to the experimental results. Therefore, the decreasing permeate flux could be explained by the low permeability of the ionic liquid and osmotic pressures. Results of these investigations are presented in chapter 2. For solvent mixtures containing up to 40 wt.% of ionic liquid the rejections of saccharides glucose, cellobiose and raffinose were experimentally determined and modeled with

the Maxwell-Stefan approach (see chapter 3). Here it was found that for increasing ionic liquid contents in the feed solution a gap evolved between the glucose rejection and the rejections of the polysaccharides. These results could be explained by the Maxwell-Stefan model with diverging decreases of solvent and solute fluxes by adding the ionic liquid to the solution. In conclusion, the Desal DL membrane was chosen to separate the glucose from poly-saccharides in ionic liquid solutions containing a minimum of 100 g L^{-1} of IL.

In chapter 4, the implementation of the physical model into a technical device or unit operation is performed. In this chapter batch filtration experiments at varying pressures were carried to determine the optimal process conditions in terms of glucose recovery and purity from a mixture of glucose, cellobiose and ionic liquid in aqueous solution.

In chapter 5 the nanofiltration process is integrated into the downstream processing of a cellulose hydrolysis with ionic liquid pretreatment. Here, additional membrane processes, namely ultrafiltration and electrodialysis are additionally investigated for the separation of particulates from the cellulose hydrolysis prior the nanofiltration process and the separation of ionic liquid from the glucose product solution downstream of the nanofiltration process.

In chapter 6 finally an economic analysis of the set up process is undertaken with respect to the investment and operating costs assuming a lifespan of the plant of 10 years. A sensitivity analysis reveals that the major cost driver of the process is the ionic liquid which has to be recycled very efficiently to run the process economically. In fact the ionic liquid recovery rate may not undercut a value of 99.7%.

1.5 References

[1] W. Marquardt, A. Harwardt, M. Hechinger, K. Kraemer, J. Viell and A. Voll; *The biorenewables opportunity - toward next generation process and product systems*; AIChE Journal **56** (9) (2010) 2228--2235

[2] M. Stoecker; *Biofuels and Biomass-To-Liquid Fuels in the Biorefinery: Catalytic Conversion of Lignocellulosic Biomass using Porous Materials*; Angewandte Chemie International Edition **47** (48) (2008) 9200--9211

[3] J. Viell and W. Marquardt; *Disintegration and dissolution kinetics of wood chips in ionic liquids*; Holzforschung **65** (4) (2011) 519--525

[4] D. A. Fort, R. C. Remsing, R. P. Swatloski, P. Moyna, G. Moyna and R. D. Rogers; *Can ionic liquids dissolve wood? Processing and analysis of lignocellulosic materials with 1-n-butyl-3-methylimidazolium chloride*; Green Chemistry **9** (1) (2007) 63--69

[5] P. Engel, R. Mladenov, H. Wulfhorst, G. Jaeger and A. C. Spiess; *Point by point analysis: how ionic liquid affects the enzymatic hydrolysis of native and modified cellulose*; Green Chemistry **12** (11) (2010) 1959--1966

[6] L. Hu, Y. Sun, L. Lin and S. J. Liu; *Catalytic conversion of glucose into 5-hydroxymethylfurfural using double catalysts in ionic liquid*; Journal of the Taiwan Institute of Chemical Engineers **43** (5) (2012) 718--723

[7] T. Klement, S. Milker, G. Jaeger, P. M. Grande, P. D. de Maria and J. Buechs; *Biomass pretreatment affects Ustilago maydis in producing itaconic acid*; Microbial Cell Factories **11** (43) (2012) 1--13

[8] F. M. A. Geilen, B. Engendahl, A. Harwardt, W. Marquardt, J. Klankermayer and W. Leitner; *Selective and Flexible Transformation of Biomass-Derived Platform Chemicals by a Multifunctional Catalytic System*; Angewandte Chemie-International Edition **49** (32) (2010) 5510--5514

[9] M. Hechinger, A. Voll and W. Marquardt; *Towards an integrated design of biofuels and their production pathways*; Computers & Chemical Engineering **34** (12) (2010) 1909--1918

[10] M. Rose and R. Palkovits; *Cellulose-Based Sustainable Polymers: State of the Art and Future Trends*; Macromolecular Rapid Communications **32** (17) (2011) 1299--1311

CHAPTER 2

Transport of ionic liquid water mixtures through polyamide and polyimide nanofiltration membranes

Parts of this chapter have been published:

C. Abels; C. Redepenning; A. Moll; T. Melin; M. Wessling, *Simple purification of ionic liquid solvents by nanofiltration in biorefining of lignocellulosic substrates,* Journal of Membrane Science 405-406 (2012) 1–10

2.1 Introduction

Ionic liquids (ILs) are synthetic, organic, ionic compounds with a melting point below 100°C. Methylimidazole is a common starting chemical for synthesizing alkyl-methyl-imidazolium cations bound in many types of ionic liquids. By chemically modifying the organic cation, ILs can be prepared in large varieties with different, tailor-made properties [1]. Hence, the term "designer solvents" has come into common use [2]. Up to now various articles have been published emphasizing numerous applications for ionic liquids, e.g. as catalysts [3--5], electrolytes [6--8], lubricants [9--11] or solvents [12, 13].

One common property among ILs is their extremely low vapor pressure due to their ionic nature - a significant advantage over typical solvents regarding environmental friendliness. Moreover ILs only evaporate at very low vacuum pressures [14]. Due to their practical non-volatility ILs are claimed to be green solvents [15]. However, recent studies prove the negative impact of ionic liquids on the environment [16]. For instance, cytotoxic effects of ILs have already been reported [17]. Nevertheless, the negative impact of water soluble ionic liquids is not fully understood up to now, because this species can easily drain off in waste-water streams.

As yet, there are just few publications on the recovery of ionic liquid via membrane technology published. Han et al. reported about employing nanofiltration to recycle ionic liquids in IL-mediated Suzuki cross coupling reactions [18]. In this study the concentration of ionic liquid in solvent did not exceed 5 g L^{-1}. Starmem nanofiltration membranes were applied to recover different hydrophobic ILs from organic solvents. The separation performance for several membranes was determined and a recovery of about 99% was achieved by application of the dense Starmem 120 membrane in a methanol system with the ionic liquid PEG-5 cocomonium methylsulfate (molecular weight: 868 Da). Nanofiltration membranes were also used for separating of 1-butyl-3-methylimidazolium tetrafluoroborate and bromophenol blue in aqueous solution and the separation of lactose from 1,3-dimethylimidazol methylsulfate. The second separation was a downstream process of an IL-catalyzed enzymatic synthesis of Nacetyllactosamine. Used as reference substance, lactose could be separated from the IL in several diafiltration steps. Again, only small amounts of about 1 vol.% of ionic liquid were filtered [19].

Moreover, Gan et al. reported about ultrafiltration of ionic liquids in mixtures with methanol, ethanol and water [20]. ILs were mixed with different solvents, basically to decrease viscosity, which strongly influenced the permeation rate. Permeate fluxes were measured and correlated to the viscosity of the system as a function of mixture composition and temperature. Since the IL was not rejected, it was not recovered. However, a more general process design with ionic liquids as highly viscous media was discussed within this study, focusing especially on the rheological properties of the investigated ILs.

In this work, nanofiltration of the water-soluble ionic liquid [MMIM][DMP] with the hydrophilic membrane Desal DK and the hydrophobic membrane Starmem 240 is investigated. In contrast to other publications the filterability of a single ionic liquid is investigated systematically, concerning process conditions such as pressure and concentration dependency of flux and rejection performance of the respective membrane. With this methodology the relevant physical phenomena of the ionic liquid transport through nanofiltration membranes shall be revealed and modeled in order to more generally understand the transport of ionic liquids through nanofiltration membranes.

2.2 Transport model

2.2.1 Maxwell-Stefan model

The transport of water and ionic liquid is described with the Maxwell-Stefan model which was extensively revised by Krishna and Wesselingh [21]. In this model the velocity u of a molecule i is balanced with its moving driving force F. If another species of molecules j is present, there is competing transport between molecules i and surrounding molecules j which can either increase the final velocity of molecule i in the case of a faster velocity of surrounding molecules or decrease its final velocity in the opposite case. The interaction of different molecules by means of disturbing the respective flow is expressed by the friction parameter ξ. The basic equation of the Maxwell-Stefan approach is:

$$F_i = \sum_{i \neq j} \xi_{i,j} \cdot x_j \cdot (u_i - u_j) \tag{2.1}$$

When the system comprises a stagnant layer such as a membrane, there are two different possibilities to model the membrane. In case (1) the membrane is modeled the same way as the moving molecules. The membrane is modeled as a large, non-moving molecule which reduces the velocity of all dissolved molecules. Then the friction parameter of the membrane and its mass fraction, respectively mole fraction in the system has to be known. The free volume theory can be applied to predict appropriate values, but its application is quite difficult due to the amount of parameters which have to be determined such as the free volume of each involved species [22].
In case (2) the membrane is modeled as homogenous background layer which is called non-structured matrix. The moving molecules are then supposed to integrally adsorb into the membrane material. In result, the mass fraction of the membrane in the system has not explicitly to be calculated. Further transformations of eq. 2.1 concern the substitution of molecule velocity u by the molar flux N and the definition

of the relevant driving forces.

$$\begin{aligned} &-\left(\frac{d\mu_i}{dy} - V_{m,i} \cdot \frac{dP}{dy} - z_i \cdot F \cdot \frac{d\Phi}{dy}\right) \cdot c \cdot x_i \\ &= \sum_{i \neq j} \xi_{i,j} \cdot \left(x_j \cdot N_i - x_i \cdot N_j\right) + \xi_{i,M} \cdot x_i \end{aligned} \tag{2.2}$$

The driving forces are the chemical potential gradient dμ (simplified: the concentration difference), the pressure gradient dP and the electric potential gradient dΦ between feed and permeate. Whereas the electric potential gradient can be neglected for neutral molecules, it has to be taken into account for charged molecules. To complete the model the mass balance has to be taken into account:

$$\sum x_i = 1 \tag{2.3}$$

The transport of charged molecules has to fulfill the rules of electroneutrality. For the feed, permeate and retentate phase one yields:

$$\sum z_i \cdot x_i = 0 \tag{2.4}$$

To calculate the mole fractions of molecules in the membrane, assumptions for their sorption into the membrane material have to be made. These assumptions will be discussed in section 2.3.4.

2.2.2 Activity coefficients

The chemical potential of a species i can be expressed by its activity.

$$\mu_i = R \cdot T \cdot ln(a_i). \tag{2.5}$$

In liquid systems the activity a_i can be calculated from:

$$a_i = x_i \cdot \gamma_i \tag{2.6}$$

In ideal mixtures the activity coefficient ai is constantly 1 by definition. Highly diluted aqueous salt solutions are usually assumed to behave ideal. Then the activity gradient can directly be translated into a concentration gradient. For non-ideal systems comprising ions the activity coefficients of the ions can be calculated by the law of Debye-Huckel [23]. If the system does not behave ideally, the activity coefficients can be derived experimentally, for example by vapor pressure measurements. Another option is the simulation of activity coefficient evolution with complex molecular simulations such as COSMO-RS.

2.2.3 Sorption of water and ionic liquid

The sorption of water and ionic liquid molecules into the membrane material has to be known in order to calculate the mole fractions of the respective species in the Maxwell-Stefan model (eq. 2.2). These values are difficult to obtain. Up to now only few results on sorption measurements with respect to liquids into nanofiltration membranes have been published [24--27]. Especially the sorption of ions is not measured directly, but derived from measurements concerning the membrane charge. The membrane charge is supposed to have a major influence on sorption according to the Donnan equilibrium. Detailed investigations take a reduction of dieelectric constant in the membrane material into account as well as a steric hindrance of the ions by the membrane [28]. In drawback the steric hindrance of the ions has to be calculated by assuming the presence of pores. Therefore Straatsma et al. have presented a simplified description combining the Donnan equilibrium with a general sorption of the ions expressed by a Freundlich isotherm [29]. This expression will be used in this work to calculate the sorption of IL molecules.

In Fig. 2.1 the modeled concentration development of water and ionic liquid, divided into cation and anion, is shown.

The sorption of ionic liquid molecules is calculated with respect to the membrane charge which is usually negative in a pH neutral environment. Therefore more cations than anions are absorbed in the membrane. According to Straatsma, the sorption

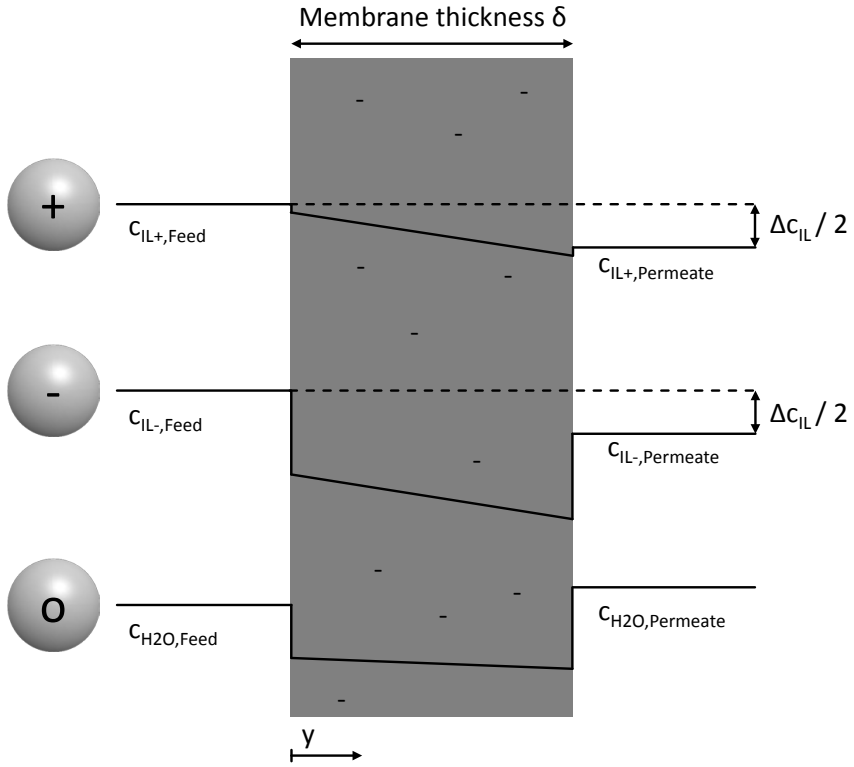

Figure 2.1: Scheme of the concentration gradients of water and IL ions within the membrane.

of the cation is calculated with:

$$c_{IL+,y=0} = K_{IL+} \cdot w_{IL+,Feed} \cdot exp(\frac{-F \cdot \Delta\Phi}{R \cdot T}) \tag{2.7}$$

The sorption of the anion is then:

$$c_{IL-,y=0} = K_{IL-} \cdot w_{IL-,Feed} \cdot exp(\frac{F \cdot \Delta\Phi}{R \cdot T}) \tag{2.8}$$

The membrane charge influences the sorption ratio of cation and anion by the condition of electroneutrality:

$$z_{IL+} \cdot x_{IL+,y=0} + z_{IL-} \cdot x_{IL-,y=0} + \frac{Q_m}{c_{IL+,y=0} + c_{IL-,y=0}} = 0 \tag{2.9}$$

As the membrane charge is not just an intrinsic property of the membrane, but does also depend on the properties of the adsorbed substance system, the membrane

charge is correlated to the feed solution by a Freundlich isotherm.

$$Q_m = Q_0 \cdot (\sum |z_i| \cdot x_i)^{K_S} \tag{2.10}$$

In this work the parameter K_s is set to 1. A sensitivity analysis concerning the membrane charge showed that the simulated results were nearly independent from the membrane charge (for values between -1 and -100 mol m^{-3}). This result can be explained by the very similar molecule sizes of cation and anion, leading to nearly identical friction forces with the water molecules or membrane. Therefore a value of -10 mol m^{-3} was used for both membranes. This value corresponds to published results [30]. The results of ζ-potential measurements are discussed in section 3.4. The sorption of water into the membrane is calculated with the law of Henry. For molecule mixtures with largely varying molecule sizes it is suggested to correlate the sorption with the mass fraction and not the mole fraction [31].

$$c_{H_2O,x=0} = K_{H_2O} \cdot w_{H_2O,Feed} \tag{2.11}$$

2.2.4 Friction coefficients

Self-friction coefficients concerning the friction between water and ionic liquid molecules have been calculated from binary diffusion coefficients.

$$\xi_{i,i} = \frac{R \cdot T}{D_{i,i}} \tag{2.12}$$

The self-diffusion coefficient of a molecule was calculated using the Stokes-Einstein correlation.

$$D_{i,i} = \frac{k_B \cdot T}{6 \cdot \pi \cdot \nu_i \cdot r_i} \tag{2.13}$$

The friction coefficients between the moving molecules were then estimated using

the geometric average.

$$\xi_{i,j} = \sqrt{\xi_{i,i} \cdot \xi_{j,j}} \tag{2.14}$$

Using eq. 2.14, it becomes obvious that the friction coefficients are crosswise equal.

$$\xi_{i,j} = \xi_{j,i} \tag{2.15}$$

The friction coefficients concerning the interaction between water and membrane were derived from pure water experiments. The friction coefficients between the ionic liquid molecules and the membrane were free fitting parameters. For simplification the ratio of cation and anion friction parameter with the membrane was fixed. It was calculated from the ratio of their respective molecular volumes. In other publications these friction parameters were derived from the ratio of the molecule radii to an assumed membrane pore, resulting in a similar result [29].

2.3 Experimental

2.3.1 Nanofiltration set-up

Nanofiltration experiments were performed with a self constructed test rig. Fig. 2.2 illustrates the process scheme.

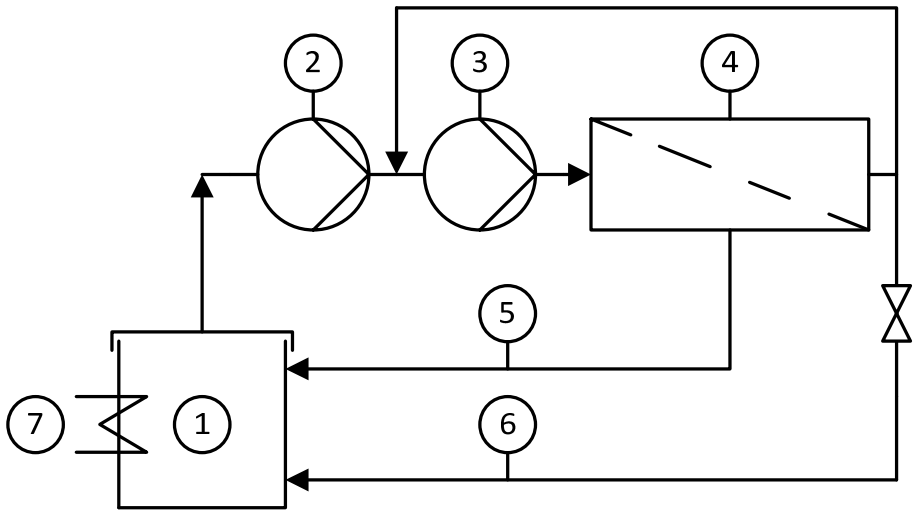

Figure 2.2: Scheme of the nanofiltration set-up. 1. Feed tank; 2. Pressurizing pump; 3. Cross flow pump; 4. Rectangular test cell; 5. Permeate pipe; 6. Retentate pipe; 7. Heat exchanger.

The test rig consists of a feed tank connected to two pumps, whereby the first pump is a membrane piston pump yielding pressures of up to 80 bar. The second pump, a gear pump, is installed in an inner circle, which is pressurized by the first pump. The gear pump allows for a well specified adjustment of feed flow across the membrane surface for controlling and minimizing concentration polarization. The membrane test cell, provided by Simatech, is designed for filtration experiments of up to 80 bar filtration pressure and for flat sheet membranes with dimensions of 0.04 m x 0.2 m. Such membranes are usually used for simulating a piece of a spiral wound module, which is the typical design for reverse osmosis / nanofiltration processes. The permeate and retentate pipes lead back into the feed tank, which allows for continuous operation. The following parameters were measured and recorded during the experiments: Total pressure, pressure drop across the test cell, feed volume flow across the membrane surface and temperatures in feed tank and retentate pipe behind the test cell.

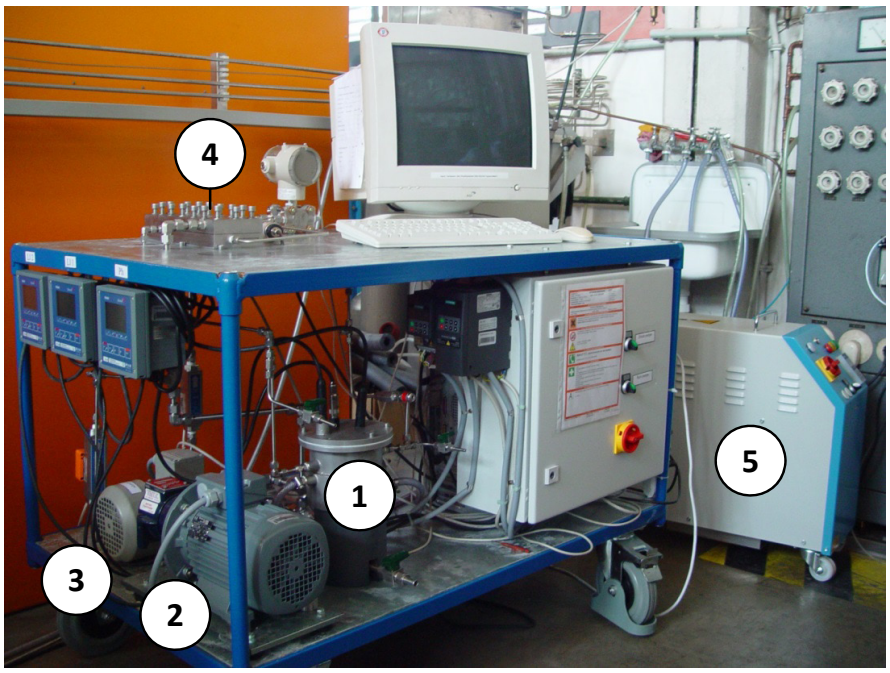

Figure 2.3: Photo of the nanofiltration set-up. 1. Feed tank; 2. Pressurizing pump; 3. Cross flow pump; 4. Rectangular test cell; 5. Heat exchanger.

Filtration experiments were carried out for pressures of 20 - 40 bar and [MMIM][DMP] / H_2O mixtures in a range of 0 wt.% - 40 wt.% ionic liquid. The temperature in all experiments was set to 25°C. As well experiments were performed with cross flow velocities of 1 m s^{-1}, 2 m s^{-1} and 2.5 m s^{-1}. A woven net-spacer was installed in the feed channel to decrease mass transfer limitations at the membrane surface. There were no observed differences in separation performance for the chosen cross-flow velocities.

2.3.2 Materials

The ionic liquid 1,3-dimethylimidazolium dimethylphosphate (in the following text [MMIM] [DMP]) was obtained in a purity of $>$98% from IoLiTec (Ionic Liquids Technologies GmbH). The IL is completely miscible with water and is hygroscopic. Due to its low melting point of about -64°C it is a so-called "room temperature ionic liquid" (RTIL). Table 2.1 lists the basic properties of [MMIM][DMP].

Table 2.1: Properties of investigated ionic liquid [MMIM][DMP].

Property	Value	Unit
Molecular formula	C_7 H_{15} N_2 O_4 P	-
Molecular weight	220	[g mol^{-1}]
Density (20°C)	1250	[kg m^{-3}]
Melting point	-64	[°C]
Viscosity	219	[mPas]
Water miscibility	Completely miscible	-
Water saturation	31	[wt.%]

2.3.3 Analytics

During nanofiltration experiments electrical conductivities of feed and permeate solution were measured as a function of temperature. Due to a linear relationship between conductivity and IL mass fraction, the concentration of IL in the feed and in the permeate could be determined with this method for ionic liquid concentrations of up to 20 wt.%. Above this concentration the electrical conductivity did not change significantly with the concentration of ionic liquid. Therefore HPLC measurements coupled with refractive index measurements were performed to determine IL concentrations for amounts of [MMIM][DMP] of up to 40 wt.%.

2.3.4 Investigated membranes

In the following experiments, one hydrophilic membrane and one hydrophobic membrane was applied: The Desal DL membrane, a polyamide membrane, which has also been used in organophilic organophilic systems [19] and the Starmem 240 membrane, which is a polyimide based asymmetric integrally skinned membrane, originally designed for filtration of organic solvents, e.g. ethanol or toluene [20]. The tested Desal DL membranes were flushed with pure water before the start of the experiments. The Starmem 240 membranes were stored in pure acetone for at least 24 h to remove preservation oils. After filtration experiments the applied membranes were stored in pure ionic liquid and reused several times.

Several membrane characterization tests were carried out. First the respective ζ-potential of the membrane surface was measured using the streaming potential

Table 2.2: Properties of investigated nanofiltration membranes. ^{a}Based on rejection of (poly-) ethylene glycols in water.

Property	Membrane	
	Desal DL	Starmem 240
Manufacturer	GE Osmonics	MET
Material of active layer	Polyamide	Polyimide
MWCO [Da]	252^a	1400^a
Isoelectric point [pH]	4.1	4.0
T_{max} [°C]	90	60
p_{max} [°C]	40	60
Pure water flux [L m^{-2} h^{-1} bar^{-1}]	4.21	0.71

method. Prior to the experiments, the membrane samples were flushed with pure water at a filtration pressure of 10 bar for at least 15 min. The Starmem 240 membrane was first stored in acetone and then flushed with pure water. The respective ζ-potential was measured using KCl solutions at concentrations of 10^{-2} mol. The channel height of the test cell was a minimum of 200 mm in order to minimize the surface conductance effect [32]. As the end parameter for the streaming potential measurements the isoelectric point was chosen. At the isoelectric point the membrane surface charge equals zero. The isoelectric points of the three investigated membranes are shown in Table 2.2.

Molecular weight cut-off (MWCO) measurements were carried out with mixtures of (poly-) ethylene glycols (PEG) at a total concentration of 20 g L^{-1} in water. (Poly-) ethylene glycols mixtures with mean molecular weights ranging from 62 to 1000 g mol^{-1} were used as reference molecules for nanofiltration processes. A rejection of 90% was defined as MWCO. Table 2.2 also depicts the MWCO. Here, one can see that the MWCO for Starmem 240 in an aqueous environment is much greater than that for the Desal membranes and is even much higher than the values declared by the manufacturer. In fact, the Starmem membrane shows 90% retention for alkenes with molecular weights of 400 Da dissolved in ethanol, as is stated by the manufacturer. This discrepancy in MWCO implies, that the rejection of a solute depends on the applied solvent system [33].

2.3.5 Osmotic pressures of [MMIM][DMP]

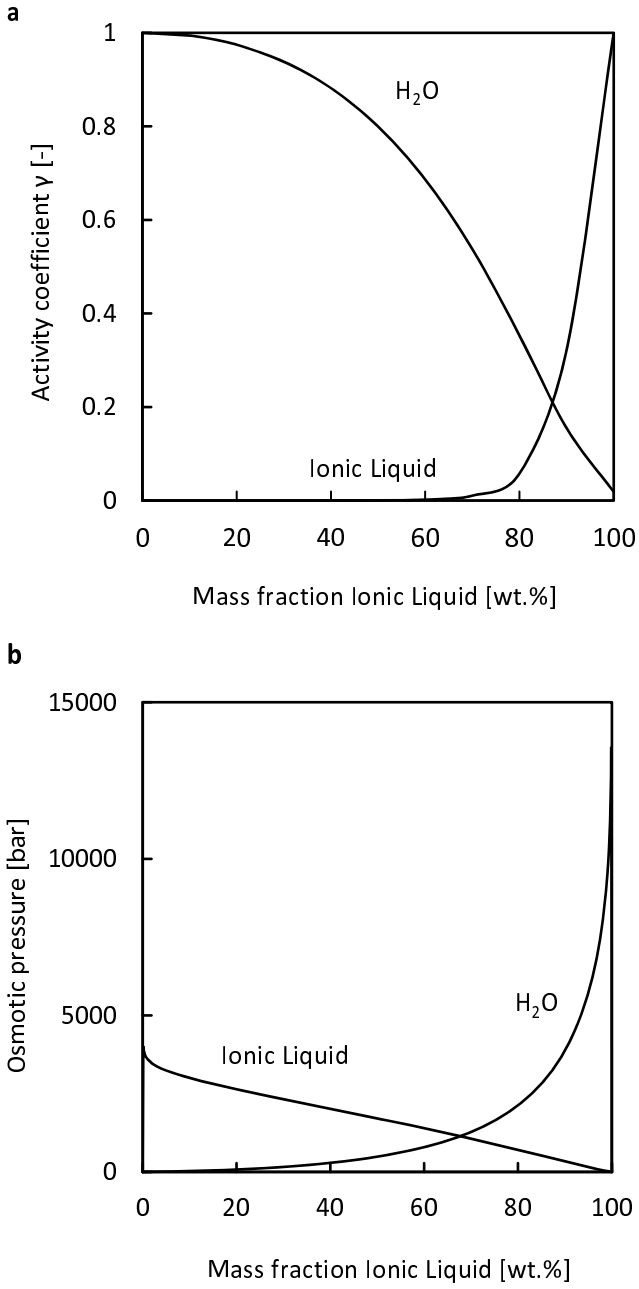

Figure 2.4: (a) Activity coefficients of [MMIM][DMP] and H_2O in binary mixtures, and (b) resulting osmotic pressures for [MMIM][DMP] and H_2O.

To apply the Maxwell-Stefan model correctly chemical potentials, respectively the activity coefficients of the diverse [MMIM][DMP] / H_2O mixtures have to be known (see eq. 2.5). Although the activity coefficients for the ionic liquid ions could be calculated with the law of Debye-Hückel, non-ideal behavior of the water activity would have to be neglected. In the investigated system, large amounts of ionic liquid are present (up to 40 wt.%), what implies a significant change of water activity. The evolutions of the respective activity coefficients a_i for [MMIM][DMP] / H_2O mixtures

have been determined by vapor liquid equilibrium (VLE) experiments at temperatures of 80°C by Kato et al. [34]. In the cited publication, the VLE data were also fitted by the UNIQUAC model which is one form of the G^E approach to predict the development of activity coefficients. In this case the G^E model with the estimated parameters (for 80°C) is used to calculate osmotic pressures for both the ionic liquid and the water. The temperature dependence of the activity coefficients is neglected. Fig. 2.4a and 2.4b illustrate the development of activity coefficients and resulting osmotic pressures depending on the mass fraction of [MMIM][DMP].

To evaluate the calculated results, reverse osmosis experiments with the membrane SWHR30 provided by DOW were performed. This membrane showed a rejection of [MMIM][DMP] of at least 99% for [MMIM][DMP] / H_2O mixtures with weight fractions of IL of up to 10 wt.%. Filtration experiments with this particular membrane were performed and the minimum pressure which had to be applied to obtain a solvent flux through the membrane was recorded.

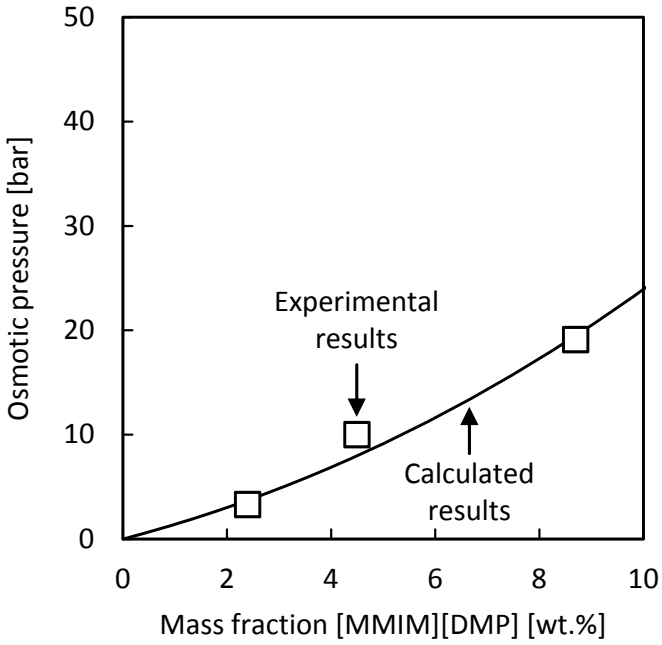

Figure 2.5: Comparison between calculated and experimental results of osmotic pressures in the reverse osmosis of aqueous solutions containing the ionic liquid [MMIM][DMP]. The employed membrane was the SWHR30 provided by DOW.

In Fig. 2.5 the comparison between the calculated results and the experimental results is shown. The experimental results confirm very well with the calculated. Therefore, it is feasible to neglect the temperature dependency of the activity coefficients.

2.4 Results

2.4.1 Results for the Desal DL membrane

In Fig. 2.6 the results for separation performance of [MMIM][DMP] from water for the Desal DL membrane are shown. Data points are experimental values, full lines represent calculated data. First the experimental data will be explained, then the calculated data in order to create a phyiscal understanding of the results.

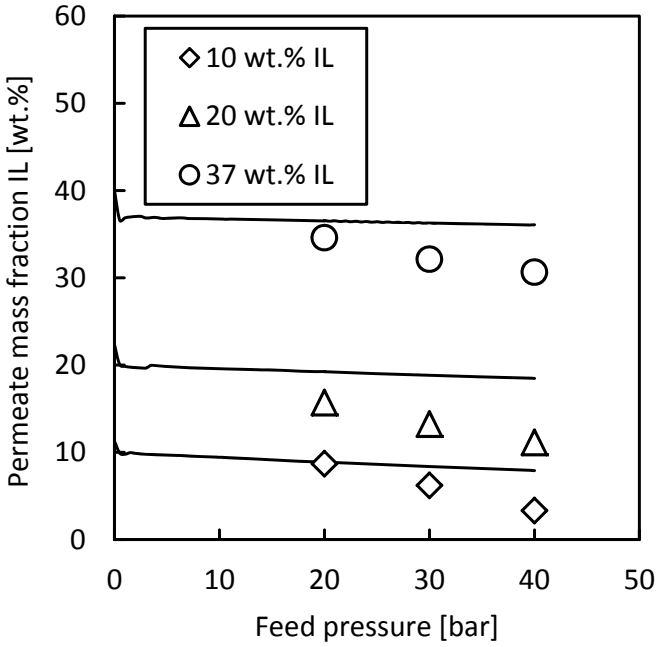

Figure 2.6: Comparison between calculated and experimental values of the permeate concentration of [MMIM][DMP] for the Desal DL membrane.

For low concentrations of ionic liquid a considerable separation of [MMIM][DMP] is observed. At a feed concentration of 10 wt.% of IL the permeate concentration is between 8.5 wt.% and 3.5 wt.% depending on the applied pressure. This equates with a rejection of 15% to 65%. But with increasing ionic liquid content the separation of ionic liquid worsens. For a feed concentration of about 40 wt.% very little rejection performance of the membrane remains. Model calculations suggest that the friction of ionic liquid in the membrane is much higher than that for water, because the ionic liquid is a much bigger molecule than water. Therefore the ionic liquid is prefereably rejected by the membrane. As well a low sorbtion rate of [MMIM][DMP] can play a role, which is plausible due to the electro-static resistance of the membrane.
The decreasing separation performance for high IL contents can be explained by os-

motic pressure effects. At high concentrations of ionic liquid, the osmotic pressure difference between feed and permeate increases considerably, as long as a separation takes place. In this case the water flux through the membrane is reduced by the osmotic pressure and the ionic liquid flux is enhanced. Exemplary calculation results are shown in the appendix. In fact, the separation performance increases for higher filtration pressures (see Fig. 2.6).

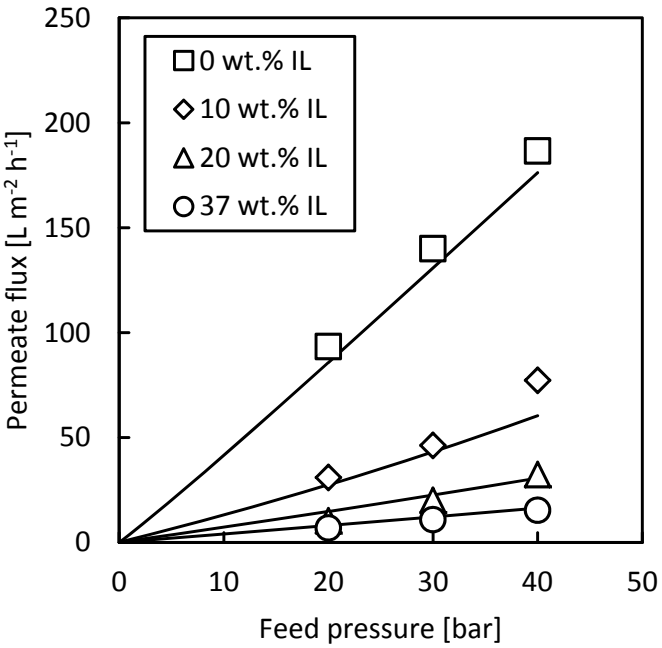

Figure 2.7: Comparison between calculated and experimental values of the permeate flux of [MMIM][DMP] / water mixtures through the Desal DL membrane.

Fig. 2.7 depicts the results for the permeate flux measurements and calculations for the Desal DL membrane. For all tested mixture compositions there is an increase in permeate flux with increasing pressure. For a pure water system the permeate flux is proportional to the applied pressure and can directly be calculated from the water permeability of the membrane.

With increasing ionic liquid concentration in the mixture the total permeate flux decreases. As well the pressure dependence of permeate flux decreases. Both effects can be explained with osmotic pressure differences between feed and permeate. These differences increase while adding ionic liquid to the solution. At high ionic liquid mass fractions separation of ionic liquid from the solution results in high osmotic pressure differences. They counteract the filtration pressure and reduce the permeate flux considerably. For concentrated ionic liquid solutions the pressure dependence of permeate flux is rather low. As discussed in Fig. 2.5 the separation of ionic liquid improves with increasing pressure. But with the increased separation

the osmotic pressure difference between feed and permeate rises. The increased pressure faces an increased osmotic pressure which works against the separation. Therefore, the permeate flux improves less than expected.

2.4.2 Results for the Starmem 240 membrane

In contrast to the Desal DL membrane the Starmem 240 membrane is not able to effectively separate [MMIM][DMP] / H_2O mixtures (see Fig. 2.8).

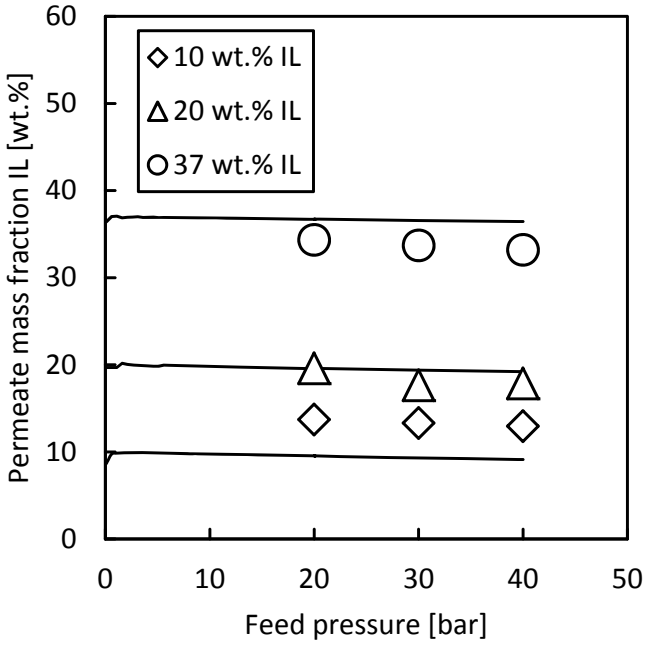

Figure 2.8: Comparison between calculated and experimental values of permeate concentration for the Starmem 240 membrane.

Even for low ionic liquid concentrations of 10 wt.% only little separation is observed. This can be explained by the relatively high MWCO of the membrane, allowing the large ionic liquid molecules to pass the membrane more easily. On the other hand the permeability of H_2O for the Starmem 240 is low (see Table 2.2). The extremely hydrophobic membrane material presumably does not absorb large amounts of water. This effect was taking into account by reducing the Henry coefficient for water sorption in the model calculations (see appendix). The permeate flux decline is much lower for the Starmem 240 than for the Desal DL membrane, as presented in Fig. 2.7. This is in good agreement with the results of Fig. 2.9, because the low separation performance indicates similar molecule velocities of the species.

The pressure dependence of separation performance and permate flux takes the same course than for the Desal DL and can be explained by osmotic pressure differences as well.

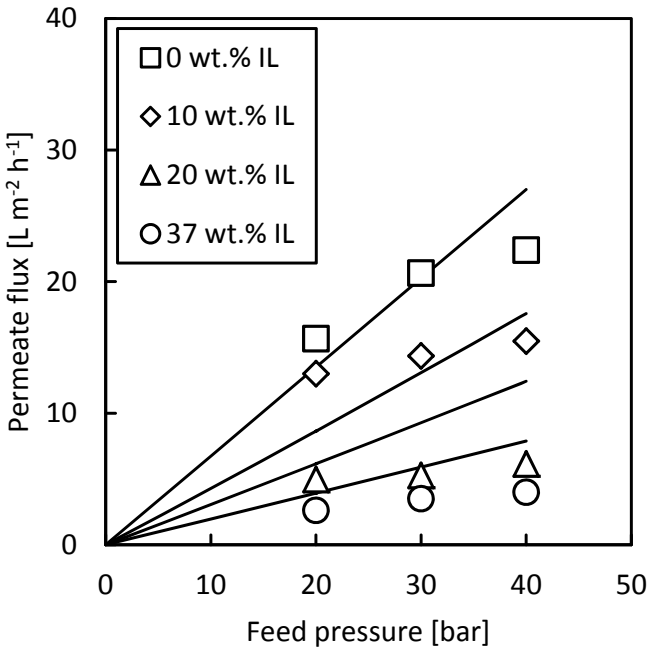

Figure 2.9: Comparison between calculated and experimental values of the permeate flux of [MMIM][DMP] / water mixtures through the Starmem 240 membrane.

2.5 Conclusion

Two different nanofiltration membranes, the Desal DL and the Starmem 240 were tested regarding their separation performance for [MMIM][DMP] / H_2O mixtures. The Desal DL membrane, which was hydrophilic, allowed for partial separation of ionic liquid from water, especially at low concentrations. The separation could be enhanced by increasing the filtration pressure. With increasing ionic liquid content a significant loss in separation performance could be observed as well as a reduction in permeate flux. In contrast, the Starmem 240 showed no significant separation of [MMIM][DMP] from water, even at low IL feed concentrations. The permeate flux decreased as well, but remained much more stable than for the Desal DL.
Model calculations with the Maxwell-Stefan model were carried out to explain these results. Calculations suggest that the ionic liquid is partially retained by both membranes due to its large molecule size and with it a high friction with the membrane material. The permeate flux reduction could be explained by osmotic pressure differences between feed and permeate due to the partial separation of IL. The worsening in separation performance for increasing ionic liquid feed concentrations could be explained by the presence of osmotic pressures as well, which counteract a separation of the substance system.
These results show that it was not possible to reveal the intrinsic membrane separation performance for the investigated substance system. The driving force in terms of filtration pressure was to low to determine the best separation performance of the respective membrane. Due to the limited operational range of nanofiltration (max. pressure of about 40 - 60 bar) it was not possible to overcome the emerging osmotic pressures of the system (see appendix).
In fact, it was not possible (1) to separate highly concentrated IL completely from water by using nanofiltration membranes, (2) to obtain a permeate flux of the mixture without any separation. Therefore, nanofiltration of ILs in aqueous solution has to be performed at rather low IL contents in order to establish an economic separation process.

2.6 References

[1] P. Wasserscheid and T. Welton; *Synthesis and Purification*; chapter 2, pages 7--55; Wiley-VCH Verlag GmbH & Co. KGaA (2008)

[2] M. Freemantle; *Ionic liquids show promise for clean separation technology*; Chemical & Engineering News **76** (34) (1998) 12--12

[3] J. P. Hallett and T. Welton; *Room-Temperature Ionic Liquids: Solvents for Synthesis and Catalysis. 2*; Chemical Reviews **111** (5) (2011) 3508--3576

[4] T. Welton; *Room-temperature ionic liquids. Solvents for synthesis and catalysis*; Chemical Reviews **99** (8) (1999) 2071--2083

[5] R. Sheldon; *Catalytic reactions in ionic liquids*; Chemical Communications **23** (2001) 2399--2407

[6] R. Kawano, H. Matsui, C. Matsuyama, A. Sato, M. A. B. H. Susan, N. Tanabe and M. Watanabe; *High performance dye-sensitized solar cells using ionic liquids as their electrolytes*; Journal of Photochemistry and Photobiology a-Chemistry **164** (1-3) (2004) 87--92

[7] M. Galinski, A. Lewandowski and I. Stepniak; *Ionic liquids as electrolytes*; Electrochimica Acta **51** (26) (2006) 5567--5580

[8] M. Ishikawa, T. Sugimoto, M. Kikuta, E. Ishiko and M. Kono; *Pure ionic liquid electrolytes compatible with a graphitized carbon negative electrode in rechargeable lithium-ion batteries*; Journal of Power Sources **162** (1) (2006) 658--662

[9] Z. G. Mu, W. M. Liu and S. Zhang; *Functional room-temperature ionic liquids as lubricants for an aluminum-on-steel system*; Chemistry Letters **33** (5) (2004) 524--525

[10] C. F. Ye, W. M. Liu, Y. X. Chen and L. G. Yu; *Room-temperature ionic liquids: a novel versatile lubricant*; Chemical Communications **21** (2001) 2244--2245

[11] F. Zhou, Y. M. Liang and W. M. Liu; *Ionic liquid lubricants: designed chemistry for engineering applications*; Chemical Society Reviews **38** (9) (2009) 2590--2599

[12] D. A. Fort, R. C. Remsing, R. P. Swatloski, P. Moyna, G. Moyna and R. D. Rogers; *Can ionic liquids dissolve wood? Processing and analysis of lignocellulosic materials with 1-n-butyl-3-methylimidazolium chloride*; Green Chemistry

9 (1) (2007) 63--69

[13] R. D. Rogers and K. R. Seddon; *Ionic liquids - Solvents of the future?*; Science **302** (5646) (2003) 792--793

[14] M. J. Earle, J. M. Esperanca, M. A. Gilea, J. N. Canongia Lopes, L. P. Rebelo, J. W. Magee, K. R. Seddon and J. A. Widegren; *The distillation and volatility of ionic liquids*; Nature **439** (7078) (2006) 831--834

[15] M. J. Earle and K. R. Seddon; *Ionic liquids. Green solvents for the future*; Pure and Applied Chemistry **72** (7) (2000) 1391--1398

[16] B. Jastorff, R. Stormann, J. Ranke, K. Molter, F. Stock, B. Oberheitmann, W. Hoffmann, J. Hoffmann, M. Nuchter, B. Ondruschka and J. Filser; *How hazardous are ionic liquids? Structure-activity relationships and biological testing as important elements for sustainability evaluation*; Green Chemistry **5** (2) (2003) 136--142

[17] P. T. P. Thi, C. W. Cho and Y. S. Yun; *Environmental fate and toxicity of ionic liquids: A review*; Water Research **44** (2) (2010) 352--372

[18] S. Han, H. T. Wong and A. G. Livingston; *Application of organic solvent nanofiltration to separation of ionic liquids and products from ionic liquid mediated reactions*; Chemical Engineering Research & Design **83** (A3) (2005) 309--316

[19] J. Krockel and U. Kragl; *Nanofiltration for the separation of nonvolatile products from solutions containing ionic liquids*; Chemical Engineering & Technology **26** (11) (2003) 1166--1168

[20] Q. Gan, M. L. Xue and D. Rooney; *A study of fluid properties and microfiltration characteristics of room temperature ionic liquids [C-10-min][NTf2] and N-8881[NTf2] and their polar solvent mixtures*; Separation and Purification Technology **51** (2) (2006) 185--192

[21] R. Krishna and J. A. Wesselingh; *The Maxwell-Stefan approach to mass transfer*; Chemical Engineering Science **52** (6) (1997) 861--911

[22] J. A. Wesselingh and A. M. Bollen; *Multicomponent diffusivities from the free volume theory*; Chemical Engineering Research & Design **75** (A6) (1997) 590--602

[23] T. R. Noordman, P. Vonk, V. H. J. T. Damen, R. Brul, S. H. Schaafsma, M. de Haas and J. A. Wesselingh; *Rejection of phosphates by a ZrO2 ultrafiltration membrane*; Journal of Membrane Science **135** (2) (1997) 203--210

[24] L. Hesse and G. Sadowski; *Modeling Liquid-Liquid Equilibria of Polyimide Solu-*

tions; Industrial & Engineering Chemistry Research **51** (1) (2012) 539--546

[25] Y. Shim, W. G. Rixey and S. Chellam; *Influence of sorption on removal of tryptophan and phenylalanine during nanofiltration*; Journal of Membrane Science **323** (1) (2008) 99--104

[26] E. Steinle-Darling, E. Litwiller and M. Reinhard; *Effects of Sorption on the Rejection of Trace Organic Contaminants During Nanofiltration*; Environmental Science & Technology **44** (7) (2010) 2592--2598

[27] A. V. Volkov, D. F. Stamatialis, V. S. Khotimsky, V. V. Volkov, M. Wessling and N. A. Plate; *Poly[1-(trimethylsilyl)-1-propyne] as a solvent resistance nanofiltration membrane material*; Journal of Membrane Science **281** (1-2) (2006) 351--357

[28] S. Deon, P. Dutournie and P. Bourseau; *Modeling nanofiltration with Nernst-Planck approach and polarization layer*; Aiche Journal **53** (8) (2007) 1952--1969

[29] J. Straatsma, G. Bargeman, H. C. van der Horst and J. A. Wesselingh; *Can nanofiltration be fully predicted by a model?*; Journal of Membrane Science **198** (2) (2002) 273--284

[30] S. Bandini and C. Mazzoni; *Modelling the amphoteric behaviour of polyamide nanofiltration membranes*; Desalination **184** (1-3) (2005) 327--336

[31] M. F. J. Dijkstra, S. Bach and K. Ebert; *A transport model for organophilic nanofiltration*; Journal of Membrane Science **286** (1-2) (2006) 60--68

[32] P. Fievet, M. Sbai, A. Szymczyk and A. Vidonne; *Determining the zeta-potential of plane membranes from tangential streaming potential measurements: effect of the membrane body conductance*; Journal of Membrane Science **226** (1-2) (2003) 227--236

[33] D. Bhanushali, S. Kloos and D. Bhattacharyya; *Solute transport in solvent-resistant nanofiltration membranes for non-aqueous systems: experimental results and the role of solute-solvent coupling*; Journal of Membrane Science **208** (1-2) (2002) 343--359

[34] R. Kato and J. Gmehling; *Measurement and correlation of vapor-liquid equilibria of binary systems containing the ionic liquids [EMIM] [(CF3SO2)(2)N], [BMIM] [(CF3SO2)(2)N], [MMIM] [(CH3)(2)PO4] and oxygenated organic compounds respectively water*; Fluid Phase Equilibria **231** (1) (2005) 38--43

2.7 Appendix

2.7.1 Nomenclature

a	activity	[-]
c	concentration	[mol m^{-3}]
D	diffusion coefficient	[m^2 sec^{-1}]
F	driving force	[N]
F	Faraday constant	96,485 [C mol^{-1}]
K	Henry coefficient	[-]
K_s	Freundlich parameter	[-]
K_B	Boltzmann constant	[$1.38 \cdot 10^{-23}$ J K^{-1}]
M	molar mass	[g mol^{-1}]
N	molar flux	[kg m^{-2} s^{-1}]
p	pressure	[Pa]
Q_0	intrinsic membrane charge	[mol m^{-3}]
Q_m	effective membrane charge	[mol m^{-3}]
R_G	gas constant	[J mol^{-1} K^{-1}]
r	radius	[m]
T	temperature	[K]
u	velocity	[m sec^{-1}]
V_m	molar volume	[m^3 mol^{-1}]
w	mass fraction	[-]
x	mole fraction	[-]
y	position in the membrane	[m]
z	valency	[-]

Greek

γ	activity coefficient	[-]
δ	active layer thickness	[m]
ζ	Zeta-Potential	[V]
ν	viscosity	[Pa sec^{-1}]
μ	chemical potential	[kJ kg^{-1}]
ζ	friction coefficient	[N sec m^{-1} mol^{-1}]
ϕ	electric potential	[V]

Subscript

i	species i
j	species j
M	membrane
IL+	ionic liquid cation
IL-	ionic liquid anion
H_2O	water

2.7.2 Model calculation results

Table 2.3: Estimated parameters for the Maxwell-Stefan model.

Parameter	Unit	Pure solvent system	Desal DL	Starmem 240
K_{H_2O}	[-]	-	0.6	0.3
$K_{[MMIM]+}$	[-]	-	0.6	0.25
$K_{[DMP]-}$	[-]	-	0.6	0.25
δ	[m]	-	$1 \cdot 10^{-07}$	$1 \cdot 10^{-07}$
Q_0	[mol m^{-3}]	-	-10	-10
$\zeta_{H_2O,[MMIM]+}$	[N sec m^{-1} mol^{-1}]	$3.70 \cdot 10^{+13}$	-	-
$\zeta_{H_2O,[DMP]-}$	[N sec m^{-1} mol^{-1}]	$3.86 \cdot 10^{+13}$	-	-
$\zeta_{[MMIM]+,[DMP]-}$	[N sec m^{-1} mol^{-1}]	$8.10 \cdot 10^{+14}$	-	-
ζ_{M,H_2O}	[N sec m^{-1} mol^{-1}]	-	$4.80 \cdot 10^{+12}$	$8.57 \cdot 10^{+12}$
$\zeta_{M,[MMIM]+}$	[N sec m^{-1} mol^{-1}]	-	$3.75 \cdot 10^{+15}$	$1.27 \cdot 10^{+15}$
$\zeta_{M,[DMP]-}$	[N sec m^{-1} mol^{-1}]	-	$4.31 \cdot 10^{+15}$	$1.46 \cdot 10^{+15}$

Table 2.4: Calculation results for the Desal DL membrane. Operating conditions: 30 bar, 25°C.

Feed [MMIM][DMP] [wt.%]	Permate [MMIM][DMP] [wt.%]	Osmotic pressure H_2O [bar]	Osmotic pressure [MMIM][DMP] [bar]	Permeate flux [L m^{-2} h^{-1}]
0	0	0.0	0.0	142.9
5	3	-10.4	134.1	75.5
10	8	-16.9	92.3	43.2
15	13	-19.5	65.0	29.6
20	19	-20.7	48.3	22.7
25	24	-21.4	37.5	18.3
30	29	-21.7	29.8	15.2
35	34	-22.0	24.1	13.0
40	39.7	-22.3	19.9	11.1

Table 2.5: Calculation results for the Starmem240 membrane. Operating conditions: 30 bar, 25°C.

Feed [MMIM][DMP] [wt.%]	Permate [MMIM][DMP] [wt.%]	Osmotic pressure H_2O [bar]	Osmotic pressure [MMIM][DMP] [bar]	Permeate flux [L m^{-2} h^{-1}]
0	0	0.0	0.0	23.1
5	4	-4.4	49.9	18.6
10	9	-8.0	41.5	15.0
15	14	-10.4	33.7	12.5
20	19	-12.2	28.1	10.6
25	24	-13.3	23.1	9.2
30	29	-14.3	19.5	8.1
35	34	-14.8	16.2	7.2
40	39	-15.3	13.7	6.4

CHAPTER 3

Transport of saccharides in ionic liquid water mixtures through polyamide and polyimide nanofiltration membranes

Parts of this chapter have been published:

C. Abels; C. Redepenning; A. Moll; T. Melin; M. Wessling, *Simple purification of ionic liquid solvents by nanofiltration in biorefining of lignocellulosic substrates,* Journal of Membrane Science 405-406 (2012) 1–10

3.1 Introduction

Ionic liquids (ILs) are new kinds of solvents which allow the processing of wooden material by means of biorefinery [1, 2]. In published process schemes the recovery of valuable products such as cellulose or lignin from the IL solution is carried out by adding water or acetone as anti-solvent [3]. Here the recovery and reuse of ionic liquid is crucial due to its high expense. In a recent publication the recovery of the hydrophobic ionic liquid 1-n-Butyl-3-methylpyridinium tetrafluoroborate from a wood dissolution process via nanofiltration is reported [4]. Whereas the permeate fluxes have been measured and fitted to a model, the rejection of solutes has not been examined in detail. The rejection of solutes in ILs is assumed to depend on the water content, especially for hydrophilic ionic liquids based on imidazole such as ethyl-methylimidazolium acetate, butyl-methylimidazolium chloride or 1,3-dimethylimidazolium phosphate [5--8]. As the ionic liquid is both, salt and solvent, two different fields of nanofiltration can be addressed, depending on the ionic liquid content in the mixture: (1) Nanofiltration of aqueous systems containing salts and organic solutes and (2) Nanofiltration of non-aqueous solvent systems containing organic solutes.

Nanofiltration of aqueous solvents containing salts has been studied extensively. In this case, especially nanofiltration of mixtures of salts and organic solutes is from interest. Few publications discuss the effect of salt addition to an aqueous solution on the rejection performance regarding organic solutes such as glucose [9--11]. Applied models assume the presence of pores in the membrane. Two general approaches are used: (1) The Maxwell-Stefan model and the (2) Nernst-Planck model [12, 13]. By assuming the presence of pores the model focuses on the rejection of the respective salt and organic solute. The sorption of these substances is calculated taking the pore size and the membrane charge into account while the water flux is assumed to depend only on the active driving force. The reduction of water sorption into the membrane at increased solute content, which is reasonable for low salt/solute concentrations, is neglected.

Nanofiltration in non-aqueous solvent systems is often referred to the field of solvent resistant nanofiltration (SRNF). Such membranes are designed for application in organic solvent recovery, e.g. toluene or acetone. Favored polymeric solvent

resistant membranes consist of compositions of polyimide or polyamide [14]. In this field several studies were published discussing the rejection of solutes in dependence of the solvent which can also comprise solvent mixtures [15--21]. Fitting of theoretical values to experimental results is performed for each respective solvent-solute-membrane system individually, for instance with the solution-diffusion approach [22].

In this work the rejection of solutes stemming from a wood dissolution process with IL via nanofiltration is examined. The experimental part focuses on the influence of the IL/water mixture composition on the solute rejection. The experimental results are modeled with the Maxwell-Stefan approach to explain trends of solute rejection. In fact, a multi-component transport is modeled comprising water, two ionic liquid molecules and the saccharide. The model is fitted to experimental results for the polyamide membrane Desal DL and the polyimide membrane Starmem 240.

3.2 Transport model

3.2.1 Maxwell-Stefan model

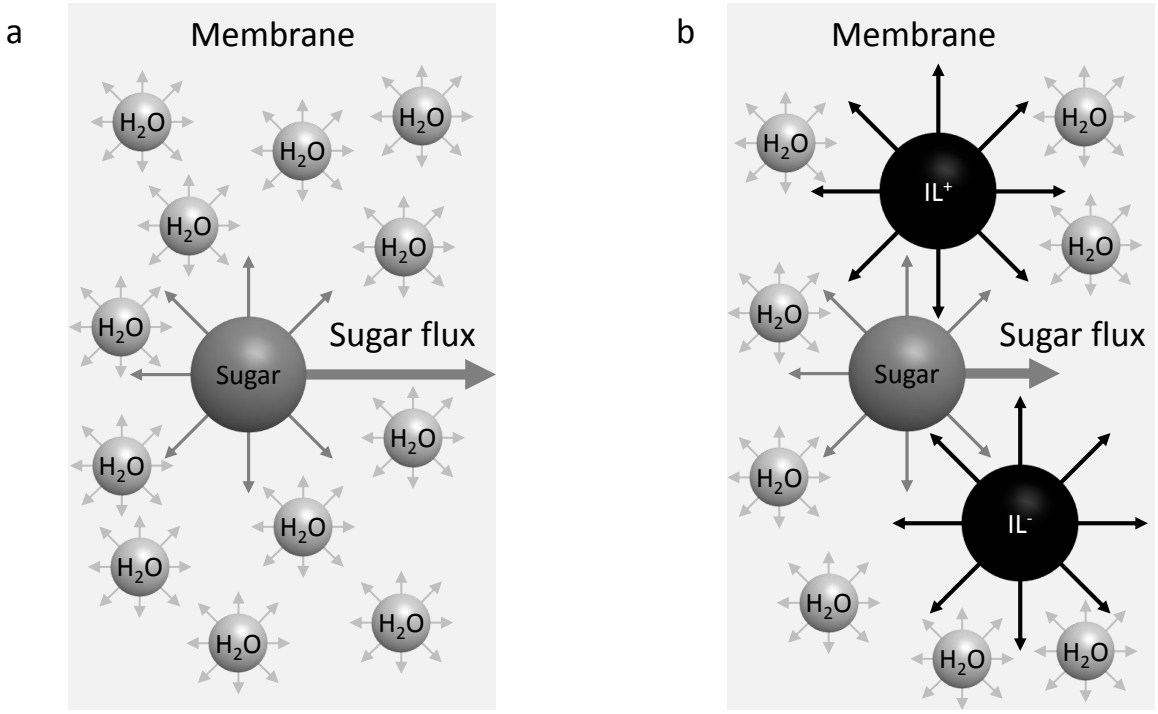

Figure 3.1: a) Friction of sugar molecule with water molecules. b) Friction of sugar molecules with water molecules and additional ionic liquid molecules.

The transport of water, ionic liquid and saccharide molecules through the nanofiltration membrane is described with the Maxwell-Stefan model which was extensively revised by Krishna and Wesselingh [13]. The basic equation of the Maxwell-Stefan approach is:

$$F_i = \sum_{i \neq j} \xi_{i,j} \cdot x_j \cdot (u_i - u_j) \tag{3.1}$$

The flux F is in balance with the velocity u of a molecule and the resistance ξ of its surrounding. The resistance can be induced by molecules from other species which are moving somehow different or from a stagnant layer such as a membrane. In this case the membrane is modeled as homogenous background layer, a so-called non-structured matrix, which does not possess an explicit mass. By replacing the molecule velocity u by the molar flux N and stating the relevant driving forces, one

yields:

$$\begin{aligned} &-\left(\frac{d\mu_i}{dy} - V_{m,i} \cdot \frac{dP}{dy} - z_i \cdot F \cdot \frac{d\Phi}{dy}\right) \cdot c \cdot x_i \\ &= \sum_{i \neq j} \xi_{i,j} \cdot \left(x_j \cdot N_i - x_i \cdot N_j\right) + \xi_{i,M} \cdot x_i \end{aligned} \tag{3.2}$$

The driving forces are the chemical potential gradient $d\mu$, the pressure gradient dP and the electric potential gradient $d\Phi$ between feed and permeate. Whereas the electric potential gradient can be neglected for neutral molecules, it has to be taken into account for charged molecules. The flux of saccharide molecules in the membrane with respect to a solvent mixture of water and ionic liquid can than be expressed as following:

$$\begin{aligned} \dot{N}_s = &\frac{(\Delta\mu - V_{m,i} \cdot \Delta P - z_i \cdot F \cdot \Delta\phi) \cdot \frac{c_s \cdot x_s}{\delta}}{\xi_{s,M} + (\xi_{s,H_2O} \cdot x_{H_2O}) + (\xi_{s,IL+} \cdot x_{IL+}) + (\xi_{s,IL-} \cdot x_{IL-})} \\ &+ \frac{\xi_{s,H_2O} \cdot x_{H_2O} \cdot \dot{N}_{H_2O}}{\xi_{s,M} + (\xi_{s,H_2O} \cdot x_{H_2O}) + (\xi_{s,IL+} \cdot x_{IL+}) + (\xi_{s,IL-} \cdot x_{IL-})} \\ &+ \frac{\xi_{s,IL+} \cdot x_{IL+} \cdot \dot{N}_{IL+}}{\xi_{s,M} + (\xi_{s,H_2O} \cdot x_{H_2O}) + (\xi_{s,IL+} \cdot x_{IL+}) + (\xi_{s,IL-} \cdot x_{IL-})} \\ &+ \frac{\xi_{s,IL-} \cdot x_{IL-} \cdot \dot{N}_{IL-}}{\xi_{s,M} + (\xi_{s,H_2O} \cdot x_{H_2O}) + (\xi_{s,IL+} \cdot x_{IL+}) + (\xi_{s,IL-} \cdot x_{IL-})} \end{aligned} \tag{3.3}$$

The effect of ionic liquid addition to an aqueous solution with a saccharide (sugar) molecule is visualized in Fig. 3.1. Fig. 3.1a shows the flux for a saccharide (sugar) molecule within the membrane in a pure water solvent. The stagnant membrane layer causes a fixed resistance $\xi_{s,M}$. Additionally, the surrounding water molecules affect the saccharide flux positively, if the water molecules move faster and negatively if they move slower. The friction forces of the water on the saccharide are rather small. In Fig. 3.1b ionic liquid molecules are added to the solution. Due to their bigger volume and their higher viscosity the ionic liquid molecules cause more friction on the saccharide molecules. If the ionic liquid molecules move slower than the water molecules they reduce the saccharide flux in comparison to a pure water system. Eq. 3.3 shows that beside the membrane friction $\xi_{s,M}$ the friction with co-flowing water and ionic liquid molecules ξ_{s,H_2O}, $\xi_{s,IL+}$ and $\xi_{s,IL-}$ restricts the flux

of saccharide molecules. The calculation results for the respective friction parameter show that the ionic liquid molecules cause far more friction on the saccharide molecules than the water molecules (see appendix).

3.2.2 Activity coefficients

The activity coefficients for mixtures of water and ionic liquid were derived from published data of vapor-liquid-equilibrium experiments [23]. The activities of the saccharide molecules were calculated with:

$$a_s = x_s \cdot \gamma_i \tag{3.4}$$

Even though the activity of the saccharide is dependent on the solvent composition, this influence is neglected. Due to the high dilution of saccharide in the mixture (concentration below 10 g L^{-1}) the activity coefficient is set to 1. Therefore the activity of the saccharide is directly calculated from the saccharide concentration, according to the simplification made for deriving the simple solution-diffusion model [13].

3.2.3 Sorption

The sorption of all species was calculated with the law of Henry based on feed mass fractions which is recommend for solvent mixtures comprising molecules with largely varying sizes [24]:

$$c_{i,M} = K_i \cdot w_{i,F} \tag{3.5}$$

Due to the charge of the ionic liquid molecules a Donnan-equilibrium between the ionic liquid molecules and the charged membrane has been implemented according to Straatsma [25]. Therefore eq. 3.5 is extended to

$$w_{IL,M} = K_{IL} \cdot w_{IL,F} \cdot exp(\frac{\pm F \cdot \Delta\Phi}{R \cdot T}) \tag{3.6}$$

3.2.4 Friction coefficients

Self-friction coefficients of the water and ionic liquid molecules and the friction coefficients of the saccharides with the solvent molecules have been calculated from the binary diffusion coefficients.

$$\xi_{i,i} = \frac{R \cdot T}{D_{i,j}} \tag{3.7}$$

The self-diffusion coefficients for water and ionic liquid molecules as well as the diffusion coefficients of the saccharides in the respective solvent have been calculated with the law of Stokes-Einstein:

$$D_i = \frac{k_B \cdot T}{6 \cdot \pi \cdot \nu_i \cdot r_i} \tag{3.8}$$

The calculation results show that the diffusivity of saccharide molecules within the ionic liquid is far lower than within the water due to its high viscosity (see Table 3.1).

Table 3.1: Calculated diffusion coefficients of investigated saccharides.

Saccharide	Radius [10^{-10} m]	Diffusion coefficient H_2O [10^{-10} m^2 sec^{-1}]	Diffusion coefficient IL [10^{-10} m^2 sec^{-1}]
Glucose	7.5	6.14	0.0281
Cellobiose	12.9	3.39	0.0155
Raffinose	9.6	4.58	0.0209

The self-friction coefficients of the saccharides were then estimated using the geometric average.

$$\xi_{i,j} = \sqrt{\xi_{i,i} \cdot \xi_{j,j}} \tag{3.9}$$

Eq. 3.9 implies that:

$$\xi_{i,j} = \xi_{j,i} \tag{3.10}$$

The friction parameter between the water molecules and the membrane was de-

rived from pure water experiments, while the friction parameters between ionic liquid molecules and membrane were fitted to experimental results. The calculated values of the friction parameters are embedded in the appendix.

3.3 Experimental

3.3.1 Nanofiltration setup

Nanofiltration experiments were carried out in a flat-sheet module, providing a membrane area of 2 mm x 8 mm. A comprehensive description of the nanofiltration setup can be found in chapter 2. During experiments the pressure was varied between 20 and 40 bar. The temperature was kept at a value of 30°C. Cross flow velocities were varied between 1 m sec^{-1} and 2.5 m sec^{-1} to check for mass transfer limitations at the membrane surface. In this range the saccharide rejection was found to be independent from cross flow velocity.

3.3.2 Materials

The investigated ionic liquid [MMIM][DMP] was provided by IoLiTec. Saccharides glucose, cellobiose and raffinose were obtained from VWR International. Raffinose is used as a substitute for cellotriose, which is the tri-saccharide occurring in the enzymatic hydrolysis of cellulose. The feed concentration of all saccharides in the experiments was set to 10 g L^{-1}. Solubility experiments were carried out to check for a complete miscibility of the diverse saccharides in [MMIM][DMP] solutions. These experiments were performed at ambient temperature of about 25°C. The results of the measurements are shown in Table 3.2. The solubility for the substances significantly decreases while adding ionic liquid to the solution. Nevertheless, for no [MMIM][DMP] solution investigated, the saccharide solubility was exceeded.

Table 3.2: Investigated saccharides and their solubilities in ionic liquid / water mixtures.

Saccharide	Molar mass [g mol^{-1}]	Solubility 0 wt.% IL [g mol^{-1}]	Solubility 20 wt.% IL [g mol^{-1}]	Solubility 40 wt.% IL [g mol^{-1}]
Glucose	180	470	340	235
Cellobiose	342	111	65	33
Raffinose	504	50	32	14

3.3.3 Analytics

The saccharides glucose, cellobiose and raffinose dissolved in various ionic liquid / water mixtures were detected via HPLC separation and refractive index measurements. Hereby the 'OrganicAcidResin + VS' column from BioRAD was used. Fig. 3.2 depicts a representative chromatogram. Due to the high viscosity of the IL, the samples had to be diluted by a factor of 50. There are small IL shoulder peaks visible at approximately 7 min. These are induced by impurities found in the technical grade of methylimidazole applied to make the ionic liquid.

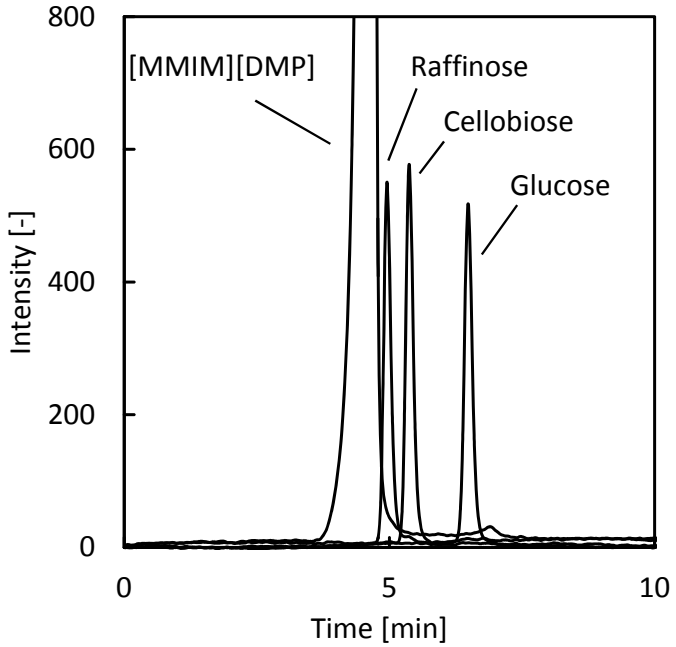

Figure 3.2: Representative HPLC-chromatogram for the ionic liquid [MMIM][DMP] and saccharides glucose, cellobiose, raffinose.

The error of the saccharide concentration measurements was determined by repeated measurements. The average error for the saccharide concentration was estimated to about 10%.

3.3.4 Investigated membranes

The Desal DL provided by GE Osmonics and the Starmem 240 provided by MET were investigated for their separation performance regarding saccharide mixtures in ionic liquid / water solvents (see Table 2.2 for detailed information on the membranes). The Desal DL membrane was flushed with pure water before experiments.

The Starmem 240 membrane was first stored in pure acetone for at least 24 h in order to remove the preservation oils. After the filtration experiments the applied membranes were stored in pure ionic liquid and reused several times.

3.4 Results

3.4.1 Saccharide rejection for the Desal DL

The rejections of glucose, cellobiose and raffinose in several ionic liquid water mixtures with IL mass fractions of up to 40 wt.% are shown in Fig. 3.3 - 3.5.

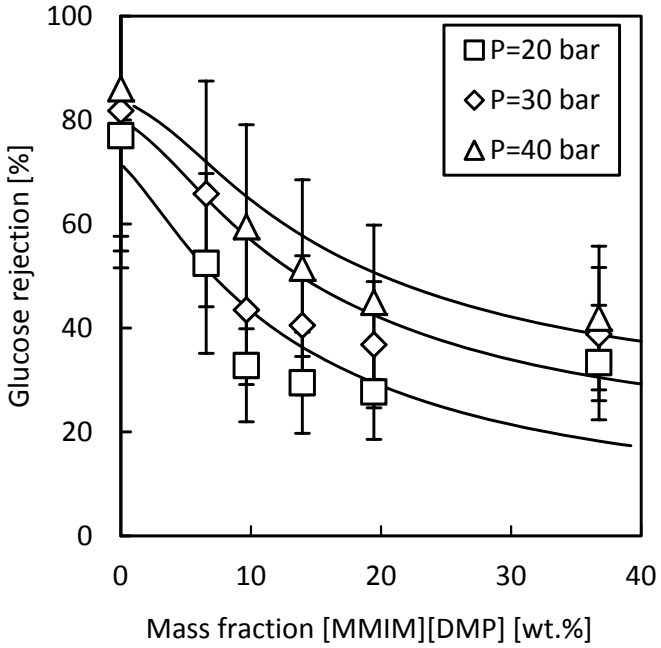

Figure 3.3: Rejection of glucose depending on feed concentration of ionic liquid [MMIM][DMP] by the Desal DL membrane. Data points reflect experimental results, straight lines reflect calculated results.

The glucose rejection was strongly dependent on the solvent mixture composition (Fig. 3.3). For pure water systems the rejection was about 80% - 85%. With increasing ionic liquid content the rejection worsened and remained at a level of about 25% - 40%. A clear pressure dependence of glucose rejection was observed. With increasing pressure the rejection increased resulting in differences of up to 10% of rejection for a change of 20 bar to 40 bar. Model calculations with the Maxwell-Stefan approach were performed. Exemplary results are shown in Table 3.3.

The glucose molecules were just partially rejected even in pure water systems. This can be explained by the small molecular weight of the glucose (180 Da) which is similar to the nominal MWCO of the Desal DK membrane (200 Da). The decrease of rejection performance can be explained by a strong decrease of the solvent mixture permeate flux. The reason can be found in the low permeability of the ionic liquid

Table 3.3: Calculation results for the Desal DL membrane. Rejected saccharide is glucose, applied pressure is 30 bar.

Feed IL $[wt.\%]$	Friction forces [N sec m^{-1} mol^{-1}]	Glucose flux [kg m^{-2} h^{-1}]	Permeate flux [kg m^{-2} h^{-1}]	Glucose rejection [-]
0	$9.58 \cdot 10^{13}$	0.28	127.7	0.78
5	$9.95 \cdot 10^{13}$	0.23	73.9	0.69
10	$1.04 \cdot 10^{14}$	0.18	41.5	0.57
15	$1.10 \cdot 10^{14}$	0.15	28.1	0.48
20	$1.15 \cdot 10^{14}$	0.12	21.0	0.42
25	$1.21 \cdot 10^{14}$	0.10	16.7	0.37
30	$1.28 \cdot 10^{14}$	0.09	13.7	0.34
35	$1.34 \cdot 10^{14}$	0.08	11.5	0.31
40	$1.41 \cdot 10^{14}$	0.07	9.6	0.29

which is added to the solution in high amounts and in strong osmotic pressures due to a partial rejection of ionic liquid by the membrane (see chapter 2). The flux of glucose decreases similarly with increasing ionic liquid concentration. This can be explained by increasing transport resistances within the solvent mixture. Table 3-3 depicts the total friction forces on a glucose molecule depending on the feed mass fraction of [MMIM][DMP] (see eq. 3.3). Obviously, the increasing amount of ionic liquid molecules in the solution increases the friction on glucose molecules as illustrated in Fig. 3.1.

The pressure dependence of glucose rejection can be explained by the driving forces which act differently on solvent and solute. While the solvent transport through the membrane is strongly pressure dependent, the transport of the solute glucose is dominated by the concentration differences between feed and permeate. Therefore a change of pressure primarily affects the solvent flux, while the solute flux remains stable.

The cellobiose rejection of the Desal DL membrane is shown in Fig. 3.4. In contrast to the glucose the cellobiose is completely retained by the membrane in a pure water solvent. These results can be explained by the higher molecular weight of cellobiose (324 g mol^{-1}). Similarly to the glucose experiments the rejection for cellobiose worsens with increasing ionic liquid content in the solvent. Nevertheless, the rejection never undercuts values of about 80%. Due to the high separation performance for cellobiose the rejection is just slightly affected by a solvent permeate flux decrease.

In Fig. 3.5 the separation performance for raffinose is shown. The molecular weight

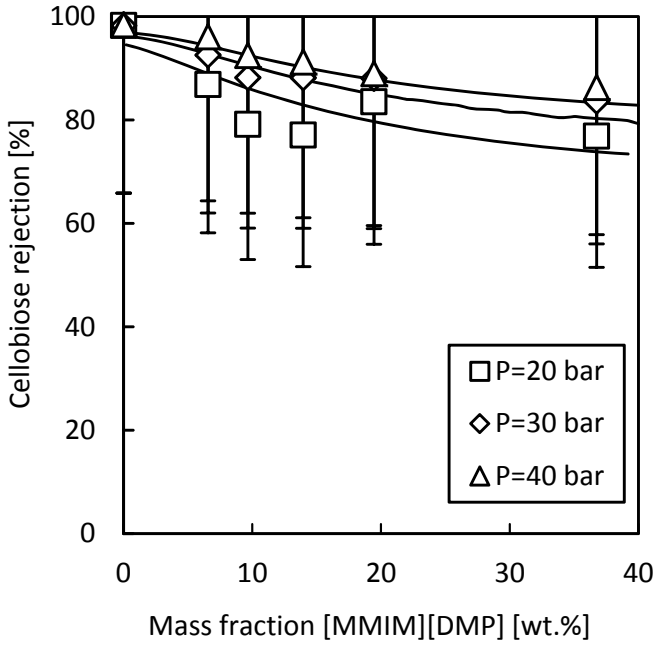

Figure 3.4: Rejection of cellobiose depending on feed concentration of ionic liquid [MMIM][DMP] by the Desal DL membrane. Data points reflect experimental results, straight lines reflect calculated results.

of this molecule is highest with 504 Da. Therefore the rejection is best, starting with an initial rejection of $>$99% for the pure water system. With increasing ionic liquid content the rejection decreases slightly to values of about 80%. This value is similar to the cellobiose rejection. In fact, the calculated diffusion coefficients for these molecules were similar, because the molecular radii are nearly the same, even though the molecular weights differ. Due to the high rejection the pressure dependence on raffinose rejection is low, as for the cellobiose.

In summary, the separation performance for all three tested saccharides decreased constantly while adding ionic liquid to the solvent mixture. At high concentrations above 20 wt.% ionic liquid the rejection stabilized at a low level. These results correspond to publications in which salt addition to an aqueous solution containing saccharides resulted in diminish of saccharide rejection [9, 10].

3.4.2 Saccharide rejection for the Starmem 240

The results for separation performance of the Starmem 240 membrane regarding saccharides in mixtures of IL and water are shown in Fig. 3.6 - Fig. 3.8. In opposite to the Desal DL membrane the rejection for all tested saccharides increased with

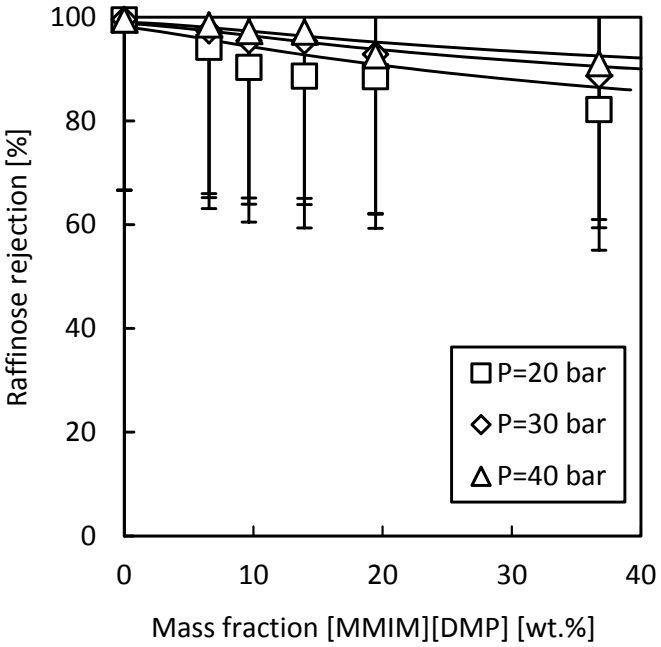

Figure 3.5: Rejection of raffinose depending on feed concentration of ionic liquid [MMIM][DMP] by the Desal DL membrane. Data points reflect experimental results, straight lines reflect calculated results.

increasing ionic liquid content in the solution.

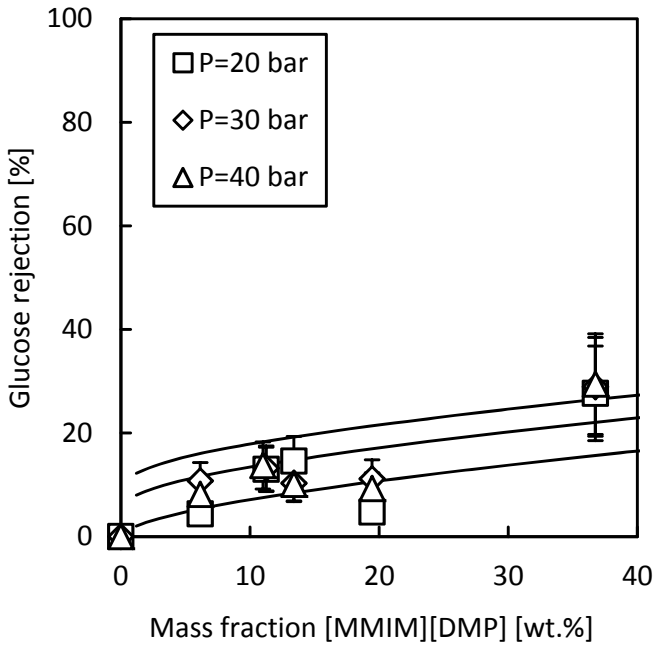

Figure 3.6: Rejection of glucose depending on feed concentration of ionic liquid [MMIM][DMP] by the Starmem 240 membrane. Data points reflect experimental results, straight lines reflect calculated results.

In Fig. 3.6 the results for the glucose rejection are shown. In pure water systems the membrane did not separate any glucose from the feed solution. With increasing ionic liquid content the membrane separated up to 20% of glucose. The low rejection for glucose can be explained with the high MWCO of the Starmem 240

membrane, which is nominal 400 Da. A clear pressure dependence on the rejection could not be measured. This can be explained by the relative stable solvent fluxes, which did not vary significantly with the applied pressure (see chapter 2). A non-linear pressure-flux correlation can result from membrane compaction which was reported for the Starmem series [26--28]. On the other hand the separation performance is reported to increase with compaction of the membrane [29]. Long-term experiments with operation times of over 80 hours showed that the membrane compaction was depending on solvent mixture. In Table 3.4 the calculation results for glucose rejection by the Starmem 240 membrane are presented.

Table 3.4: Calculation results for the Starmem 240 membrane. Rejected saccharide is glucose, applied pressure is 30 bar.

Feed IL $[wt.\%]$	Friction forces [N sec m^{-1} mol^{-1}]	Glucose flux [kg m^{-2} h^{-1}]	Permeate flux [kg m^{-2} h^{-1}]	Glucose rejection [-]
0	2.66·10^{12}	0.18	19.4	0.08
5	3.46·10^{12}	0.14	15.8	0.11
10	4.48·10^{12}	0.11	12.5	0.14
15	5.53·10^{12}	0.09	10.2	0.15
20	6.61·10^{12}	0.07	8.6	0.17
25	7.73·10^{12}	0.06	7.3	0.19
30	8.89·10^{12}	0.05	6.2	0.20
35	1.01·10^{13}	0.04	5.4	0.22
40	1.13·10^{13}	0.04	4.7	0.23

As for the Desal DL membrane the presence of ionic liquid molecules in the solvent increases the friction on glucose molecules according to eq. 3.3. In result, the glucose flux decreases. In contrast to the Desal DL membrane the total permeate flux reduction for the Starmem 240 membrane is less significant. Therefore, the glucose rejection increases, because the total permate flux is more stable than the glucose flux. Calculations predict a more significant pressure dependence on separation performance. The differences between experimental and calculated values can be explained by compaction of the Starmem 240 membrane during experiments which was neglected in the model.

In Fig. 3.7 and Fig. 3.8 the results for the cellobiose and raffinose rejection are shown. As for the glucose the separation of the saccharides increases with increasing ionic liquid content. Due to the higher molecular weight of these substances they are separated in a higher degree by the Starmem 240 membrane. However, the pressure dependence on rejection was found to be low which is contrary to sim-

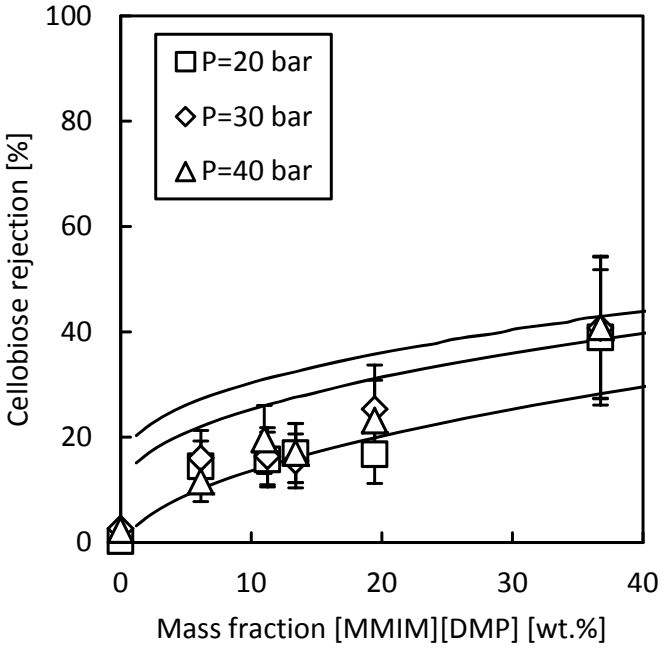

Figure 3.7: Rejection of cellobiose depending on feed concentration of ionic liquid [MMIM][DMP] by the Starmem 240 membrane. Data points reflect experimental results, straight lines reflect calculated results.

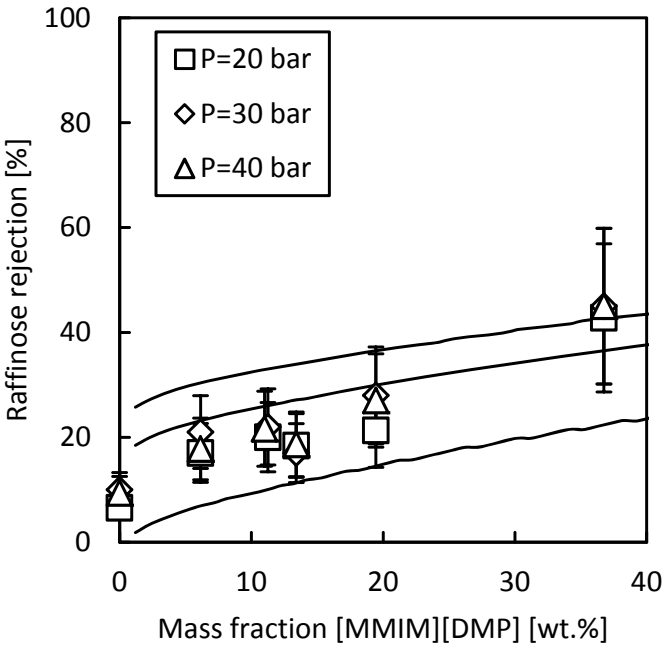

Figure 3.8: Rejection of raffinose depending on feed concentration of ionic liquid [MMIM][DMP] by the Starmem 240 membrane. Data points reflect experimental results, straight lines reflect calculated results.

ulated results.

3.5 Conclusion

Two different nanofiltration membranes, the Desal DL and the Starmem 240 were tested on their separation performance regarding saccharides in water/ ionic liquid mixtures. Mixtures containing the ionic liquid [MMIM][DMP] were concentrated up to 40 wt.%. The separation performance for glucose, cellobiose and raffinose was tested for pressures of 20 - 40 bar at ambient temperature.

The separation performance for the Desal DL membrane was best for a pure water solvent. In such a solvent a glucose rejection of up to 85% and a cellobiose and raffinose rejection of up to $>$99% was reached. With increasing ionic liquid content in the mixture, the rejection worsened for all three substances. For glucose the rejection dropped to about 25% at a feed concentration of 40 wt.% ionic liquid. For cellobiose and raffinose the rejection decreased less, to a value of about 85%. The separation performance for all three substances was dependent on the pressure. It increased with increasing pressures. Whereas the pressure dependence was significant for glucose, it was low for cellobiose and raffinose.

The results for the Starmem 240 membranes were different. In pure water solvent there was hardly a rejection of the diverse saccharides observed. With increasing ionic liquid content the separation performance increased for all three substances to values of about 20% - 40% at 40 wt.% of [MMIM][DMP]. As for the Desal DL membrane the rejection of the respective saccharide increased with increasing molecular weight. In contrast to the Desal DL membrane the rejection was hardly dependent on pressure. With increasing pressure the rejection increased.

A Maxwell-Stefan model was set up to simulate the experimental results of saccharide rejection. For both membranes the flux of glucose decreased with increasing ionic liquid content. This effect could be explained with increasing friction forces on the saccharide molecules in presence of ionic liquid molecules. The opposite evolution of saccharide rejection for the tested membranes can be explained by differing developments of permeate fluxes. Whereas for the Desal DL membrane a strong permeate flux decline is observed, the permeate flux for the Starmem 240 reduces moderately.

For the Starmem 240 membrane the permeate flux decline was very much lower than for the Desal DL membrane due to a better permeability of the ionic liquid. In

this case the increasing transport resistance for the saccharide molecules with increasing ionic liquid content in the membrane affected the rejection performance positively. The bigger ionic liquid molecules filled the membrane and therefore blocked the transport of saccharides more than the water molecules. In fact, diffusion of saccharides in ionic liquid is way much slower than for water. Therefore, the saccharide flux decreased significantly. Because the solvent flux decreased just slightly, the separation performance engaged with increasing ionic liquid content for the Starmem 240 membrane.

For the Desal DL a clear pressure dependence on saccharide separation was observed as predicted by the model. As the solvent mixture permeates through the membrane due to the applied pressure, the solute flux is induced by concentration differences between feed and permeate. Hence, an increase in pressure encourages the solvent flux, while the solute flux remains nearly stable. However, for the Starmem 240 membrane no pressure dependence could be found. This was explained by compaction effects which have not been included in the model.

3.6 References

[1] I. Kilpelainen, H. Xie, A. King, M. Granstrom, S. Heikkinen and D. S. Argyropoulos; *Dissolution of wood in ionic liquids*; Journal of Agricultural and Food Chemistry **55** (22) (2007) 9142--9148

[2] D. A. Fort, R. C. Remsing, R. P. Swatloski, P. Moyna, G. Moyna and R. D. Rogers; *Can ionic liquids dissolve wood? Processing and analysis of lignocellulosic materials with 1-n-butyl-3-methylimidazolium chloride*; Green Chemistry **9** (1) (2007) 63--69

[3] N. Sun, M. Rahman, Y. Qin, M. L. Maxim, H. Rodriguez and R. D. Rogers; *Complete dissolution and partial delignification of wood in the ionic liquid 1-ethyl-3-methylimidazolium acetate*; Green Chemistry **11** (5) (2009) 646--655

[4] S. Hazarika, N. N. Dutta and P. G. Rao; *Dissolution of lignocellulose in ionic liquids and its recovery by nanofiltration membrane*; Separation and Purification Technology **97** (2012) 123--129

[5] A. S. da Silva, S. H. Lee, T. Endo and E. P. S. Bon; *Major improvement in the rate and yield of enzymatic saccharification of sugarcane bagasse via pretreatment with the ionic liquid 1-ethyl-3-methylimidazolium acetate ([Emim] [Ac])*; Bioresource Technology **102** (22) (2011) 10505--10509

[6] Y. Fukaya, K. Hayashi, M. Wada and H. Ohno; *Cellulose dissolution with polar ionic liquids under mild conditions: required factors for anions*; Green Chemistry **10** (1) (2008) 44--46

[7] R. P. Swatloski, S. K. Spear, J. D. Holbrey and R. D. Rogers; *Dissolution of Cellose with Ionic Liquids*; Journal of the American Chemical Society **124** (18) (2002) 4974--4975

[8] M. Zavrel, D. Bross, M. Funke, J. Buechs and A. C. Spiess; *High-throughput screening for ionic liquids dissolving (ligno-)cellulose*; Bioresource Technology **100** (9) (2009) 2580--2587

[9] G. Bargeman, J. M. Vollenbroek, J. Straatsma, C. G. P. H. Schroen and R. M. Boom; *Nanofiltration of multi-component feeds. Interactions between neutral and charged components and their effect on retention*; Journal of Membrane Science **247** (1-2) (2005) 11--20

[10] A. W. Mohammad, R. K. Basha and C. P. Leo; *Nanofiltration of glucose solution*

containing salts: Effects of membrane characteristics, organic component and salts on retention; Journal of Food Engineering **97** (4) (2010) 510--518

[11] J. Q. Luo and Y. H. Wan; *Effect of highly concentrated salt on retention of organic solutes by nanofiltration polymeric membranes*; Journal of Membrane Science **372** (1-2) (2011) 145--153

[12] J. Schaep, C. Vandecasteele, A. W. Mohammad and W. R. Bowen; *Modelling the retention of ionic components for different nanofiltration membranes*; Separation and Purification Technology **22-3** (1-3) (2001) 169--179

[13] R. Krishna and J. A. Wesselingh; *The Maxwell-Stefan approach to mass transfer*; Chemical Engineering Science **52** (6) (1997) 861--911

[14] P. Vandezande, L. E. M. Gevers and I. F. J. Vankelecom; *Solvent resistant nanofiltration: separating on a molecular level*; Chemical Society Reviews **37** (2) (2008) 365--405

[15] D. Bhanushali, S. Kloos and D. Bhattacharyya; *Solute transport in solvent-resistant nanofiltration membranes for non-aqueous systems: experimental results and the role of solute-solvent coupling*; Journal of Membrane Science **208** (1-2) (2002) 343--359

[16] S. Darvishmanesh, J. Degreve and B. Van der Bruggen; *Mechanisms of solute rejection in solvent resistant nanofiltration: the effect of solvent on solute rejection*; Physical Chemistry Chemical Physics **12** (40) (2010) 13333--13342

[17] J. Geens, K. Peeters, B. Van der Bruggen and C. Vandecasteele; *Polymeric nanofiltration of binary water-alcohol mixtures: Influence of feed composition and membrane properties on permeability and rejection*; Journal of Membrane Science **255** (1-2) (2005) 255--264

[18] E. Gibbins, M. D'Antonio, D. Nair, L. S. White, L. M. F. dos Santos, I. F. J. Vankelecom and A. G. Livingston; *Observations on solvent flux and solute rejection across solvent resistant nanofiltration membranes*; Desalination **147** (1-3) (2002) 307--313

[19] D. Q. Shi, Y. Kong, J. X. Yu, Y. F. Wang and J. R. Yang; *Separation performance of polyimide nanofiltration membranes for concentrating spiramycin extract*; Desalination **191** (1-3) (2006) 309--317

[20] E. S. Tarleton, J. P. Robinson, C. R. Millington and A. Nijmeijer; *Non-aqueous nanofiltration: solute rejection in low-polarity binary systems*; Journal of Membrane Science **252** (1-2) (2005) 123--131

[21] E. S. Tarleton, J. P. Robinson, C. R. Millington, A. Nijmeijer and M. L. Taylor; *The influence of polarity on flux and rejection behaviour in solvent resistant nanofiltration - Experimental observations*; Journal of Membrane Science **278** (1-2) (2006) 318--327

[22] J. G. Wijmans and R. W. Baker; *The Solution-Diffusion Model - a Review*; Journal of Membrane Science **107** (1-2) (1995) 1--21

[23] R. Kato and J. Gmehling; *Measurement and correlation of vapor-liquid equilibria of binary systems containing the ionic liquids [EMIM] [(CF3SO2)(2)N], [BMIM] [(CF3SO2)(2)N], [MMIM] [(CH3)(2)PO4] and oxygenated organic compounds respectively water*; Fluid Phase Equilibria **231** (1) (2005) 38--43

[24] M. F. J. Dijkstra, S. Bach and K. Ebert; *A transport model for organophilic nanofiltration*; Journal of Membrane Science **286** (1-2) (2006) 60--68

[25] J. Straatsma, G. Bargeman, H. C. van der Horst and J. A. Wesselingh; *Can nanofiltration be fully predicted by a model?*; Journal of Membrane Science **198** (2) (2002) 273--284

[26] S. S. Luthra, X. J. Yang, L. M. F. dos Santos, L. S. White and A. G. Livingston; *Homogeneous phase transfer catalyst recovery and re-use using solvent resistant membranes*; Journal of Membrane Science **201** (1-2) (2002) 65--75

[27] J. A. Whu, B. C. Baltzis and K. K. Sirkar; *Nanofiltration studies of larger organic microsolutes in methanol solutions*; Journal of Membrane Science **170** (2) (2000) 159--172

[28] X. J. Yang, A. G. Livingston and L. F. dos Santos; *Experimental observations of nanofiltration with organic solvents*; Journal of Membrane Science **190** (1) (2001) 45--55

[29] J. T. Scarpello, D. Nair, L. M. F. dos Santos, L. S. White and A. G. Livingston; *The separation of homogeneous organometallic catalysts using solvent resistant nanofiltration*; Journal of Membrane Science **203** (1-2) (2002) 71--85

3.7 Appendix

3.7.1 Nomenclature

a	activity	[-]
c	concentration	[mol m^{-3}]
D	diffusion coefficient	[m^2 sec^{-1}]
F	driving force	[N]
F	Faraday constant	96,485 [C mol^{-1}]
K	Henry coefficient	[-]
K_B	Boltzmann constant	[$1.38 \cdot 10^{-23}$ J K^{-1}]
M	molar mass	[g mol^{-1}]
N	molar flux	[kg m^{-2} s^{-1}]
p	pressure	[Pa]
Q_0	intrinsic membrane charge	[mol m^{-3}]
Q_m	effective membrane charge	[mol m^{-3}]
R_G	gas constant	[J mol^{-1} K^{-1}]
r	radius	[m]
T	temperature	[K]
u	velocity	[m sec^{-1}]
V_m	molar volume	[m^3 mol^{-1}]
w	mass fraction	[-]
x	mole fraction	[-]
y	position in the membrane	[m]
z	valency	[-]

Greek

γ	activity coefficient	[-]
δ	active layer thickness	[m]
ζ	Zeta-Potential	[V]
ν	viscosity	[Pa sec^{-1}]
μ	chemical potential	[kJ kg^{-1}]
ζ	friction coefficient	[N sec m^{-1} mol^{-1}]
ϕ	electric potential	[V]

Subscript

i	species i
j	species j
M	membrane
IL+	ionic liquid cation
IL-	ionic liquid anion
H_2O	water
s	saccharide / sguar

3.7.2 Model calculation results

Table 3.5: Estimated parameters for the Maxwell-Stefan model. Part 1

Parameter	Unit	Pure solvent system	Desal DL	Starmem 240
K_{H_2O}	[-]	-	0.6	0.3
$K_{[MMIM]+}$	[-]	-	0.6	0.25
$K_{[DMP]-}$	[-]	-	0.6	0.25
δ	[m]	-	$1 \cdot 10^{-07}$	$1 \cdot 10^{-07}$
Q_0	[mol m^{-3}]	-	-10	-10
$\zeta_{H_2O,[MMIM]+}$	[N sec m^{-1} mol^{-1}]	$3.70 \cdot 10^{+13}$	-	-
$\zeta_{H_2O,[DMP]-}$	[N sec m^{-1} mol^{-1}]	$3.86 \cdot 10^{+13}$	-	-
$\zeta_{[MMIM]+,[DMP]-}$	[N sec m^{-1} mol^{-1}]	$8.10 \cdot 10^{+14}$	-	-
ζ_{M,H_2O}	[N sec m^{-1} mol^{-1}]	-	$4.80 \cdot 10^{+12}$	$8.57 \cdot 10^{+12}$
$\zeta_{M,[MMIM]+}$	[N sec m^{-1} mol^{-1}]	-	$3.75 \cdot 10^{+15}$	$1.27 \cdot 10^{+15}$
$\zeta_{M,[DMP]-}$	[N sec m^{-1} mol^{-1}]	-	$4.31 \cdot 10^{+15}$	$1.46 \cdot 10^{+15}$

Table 3.6: Estimated parameters for the Maxwell-Stefan model. Part 2

Parameter	Unit	Pure solvent system	Desal DL	Starmem 240
$K_{Glucose}$	[-]	-	$3.00 \cdot 10^{-03}$	$3.00 \cdot 10^{-04}$
$K_{Cellobiose}$	[-]	-	$8.00 \cdot 10^{-05}$	$8.00 \cdot 10^{-05}$
$K_{Raffinose}$	[-]	-	$1.00 \cdot 10^{-04}$	$5.00 \cdot 10^{-05}$
$\zeta_{Glucose,H_2O}$	[N sec m^{-1} mol^{-1}]	$4.06 \cdot 10^{+12}$	-	-
$\zeta_{Glucose,[DMP]+}$	[N sec m^{-1} mol^{-1}]	$8.52 \cdot 10^{+13}$	-	-
$\zeta_{Glucose,[DMP]-}$	[N sec m^{-1} mol^{-1}]	$8.89 \cdot 10^{+13}$	-	-
$\zeta_{M,Glucose}$	[N sec m^{-1} mol^{-1}]	-	$4.80 \cdot 10^{+12}$	$8.57 \cdot 10^{+12}$
$\zeta_{Cellobiose,H_2O}$	[N sec m^{-1} mol^{-1}]	$7.35 \cdot 10^{+12}$	-	-
$\zeta_{Cellobiose,[DMP]+}$	[N sec m^{-1} mol^{-1}]	$1.54 \cdot 10^{+14}$	-	-
$\zeta_{Cellobiose,[DMP]-}$	[N sec m^{-1} mol^{-1}]	$1.61 \cdot 10^{+14}$	-	-
$\zeta_{M,Cellobiose}$	[N sec m^{-1} mol^{-1}]	-	$4.80 \cdot 10^{+12}$	$8.57 \cdot 10^{+12}$
$\zeta_{Raffinose,H_2O}$	[N sec m^{-1} mol^{-1}]	$5.45 \cdot 10^{+12}$	-	-
$\zeta_{Raffinose,[DMP]+}$	[N sec m^{-1} mol^{-1}]	$1.14 \cdot 10^{+14}$	-	-
$\zeta_{Raffinose,[DMP]-}$	[N sec m^{-1} mol^{-1}]	$1.19 \cdot 10^{+14}$	-	-
$\zeta_{M,Raffinose}$	[N sec m^{-1} mol^{-1}]	-	$4.80 \cdot 10^{+12}$	$8.57 \cdot 10^{+12}$

CHAPTER 4

Separation of glucose from cellobiose in ionic liquid water mixtures via nanofiltration

4.1 Introduction

Cellulose can be converted to glucose by enzymatic hydrolysis. For a fast and complete conversion of cellulose enzyme mixtures are employed comprising endoglucanases and exoglucanases. These enzymes reduce the endings of the cellulose chains, respectively random regions within the cellulose fibers with the simultaneous release of polysaccharides and the disaccharide cellobiose. Cellobiose is strongly product inhibiting, resulting in a decreasing enzyme activity during the batch hydrolysis. To release the cellobiose product inhibition, the enzyme β-D-glucosidase can be added to the mixture for a conversion of cellobiose to glucose, though glucose is product inhibited as well [1--3].

To achieve high conversion rates of cellulose, its crystallinity can be reduced to extend the range of accessible regions for the enzymes. For this purpose cellulose is pretreated with organic solvents such as ethanol (in the Organosolv process for instance) or strong salt solutions such as ionic liquids. A solvent pretreatment of cellulose or lignocellulosic matter can lead to a partial conversion to sugars. Nevertheless, the release of sugars is far less than by an enzymatic hydrolysis and can therefore not replace it up to now [4--7].

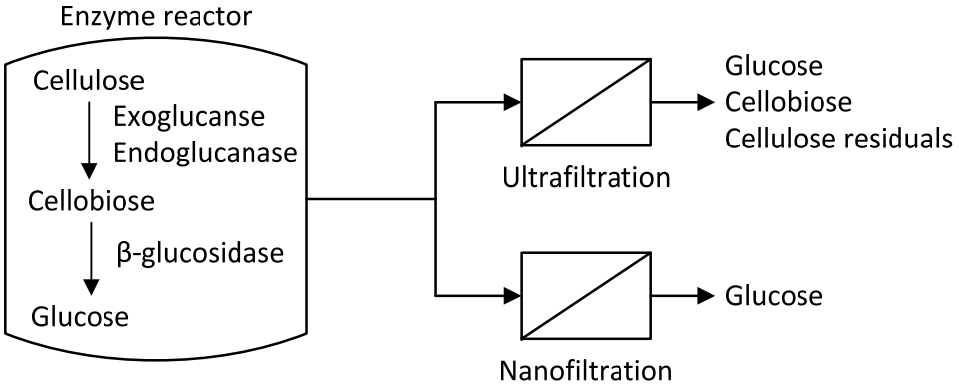

Figure 4.1: a) Friction of sugar molecule with water molecules. b) Friction of sugar molecules with water molecules and additional ionic liquid molecules.

For a complete and fast conversion of cellulose to glucose it is necessary to remove the product during the enzymatic hydrolysis. Several publications deal with the implementation of membrane separations into an enzymatic reactor [8--14]. Interestingly, in all these publications micro- or ultrafiltration membranes are employed which allow the passage of not just glucose, but of intermediates of the cellulose hydrolysis as well (see Fig. 4.1). Therefore, the productivity of these reactors could

just be enhanced to a certain permeation rate. Further increase of the permeate flux resulted in a decrease of productivity.

In most of the publications, problems during the membrane operation such as concentration polarization were taken into account for the observed decrease of product yield. In only one publication the simultaneous loss of intermediates during the membrane operation was mentioned as possible reason for the decrease of productivity [12]. Due to the high MWCO of the ultrafiltration membranes the loss of intermediates from the cellulose hydrolysis can not be avoided. Therefore, we suggest implementing a nanofiltration membrane for the selective recovery of glucose from the hydrolysis reactor.

In this work a nanofiltration membrane, namely the Desal DL provided by GE Osmonics, is investigated for its separation performance regarding mixtures of glucose and cellobiose. Target approach is to separate the glucose from higher polysaccharides to allow for a complete conversion of cellulose (fragments) to the final product glucose. In this work the feasibility of glucose separation is investigated for a batch process. Key parameters in this study are the product yield and the separation performance of glucose.

4.2 Experimental

4.2.1 Batch filtration setup

Fig. 4.2 shows the setup which was used for nanofiltration experiments. The feed volume of the stainless steel cell was 1 L. The membrane area was about 100 cm^2. The experiments were carried out at ambient temperature of about 25°C. The employed membrane was a Desal DL, obtained from GE Osmonics. Batch filtration experiments were run until a permeate yield of 90% was reached. Samples were taken each 10% of permeate yield. The outflowing permeate was collected and its final concentration measured after reaching the 90% permeate yield. In addition, the retentate concentration after 90% of permeate yield was recorded.

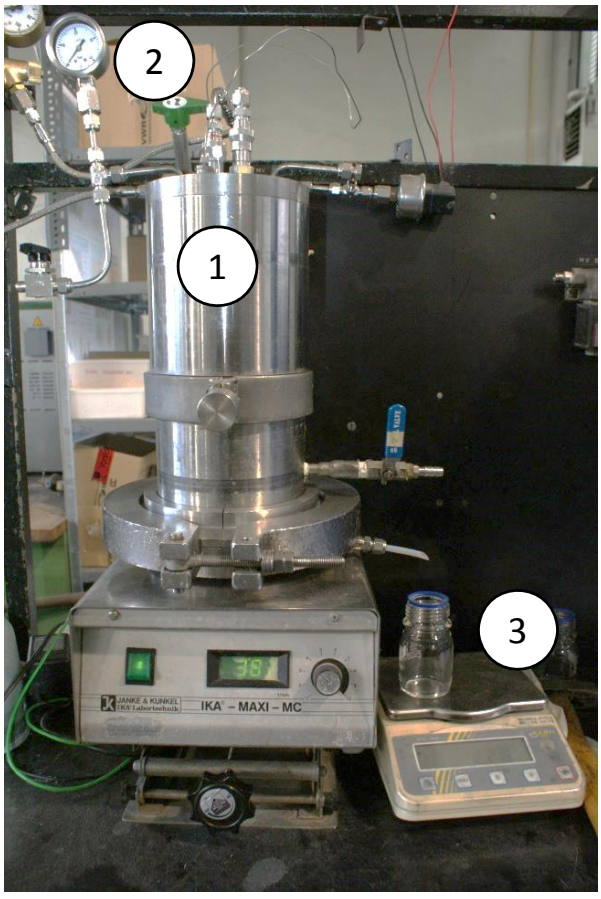

Figure 4.2: Experimental set-up used for ultra- and nanofiltration batch experiments: 1. Stainless steel test cell; 2. Pressure control; 3. Weighing balance.

The glucose concentration of the collected permeate was compared to the initial feed concentration to determine the glucose recovery. Hence, the glucose recovery R_G (at 90% permeate yield) was calculated with:

$$R_G = \frac{c_{G,P}}{c_{G,F}} \cdot 0.9 \tag{4.1}$$

As well the separation performance S_G of saccharide mixtures comprising glucose and cellobiose was calculated by dividing the glucose recovery by the cellobiose recovery (at 90% permeate yield):

$$S_G = \frac{c_{G,P}/c_{G,F}}{c_{C,P}/c_{C,F}} \tag{4.2}$$

4.2.2 Analytics

The standard system, which was tested, contained 10 g L^{-1} of α-glucose and 10 g L^{-1} of cellobiose provided by VWR. The feed solution contained 100 g L^{-1} of ionic liquid 1,3-dimethyl-phosphate [MMIM][DMP] which was provided by IoLiTec. The concentrations of glucose, cellobiose and ionic liquid in aqueous solution were determined via HPLC separation and refractive index measurements. Hereby the ÖrganicAcidResin + VSc̈olumn from BioRAD was used. Fig. 3.2 depicts a representative chromatogram. Due to the high viscosity of the IL, the samples had to be diluted by a factor of 50.

4.3 Results

4.3.1 Yield dependence of saccharide separation

In Fig. 4.3 the separation performance of the Desal DL membrane regarding diverse saccharides in mixtures of water and ionic liquid [MMIM][DMP] is shown.

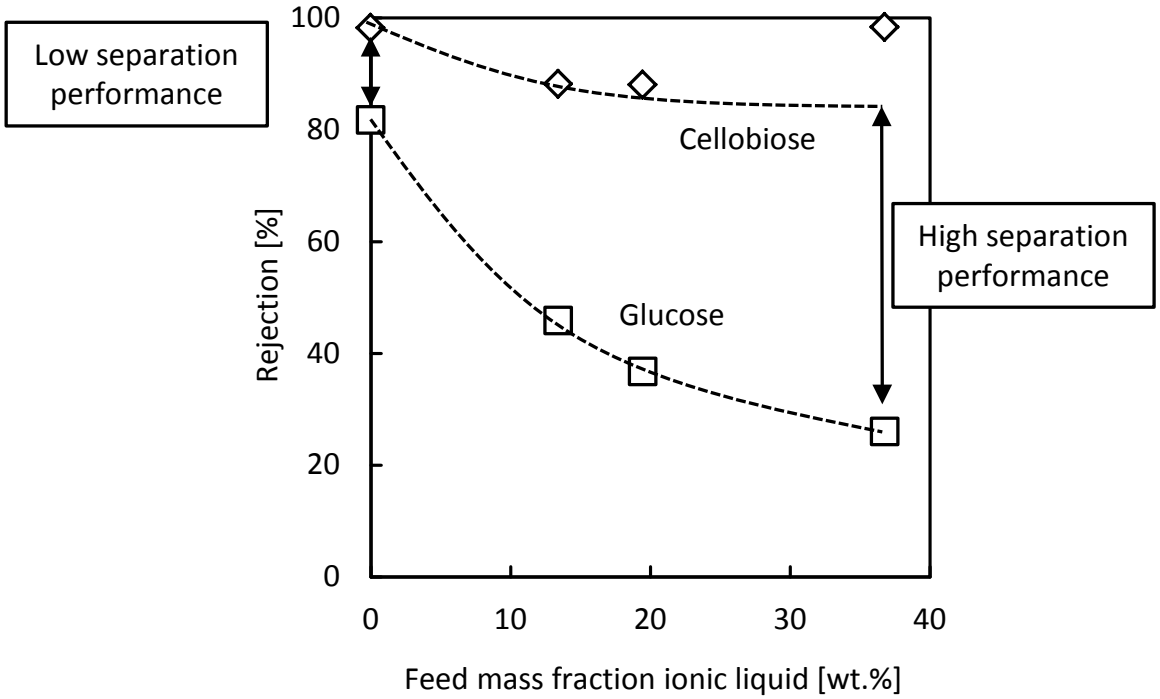

Figure 4.3: Separation performance of Desal DL membrane for diverse saccharides depending on ionic liquid content. The filtration pressure was set to 30 bar. The permeate yield was close to 0%.

With increasing ionic liquid content the rejection of glucose drops dramatically, whereas the cellobiose rejection is less dependent on ionic liquid concentration. The results were obtained for permeate yields of close to 0% by taking a 5 ml sample from a 1 L feed tank. However, in a batch filtration process the feed solution is at the same time the retentate, therefore the solute concentrations in the feed vary during the filtration process. In chapter 2 and 3 a Maxwell-Stefan model was set up in order to simulate the saccharide and ionic liquid rejection depending on the ionic liquid feed concentration. This model allows the prediction of saccharide and ionic liquid permeate concentrations depending on the permeate yield. The key results of the batch process simulations are shown in Table 4.1.

Relevant simulation results are the separation performance of glucose from cellobiose

Table 4.1: Calculation results for the batch filtration of glucose, cellobiose and ionic liquid in aqueous solution. Initial feed concentrations were 10 g L^{-1} glucose and cellobiose and 100 g L^{-1} ionic liquid. Feed pressure was set to 30 bar. Simulated membrane was Desal DL.

Permeate yield [-]	IL permeate concentration [g L^{-1}]	Glucose recovery [%]	Glucose separation [-]
0.10	86.7	4.8	4.37
0.20	87.4	10.0	4.27
0.30	88.2	15.6	4.17
0.40	89.1	21.8	4.05
0.50	90.1	28.6	3.91
0.60	91.2	36.3	3.75
0.70	92.5	45.3	3.56
0.80	94.0	56.5	3.30
0.90	96.0	72.5	2.89

and the glucose recovery rate. As shown in Table 4.1 the permeate concentration of glucose increases with increasing permeate yield from about 5% to about 73% by collecting permeate to a yield of 90%. Simultaneously with glucose, cellobiose is permeating, resulting in a decreasing separation performance. These calculation results can be explained with the varying ionic liquid content in the feed. Initially, the saccharides are highly rejected by the membrane due to the low ionic liquid content of 10 wt.% in the feed (see Fig. 4.3). While the ionic liquid is (partially) rejected by the membrane, its feed concentration increases with ongoing filtration. At high permeate yields the rejection of saccharides is correspondingly low and the current permeate concentrations increase.

4.3.2 Pressure dependence of saccharide separation

In Fig. 4.4a the experimental results of the separation performance regarding glucose / cellobiose mixtures at a feed pressure of 10 bar are shown. Depending on the permeate yield the current permeate concentration of glucose, cellobiose and ionic liquid varies. The higher the permeate yield the more of the respective solute can be found in the permeate probe. Especially the glucose and ionic liquid concentrations increase considerably with ongoing filtration. In contrast, the cellobiose concentration in the permeate probes remains low, especially for permeate yields below 80%, allowing for an efficient separation of glucose from cellobiose. As predicted, the rejection of all three substances is strongly dependent on the ionic liquid content in

the feed.

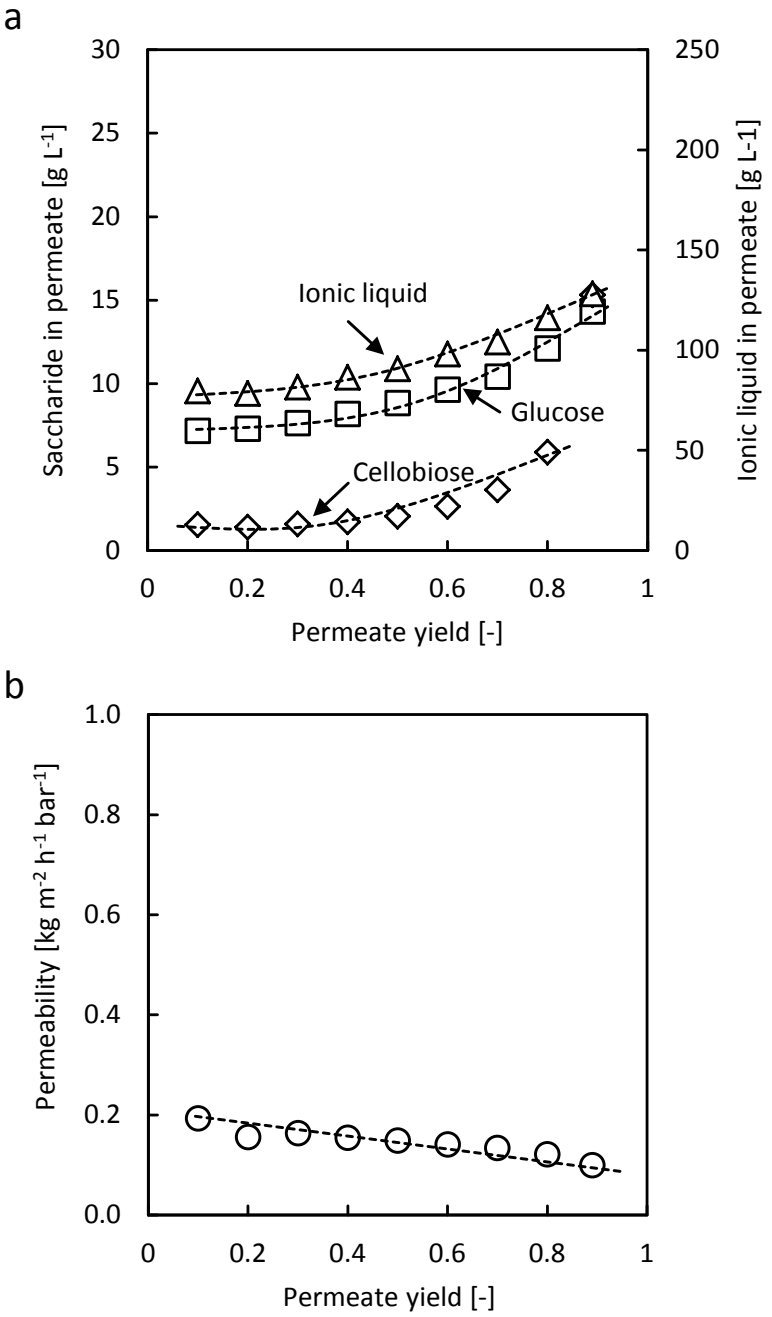

Figure 4.4: a) Current permeate concentrations of saccharides and ionic liquid depending on the permeate yield. b) Membrane permeability depending on flux. The filtration pressure was set to 10 bar, initial feed concentrations of saccharides and ionic liquid were 10 g L^{-1}, respectively 100 g L^{-1}. The employed membrane was the Desal DL.

In Fig. 4.4b the membrane permeability depending on the permeate yield is shown. The permeate flux slightly decreases for increasing permeate yields. The ionic liquid feed concentration increases significantly to values of about 300 g L^{-1} during the filtration process (results not shown). Along with the increasing ionic liquid feed concentration the permeate flux drops due to the low permeability of the ionic liquid and increasing osmotic pressures (see chapter 2).

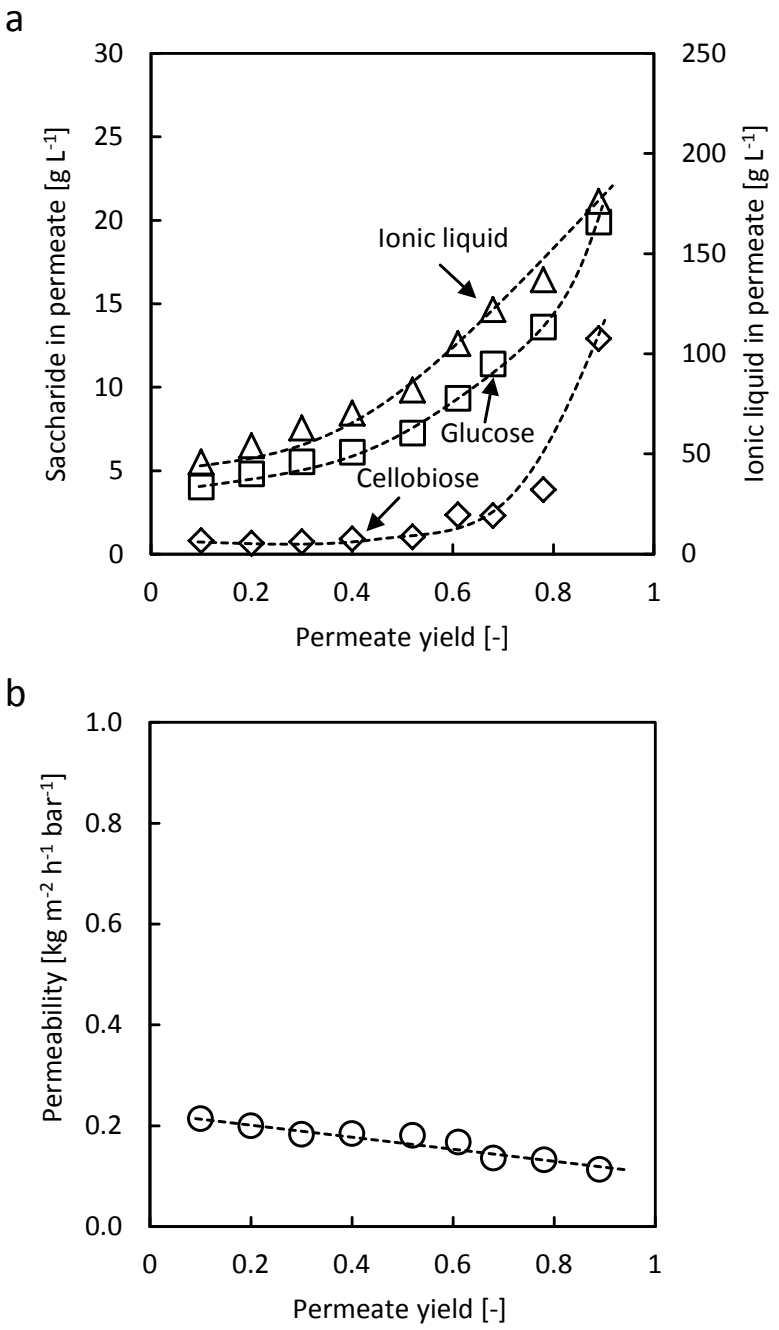

Figure 4.5: a) Current permeate concentrations of saccharides and ionic liquid depending on the permeate yield. b) Membrane permeability depending on flux. The filtration pressure was set to 20 bar, initial feed concentrations of saccharides and ionic liquid were 10 g L^{-1}, respectively 100 g L^{-1}. The employed membrane was the Desal DL.

In Fig. 4.5a the evolutions of saccharide and ionic liquid permeate concentrations depending on the permeate yield for a feed pressure of 20 bar are shown. In comparison to the results for 10 bar (see Fig. 4.4a) the initial permeate concentrations of all three substances are lower. During the filtration process the permeate concentrations increase faster with permeate yield and finally reach higher values than as for 10 bar at a permeate yield of about 60%. The observed membrane perme-

ability for 20 bar is shown in Fig. 4.5b. It is higher than for 10 bar (see Fig. 4.4b), because at 20 bar the effect of osmotic pressure, which reduces the permeate flux, is lower.

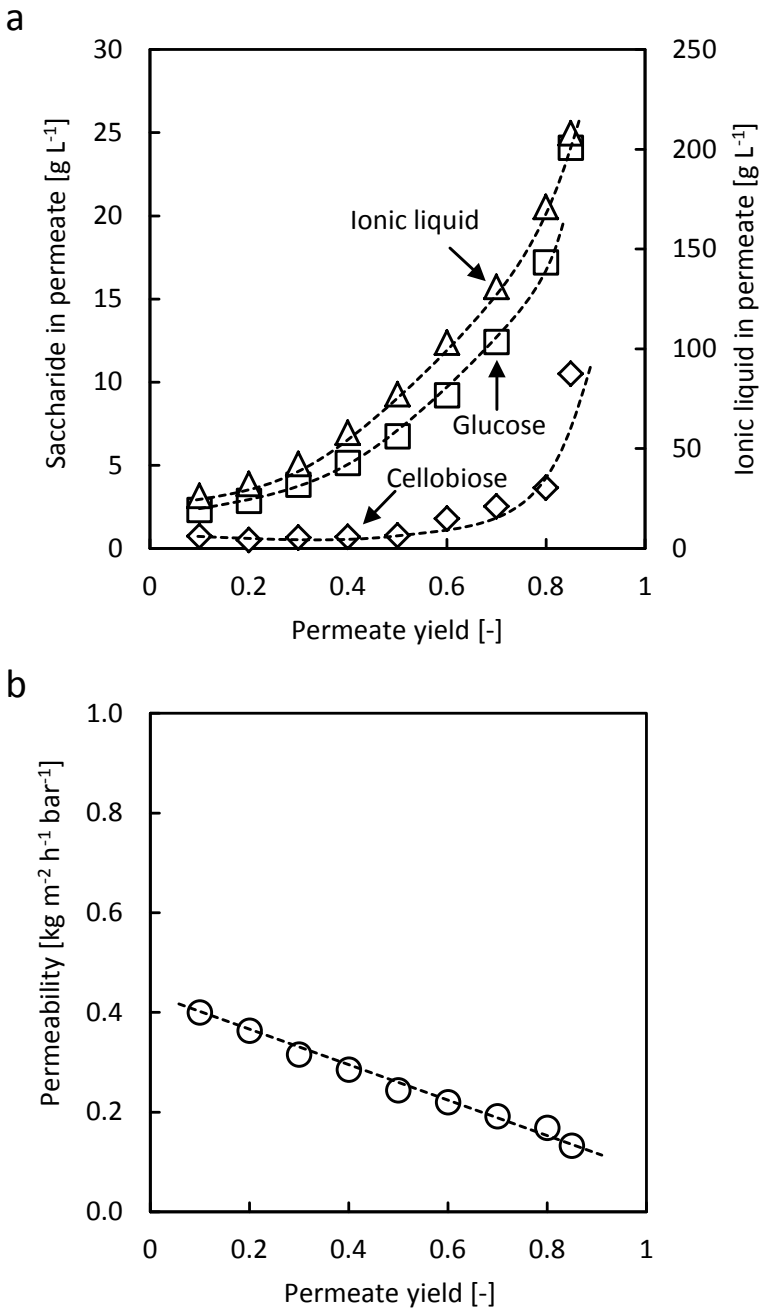

Figure 4.6: a) Current permeate concentrations of saccharides and ionic liquid depending on the permeate yield. b) Membrane permeability depending on flux. The filtration pressure was set to 30 bar, initial feed concentrations of saccharides and ionic liquid were 10 g L^{-1}, respectively 100 g L^{-1}. The employed membrane was the Desal DL.

In Fig. 4.6a the evolutions of saccharide and ionic liquid permeate concentrations depending on the permeate yield for a feed pressure of 30 bar are shown. The initial permeate concentrations are the lowest compared to the results for 10 and 20 bar (see Fig. 4.4a and 4.5a). In opposite the permeate concentrations for high permeate

yields above 60% are highest. The permeate flux for 30 bar is shown in Fig. 4.4b. It is highest in comparison to 10 bar and 20 bar (see Fig. 4.2b and 4.3b). It decreases significantly due to the rising ionic liquid feed concentration and resulting osmotic pressures.

Table 4.2: Experimental results for the recovery of glucose from a feed mixture containing 10 g L^{-1} of glucose, 10 g L^{-1} of cellobiose and 100 g L^{-1} of ionic liquid. The permeate yield was 90%. The employed membrane was the Desal DL. Feed pressure was varied between 10 bar and 30 bar.

Feed pressure [bar]	IL permeate concentration [g L^{-1}]	Glucose recovery [-]	Glucose separation [%]
10	91.6	0.88	2.58
20	86.4	0.86	3.96
30	80.0	0.77	5.38

In Table 4.2 the results for the accumulated permeate concentrations of saccharides and ionic liquid are shown. The pressure was varied between 10 and 30 bar. The final permeate yield was kept constant at a value of 90%. The saccharide and ionic liquid permeate concentrations were both highest for low feed pressures. This is in good agreement with the results for the saccharide rejection discussed in chapter 2. Therefore the glucose recovery rate is best at low feed pressures. On the other hand the separation performance regarding the glucose / cellobiose mixture decreases with increasing feed pressures. In addition, the filtration time is significantly reduced by a factor of about 4 by increasing the pressure from 10 bar to 30 bar. Therefore, an operational point of 30 bar is chosen for an optimal recovery of glucose in terms of selectivity and filtration time.

4.3.3 Concentration dependence of saccharide separation

To determine the influence of saccharide feed concentration on the separation performance, experiments were carried out with solutions containing 2 g L^{-1}, 5 g L^{-1} and 10 g L^{-1} of saccharide. In this range the feed concentration of saccharides are expected after enzymatic hydrolysis of 10 g L^{-1} of cellulose.

In Fig. 4.7 the results for feed solutions containing 2 g L^{-1} and 10 g L^{-1} of saccharides are shown. The permeate concentrations were normalized to the respective feed concentration in order to be comparable. There is no significant difference in

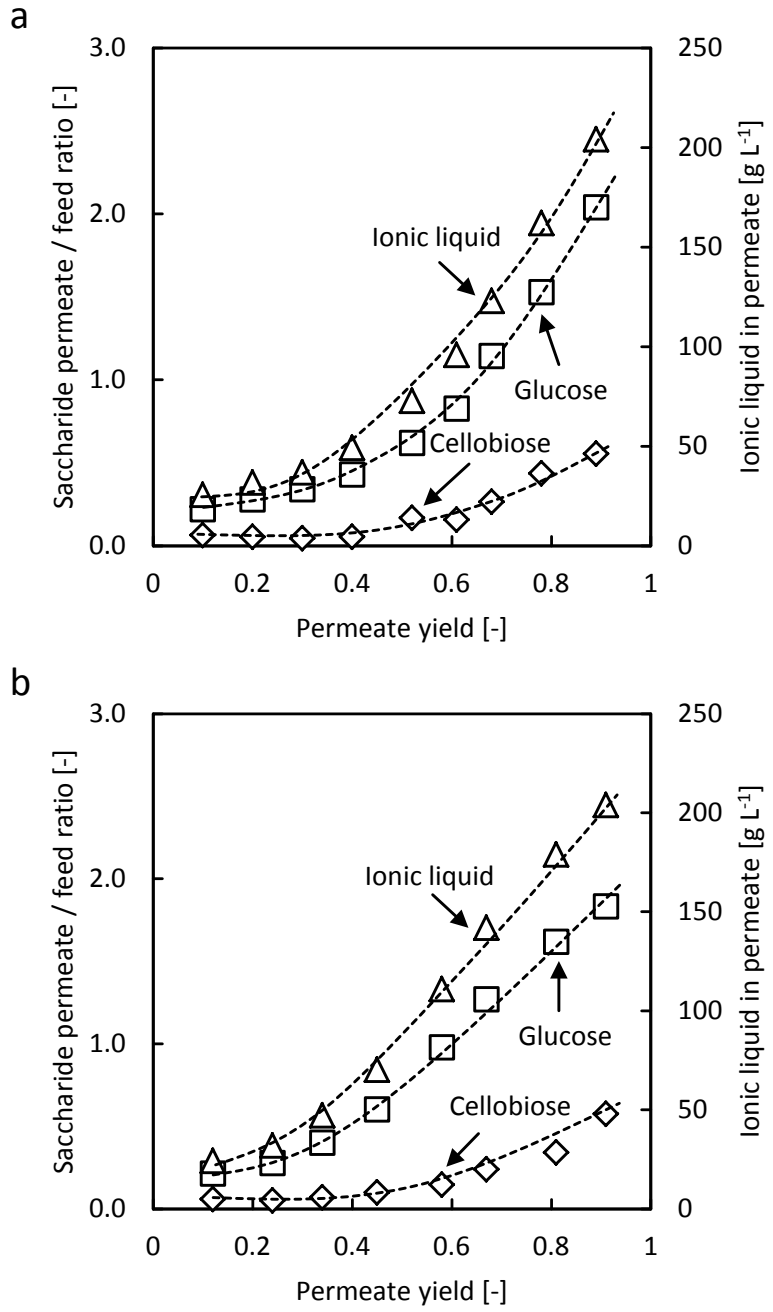

Figure 4.7: a) Permeate concentrations of saccharides and ionic liquid depending on the permeate yield. The initial feed concentrations of saccharides were 2 g L^{-1} and ionic liquid concentration was 100 g L^{-1}. b) The initial feed concentrations of saccharides and ionic liquid were 10 g L^{-1}, respectively 100 g L^{-1}. The permeate concentrations were normalized to the respective feed concentration. The filtration pressure was set to 30 bar. The tested membrane was the Desal DL.

permeate concentration at varying feed concentrations. The saccharide concentrations are too low to have a significant influence on the separation performance of the membrane.

The accumulated permeate concentrations for the diverse solutions at a permeate yield of 90% are listed in Table 3. It can be seen, that the glucose recovery is about

Table 4.3: Experimental results for the recovery of glucose from a feed mixture containing 10 g L^{-1} of glucose, 10 g L^{-1} of cellobiose and 100 g L^{-1} of ionic liquid. The permeate yield was 90%. The employed membrane was the Desal DL. Saccharide feed concentration was varied between 2 g L^{-1} and 10 g L^{-1}.

Saccharide feed concentration [g L^{-1}]	IL permeate concentration [g L^{-1}]	Glucose recovery [-]	Glucose separation [%]
2	79.3	0.74	4.14
5	82.3	0.71	4.75
10	80.0	0.71	4.80

70% - 75%, independent of the feed concentration of saccharide. The cellobiose / glucose ratio in the permeate is about 0.20, independent of the saccharide concentration as well. It can be stated, that the separation of glucose and cellobiose does not depend on the feed concentration of saccharide in a concentration range of 2 g L^{-1} - 10 g L^{-1}.

4.4 Conclusion

Separation of glucose from cellobiose in mixtures of ionic liquid and water was investigated for a batch filtration process. The dependency of permeate yield, filtration pressure and saccharide concentration on glucose purification and recovery rate was examined in detail. Based on calculation results for the glucose and cellobiose rejection in solutions containing 0 - 40 wt.% of ionic liquid, the recovery rate RG of glucose and the separation performance SG regarding glucose / cellobiose mixtures from a batch process were predicted. The calculation results show, that the glucose recovery increases significantly with increasing permeate yield. A sufficient glucose recovery of about 70% can be reached at a permeate yield of at least 90% at 30 bar. In opposite the separation performance declines constantly with increasing permeate yield from about 4.4 at 10% permeate yield to 2.9 at 90% permeate yield. Experimental results concerning the recovery rate and separation performance for glucose depending on the permeate yield confirm the calculations. For a feed pressure of 30 bar and a permeate yield of 90% the glucose recovery reached 73%, while the separation performance S was 3, which is in good agreement with the calculation results. In addition, the influence of the feed pressure and the initial saccharide feed concentration was investigated. It could be shown that a feed pressure variation between 10 - 30 bar results in differences concerning the glucose recovery and separation. While the glucose recovery decreases for increasing pressures, the separation performance increases. In contrast, the initial saccharide feed concentration does not affect the recovery rate or separation performance, due to the small solute concentration in the feed solution, which is between 2 g L^{-1} and 10 g L^{-1}.

4.5 References

[1] M. E. Himmel, S. Y. Ding, D. K. Johnson, W. S. Adney, M. R. Nimlos, J. W. Brady and T. D. Foust; *Biomass recalcitrance: Engineering plants and enzymes for biofuels production*; Science **315** (5813) (2007) 804--807

[2] R. M. F. Bezerra and A. A. Dias; *Discrimination among eight modified Michaelis-Menten kinetics models of cellulose hydrolysis with a large range of substrate/enzyme ratios*; Applied Biochemistry and Biotechnology **112** (3) (2004) 173--184

[3] P. Andric, A. S. Meyer, P. A. Jensen and K. Dam-Johansen; *Reactor design for minimizing product inhibition during enzymatic lignocellulose hydrolysis: I. Significance and mechanism of cellobiose and glucose inhibition on cellulolytic enzymes*; Biotechnology Advances **28** (3) (2010) 308--324

[4] H. Zhang, J. Wu, J. Zhang and J. S. He; *1-Allyl-3-methylimidazolium chloride room temperature ionic liquid: A new and powerful nonderivatizing solvent for cellulose*; Macromolecules **38** (20) (2005) 8272--8277

[5] P. Sannigrahi, S. J. Miller and A. J. Ragauskas; *Effects of organosolv pretreatment and enzymatic hydrolysis on cellulose structure and crystallinity in Loblolly pine*; Carbohydrate Research **345** (7) (2010) 965--970

[6] P. Engel, R. Mladenov, H. Wulfhorst, G. Jaeger and A. C. Spiess; *Point by point analysis: how ionic liquid affects the enzymatic hydrolysis of native and modified cellulose*; Green Chemistry **12** (11) (2010) 1959--1966

[7] H. Zhao, C. I. L. Jones, G. A. Baker, S. Xia, O. Olubajo and V. N. Person; *Regenerating cellulose from ionic liquids for an accelerated enzymatic hydrolysis*; Journal of Biotechnology **139** (1) (2009) 47--54

[8] R. G. Henley, R. Y. K. Yang and P. F. Greenfield; *Enzymatic Saccharification of Cellulose in Membrane Reactors*; Enzyme and Microbial Technology **2** (3) (1980) 206--208

[9] F. Alfani, D. Albanesi, M. Cantarella, V. Scardi and A. Vetromile; *Kinetics of Enzymatic Saccharification of Cellulose in a Flat-Membrane Reactor*; Biomass **2** (4) (1982) 245--253

[10] I. Ohlson, G. Tragardh and B. Hahnhagerdal; *Enzymatic-Hydrolysis of Sodium-Hydroxide-Pretreated Sallow in an Ultrafiltration Membrane Reactor*;

Biotechnology and Bioengineering **26** (7) (1984) 647--653

[11] S. Kinoshita, J. W. Chua, N. Kato, T. Yoshida and H. Taguchi; *Hydrolysis of Cellulose by Cellulases of Sporotrichum-Cellulophilum in an Ultrafilter Membrane Reactor*; Enzyme and Microbial Technology **8** (11) (1986) 691--695

[12] K. Belafi-Bako, A. Koutinas, N. Nemestothy, L. Gubicza and C. Webb; *Continuous enzymatic cellulose hydrolysis in a tubular membrane bioreactor*; Enzyme and Microbial Technology **38** (1-2) (2006) 155--161

[13] Q. Gan, S. J. Allen and G. Taylor; *Design and operation of an integrated membrane reactor for enzymatic cellulose hydrolysis*; Biochemical Engineering Journal **12** (3) (2002) 223--229

[14] P. Andric, A. S. Meyer, P. A. Jensen and K. Dam-Johansen; *Reactor design for minimizing product inhibition during enzymatic lignocellulose hydrolysis II. Quantification of inhibition and suitability of membrane reactors*; Biotechnology Advances **28** (3) (2010) 407--425

CHAPTER 5

Membrane-based recovery of glucose from enzymatic hydrolysis of ionic liquid pretreated cellulose

Parts of this chapter have been published:
C. Abels; K. Thimm; H. Wulfhorst; A.C. Spiess; M. Wessling, *Membrane-based recovery of glucose from enzymatic hydrolysis of ionic liquid pretreated cellulose,* Bioresource Technology 149 (2013) 58–64

5.1 Introduction

Future biofuel production may be based on the utilization of lignocellulosic feedstock. For the efficient conversion of raw material to fuel, numerous sub-processes have to be managed and optimized such as (1) the separation of the diverse raw material fractions, namely cellulose, hemicellulose and lignin (2) conversion of cellulose to glucose and (3) fermentation of glucose to the final product which can be ethanol or a platform chemical such as itaconic acid [1--3].

The conversion of cellulose to glucose can be carried out by enzymatic hydrolysis with cellulases [4]. In general, cellulase mixtures are used to convert cellulose with a polymerization degree of up to 1500 down to the monosaccharide glucose. The commercial cellulase preparation Celluclast® for instance comprises endoglucanase, exoglucanase and β-glucosidase. While endoglucanase and exoglucanase degrade the cellulose to the disaccharide cellobiose, β-glucosidase is specialized on the conversion of cellobiose to glucose. Both reactions are product inhibited [5, 6].

Due to the relatively low reaction rates which were observed for native cellulose conversion, two strategies were developed to increase the activity of the enzymes: (A) reducing the crystallinity of cellulose with a strong solvent to increase the accessibility for the enzymes and (B) reducing the product inhibition by continuous removal of the final product glucose.

Several solvents for lignocellulosic biomass pretreatment were investigated in literature, such as organic acids [7], alcohol / water mixtures [8] and ionic liquids [9, 10]. Especially ionic liquids were examined for their ability not just to dissolve ligno-cellulosic biomass efficiently but simultaneously to decrease the crystallinity of cellulose [11--13]. In the cited publications an increase of product yield by pretreatment with ionic liquid was proven, e.g. for 1-butyl-3-methyl-imidazolium chloride [BMIM][Cl], 1-ethyl-3-methyl-imidazolium acetate [EMIM][Ac] or 1,3-dimethyl-imidazolium dimethylphosphate [MMIM][DMP]. In presence of tested ionic liquids a decrease in enzyme activity was observed, however for [MMIM] [DMP] the activity decreased to a lesser extent [12].

In order to reduce the product inhibition of β-glucosidase, the removal of glucose from enzymatic hydrolysis was investigated by means of a membrane reactor [14, 15]. The employed ultrafiltration membranes allowed for an increased productivity

of the reactor due to the continuous removal of inhibiting product. However, the productivity decreased again, when a certain permeate flux was exceeded. Most researchers explained this phenomenon with the accumulation of cellulose onto the membrane surface preventing its hydrolysis by the enzymes. Likewise, the simultaneous loss of intermediates such as cellobiose into the permeate was identified as limiting factor for permeate flux [14].

Until now the recovery of ionic liquid from such enzymatic conversions is discussed in only few papers. Chromatographic techniques have already been applied [16, 17] as well as extraction [18]. Whereas the chromatographic separation of ionic liquid is more likely to be applied in lab-scale applications, extraction seems to be a process which can be adapted to industrial scale of biofuel production. The extraction process aimed at the recovery of ionic liquid from a wood dissolution process with the target product cellulose.

In this work, the downstream-processing after enzymatic hydrolysis of cellulose originating from wood pretreated in ionic liquids is discussed. Therefore, a complete downstream process for the recovery of glucose from ionic liquid-assisted enzymatic hydrolysis of cellulose is technically and economicaly evaluated. The process aims at a high product yield and purity of glucose as well as a close to complete recovery of the intermediate cellobiose and the pretreatment solvent ionic liquid. Lab-scale experiments are carried out for each unit operation to prove its technical feasibility. Particular substances stemming from the cellulose hydrolysis reaction, such as large polymeric cellulose residuals > 10 kDa, are retained by ultrafiltration and returned to the hydrolysis reactor. Nanofiltration is applied to purify the glucose product solution from molecular impurities such as small oligosaccharides like cellobiose with molecular weights > 300 Da. Finally, the ionic liquid, which is of similar size as the product glucose ($\sim$ 200 Da), is recovered from the product solution via charge exclusive electrodialysis and returned to the pretreatment reactor. To evaluate the entire downstream process the mass and energy balances obtained from the experimental results are introduced into a techno-economic calculation of the production costs for glucose from cellulose including the investigated membrane downstream process.

5.2 Materials and Methods

5.2.1 Materials

The investigated ionic liquid [MMIM][DMP] was provided by IoLiTec, Heilbronn, Germany. α-cellulose as well as the saccharides glucose and cellobiose were obtained from VWR International, Darmstadt, Germany. The enzyme preparation Celluclast® was provided by Sigma-Aldrich, Schnelldorf, Germany.

5.2.2 Hydrolysis reactor

Enzymatic hydrolysis was carried out in a 2 Liter reactor with 10 g L^{-1} of α-cellulose. The concentration of commercial enzyme mixture Celluclast® was 0.5 g L^{-1} with an activity of 700 EGU g L^{-1} as declared by the supplier. The pH during the hydrolysis was controlled to a value of 4.8 via 0.1 M sodium acetate buffer solution. The temperature was set to 45°C. The enzymatic hydrolysis was carried out for 100 hours. After this time no more conversion of cellulose to glucose or cellobiose was observed. Two experiments were carried out. One with and one without pretreatment of the cellulose with ionic liquid 1,3-dimethyl-imidazolium dimethylphosphate [MMIM][DMP]. In the pretreatment experiment the cellulose was dissolved in ionic liquid and heated up to 100°C for 1 hour. Afterwards the solution was mixed with the buffer solution to obtain an IL concentration of 100 g L^{-1}. In the experiment without ionic liquid pretreatment the IL was added to the buffer solution before start of the enzymatic hydrolysis of untreated cellulose. The remaining ionic liquid is known to reduce the enzymatic activity during hydrolysis [12]. Due to the same amount of ionic liquid present in the hydrolysis experiments both reaction times could be compared fairly.

5.2.3 Batch filtration device

Ultra- and nanofiltration experiments were performed in a stainless steel batch filtration cell allowing for pressures of 1 - 100 bar. The feed volume was 1 L. The mem-

brane area was about 125 cm^2. The experiments were carried out at ambient temperature of about 25°C. After hydrolysis the hydrolysate was cooled down to room temperature and then filtrated. For ultrafiltration experiments a NPO30 membrane from Microdyn Nadir with a nominal MWCO of 10 kDa was used. The membrane's active layer is made of polyethersulfone. The filtration pressure was set to 1 bar. During the filtration the collected permeate weight was recorded with a balance. The feed solution in the batch filtration cell was continuously mixed with a magnetic stirrer at 500 rpm to reduce the accumulation of particles on the membrane surface. Nevertheless, a strong flux decline was observed during the experiment. Hence, the permeate yield for the ultrafiltration was limited to 60% to allow for a reasonable average permeate flux. It could be stabilized by (a) operating a cross flow module to prevent accumulation of particles on the membrane surface more effectively (b) elevating the pretreatment time and temperature of the cellulose with hot ionic liquid to decrease the amount of particular residuals.
The ultrafiltrated hydrolysate was refiltered using a nanofiltration membrane. The employed membrane was a Desal DL, obtained from GE Osmonics. The active layer of the membrane, consisting of polyamide, was successfully tested on its solvent resistance towards ionic liquid. The feed solution in the batch filtration cell was continuously mixed with a magnetic stirrer at 500 rpm to avoid concentration polarization. The filtration pressure was set to 30 bar which allowed for the best separation performance of glucose from cellobiose (tests were carried out at pressures between 10 bar and 30 bar). The glucose recovery increased continuously with the permeate yield. Hence, a batch filtration of the hydrolysate was run until a permeate yield of 90% was reached. Samples were taken at every 10% of collected permeate. The recovered permeate was collected and its final concentration measured after reaching 90% permeate yield.

5.2.4 Electrodialysis set-up

A batch electrodialysis set-up was used to process the ultra- and nanofiltrated hydrolysate (see Fig. 5.1). The stack consisted of 5 chambers which were separated by alternating cation exchange membranes (CEM) and anion exchange membranes (AEM). This stack configuration is called conventional electrodialysis (CED) and al-

lows for the removal of salt, in this case the ionic liquid, from a feed solution. The membrane area in each compartment was 49 cm^2.

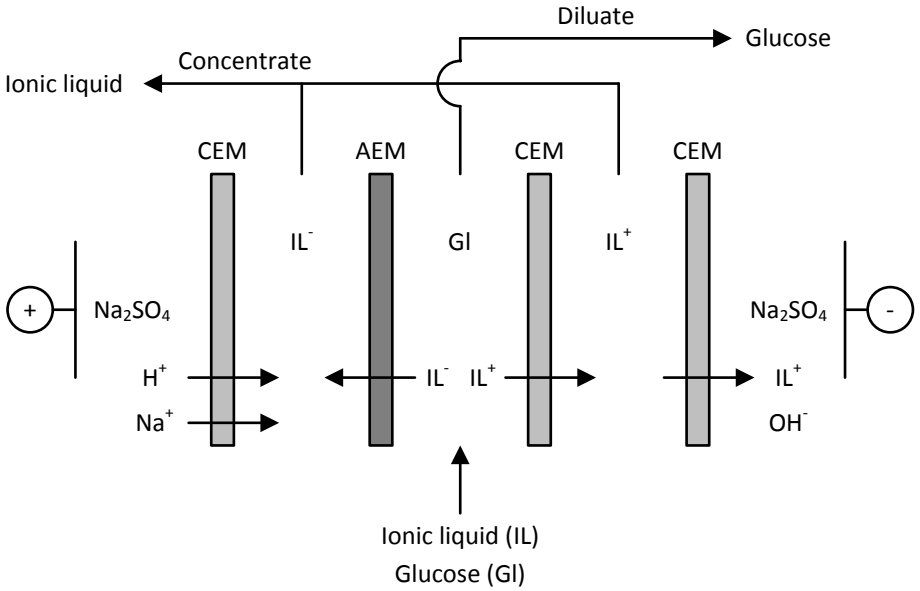

Figure 5.1: Scheme of the electrodialysis set-up. AEM - Anion Exchange Membrane. CEM - Cation Exchange Membrane.

The electrodialysis membranes were provided by Fumatech. As cation exchange membranes the Fumasep FKB membranes were chosen and as anion exchange membranes the Fumasep FAB membranes. Both types of membranes were made of polyether ether ketone as a basepolymer. During the experiments the temperature was controlled to 25°C by an external heat exchanger. The feed compartment in the middle of the stack was flushed with the hydrolysate stemming from the nanofiltration. Due to their electric charge the ionic liquid ions migrate from the diluate chamber into the neighboring chambers, where they concentrated.

The flow velocity was set to 100 ml sec^{-1} to prevent concentration polarization. The neighboring compartments were flushed with water containing about 10 g L^{-1} of ionic liquid to ensure a minimum conductivity in the whole stack at the start-up of the experiment. During operation these chambers were enriched with ionic liquid cations and anions stemming from the feed (diluate) chamber. The flow velocity was set to 100 mL sec^{-1} as well. The concentrate chamber outlets were connected to one tank to allow the separated ionic liquid cations and anions to recombine. The outer electrode compartments were rinsed with 0.1 M $NaSO_4$ solution. From these electrode compartments ions migrate across the ion exchange membranes to compensate ionic charge transported by the IL ions.

During operation the current was controlled to 1 A, resulting in a current density of 0.02 A cm^{-2}. The voltage was automatically adapted to the required current, depending on the electrical resistance of the stack. The voltage and current were recorded continuously. Samples from the feed tank and the concentrate tank were taken each hour.

5.2.5 Analytics

The saccharides glucose, cellobiose and the ionic liquid [MMIM][DMP] concentrations were determined by a Agilent 1100 HPLC-system equipped with a binary pump, degasser, autosampler, column thermostat, refractive index detector and Agilent Chemstation software. A 250 mm x 8 mm organic acid resin HPLC-column with a 40 x 8 mm guard column from Chromatographie Service, Langerwehe, Germany was used for separation. HPLC eluent was 5 mmol L^{-1} sulfuric acid with a flow rate of 0.8 mL min^{-1} at 50°C. Run time was 15 min. All components were detected with a refractive index detector. All samples were filtered through a 0.45 μm cellulose acetate membrane filter prior to analysis. Mixed sugar standards were used for quantification of glucose and cellobiose. Standard sample injection volume was 50 μL. The linear calibration range for all components was 0-200 mg L^{-1}. The correlation coefficients of the calibration curves were 0.9998 or better. Due to the high viscosity of the ionic liquid the samples had to be diluted up to a factor of 50.

5.3 Results and discussion

5.3.1 Ionic liquid pretreatment and enzymatic hydrolysis of cellulose

The pretreatment of cellulose with hot ionic liquid is suggested to decrease its crystallinity and increase its accessible surface area [12]. Thus, a higher conversion rate to fermentable sugars is expected. In Fig. 5.2 the results for the enzymatic hydrolysis of cellulose with and w/o ionic liquid pretreatment are shown.

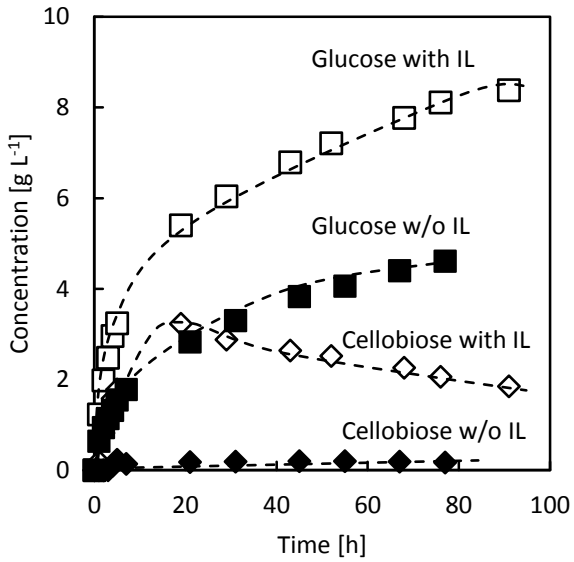

Figure 5.2: Comparison of the enzymatic hydrolysis of 10 g l^{-1} cellulose with and w/o ionic liquid pretreatment. The Celluclast® concentration was 0.5 g l^{-1}. The pH was set to 4.8 (0.1 M sodium acetate), the temperature to 45°C. Ionic liquid concentration during enzymatic hydrolysis was 100 g l^{-1} in both experiments.

Without ionic liquid pretreatment, the glucose concentration rose constantly to a value of about 5 g L^{-1}, whereas the cellobiose concentration remained below 1 g L^{-1} during the whole conversion process (see black dots in Figure 5.2). The maximum product yield of glucose was reached after about 70 h of hydrolysis. A conversion of about 45% was achieved. Reasons for the low conversion yield are supposed to be (a) product inhibition of β-glucosidase by glucose and (b) low accessibility of the cellulose for the enzymes due to the cellulose crystallinity. Product inhibition due to the formation of cellobiose should be negligible due to its low concentrations.

In a second run the cellulose was pretreated with the ionic liquid [MMIM][DMP] as described in section 5.2.2. The progress of glucose and cellobiose formation during hydrolysis is presented by white dots in Fig. 5.2. Due to the same amount of ionic liquid in the hydrolysis mixture the activity loss of enzymes is assumed to be equal. Hence, a similar reaction time was observed. A final glucose concentration of about 8 g L^{-1} was achieved after 80 hours. The higher final glucose concentration can be explained by a higher accessibility of cellulose chains after the ionic liquid pretreatment. The increasing cellobiose concentration in the first 20 hours of the experiment can be attributed to the amorphous structure of the pretreated cellulose which allowed the endo- and exoglucanases to hydrolyze more cellulose than in the first experiment. Summation of glucose concentration (8 g L^{-1}) and cellobiose concentration (2 g L^{-1}) shows that the cellulose conversion (initially 10 g L^{-1} of cellulose) was nearly complete (90%). The conversion of cellulose could even be increased to 99% by increasing the pretreatment temperature, pretreatment time or by switching to a more effective ionic liquid [1, 19]. Nevertheless, in a technical process the possibility of incomplete conversion has always to be taken into account. In following subsections downstream processing of the pretreated hydrolysate will be discussed.

5.3.2 Ultra- and nanofiltration of the hydrolysate

Before starting the ultra- and nanofiltration experiments the hydrolysate was cooled down to ambient temperature. It contained a significant amount of particular substances, namely cellulose residuals and enzymes. To recover these particulates and macromolecules ultrafiltration was performed. During the ultrafiltration experiment rejected particulates concentrated in time in the feed tank and and partly deposited onto the membrane surface. Hence, the permeate flux dropped from initially 38 L m^{-2} h^{-1} to 15 L m^{-2} h^{-1}. A permeate yield of 60% was achieved within 5 hours. The ultrafiltrated hydrolysate did not contain any particulates. HPLC measurements showed that the saccharide concentrations as well as the ionic liquid concentration were equal in permeate and retentate.

The ultrafiltrated hydrolysate was then processed with the Desal DL nanofiltration membrane to separate glucose from cellobiose. Hereby it is assumed that feeding

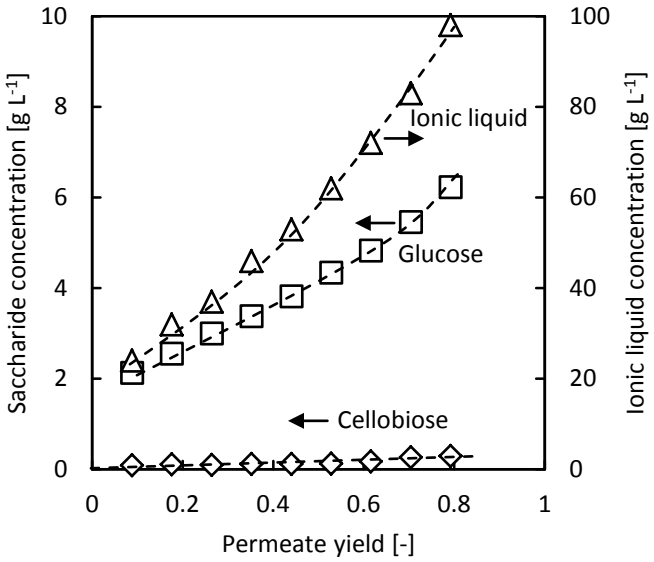

Figure 5.3: Development of glucose, cellobiose and ionic liquid concentrations in the collected permeate during nanofiltration. Membrane was the Desal DL from GE Osmonics. The filtration pressure was set to 30 bar. The temperature during filtration was 22°C.

of glucose as nutrient allows for the highest product yield in the subsequent fermentation. The impact of nutrient on a fermentation has to be investigated for each substance system individually. In this case the saccharide solution shall be fermented by the yeast ustilago maydis to itaconic acid. For this system it could be shown, that feeding xylose instead of glucose has a negative impact on the fermentation performance [2]. Nevertheless, the impact of residual cellobiose in the nutrient media on the fermentation has yet not been investigated.

Similar to the ultrafiltration experiment a strong permeate flux decline during filtration was observed. It dropped from initially 9 L m^{-2} h^{-1} to about 2 L m^{-2} h^{-1}. In contrast to the ultrafiltration experiment the flux reduction could not be explained by concentration polarization effects, but by increasing ionic liquid content in the feed solution. Therefore, flux reduction could be explained by the low permeability of the ionic liquid through the nanofiltration membrane and an increasing osmotic pressure for the ionic liquid / water mixture [20].

In Fig. 5.3 the permeate concentrations of glucose, cellobiose and ionic liquid depending on the permeate yield are shown. The initial rejection of glucose was about 70%, resulting in a permeate concentration of about 2 g L^{-1} glucose at a permeate yield of 10%. During the filtration process the rejection of glucose diminished. At a permeate yield of 90% the permeate concentration of glucose was found to be 6 g L^{-1}.

The initial permeate concentration of ionic liquid was about 30 g L^{-1}. During the filtration process the ionic liquid concentration in the permeate samples increased considerably to a value of about 100 g L^{-1} at a permeate yield of 80%. In contrast, the permeate concentration of cellobiose remained at a very low level of about 0.25 g L^{-1} during the whole filtration process. Due to the small amount of residual cellobiose in the final glucose product solution its impact on a fermentation is assumed to be negligible.

5.3.3 Electrodialysis of the filtrated hydrolysate

Electrodialysis was applied to separate ionic liquid from the ultra- and nanofiltrated hydrolysate containing about 6 g L^{-1} of glucose. The glucose as neutral molecule was assumed not to be affected by the electro-chemical driving force and to remain in the feed solution. Experimental results for the separation of ionic liquid from glucose are presented in Fig. 5.4 and support our hypothesis.

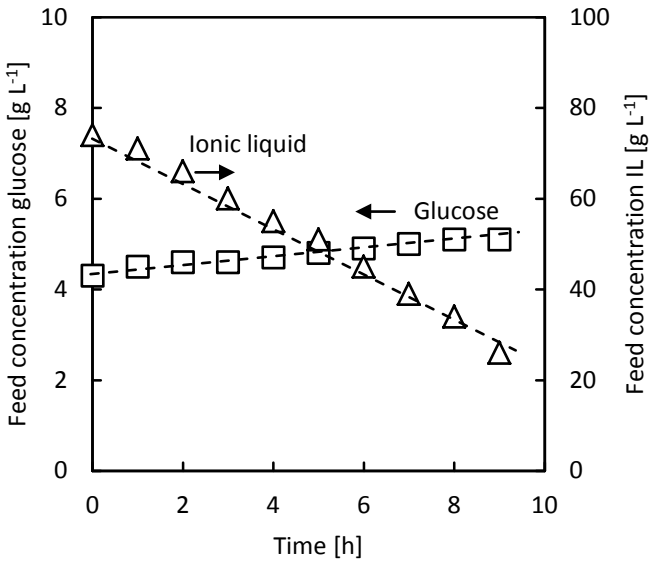

Figure 5.4: Development of glucose and ionic liquid concentrations in the nanofiltrated hydrolysate during electrodialysis. The electrodialysis was carried out at constant current of 1 A. The temperature was controlled to 25°C. Flow velocity was set to 100 mL sec^{-1}. Electrode compartments were rinsed with 0.1 M $NaSO_4$ solution.

The graph shows the development of glucose and ionic liquid concentrations in the feed (diluate) compartment. The concentration of ionic liquid decreased linearly over time. This result can be explained by the constant current density during the experiment. The concentration of ionic liquid decreased from 78 g L^{-1} to 26 g L^{-1}

within 9 hours. Considering a constant current of 1 A and a constant feed volume of 1 L the current efficiency was about 70%. The concentration of glucose increased slightly during operation, because the ionic liquid was depleted in the diluate and hence did not account to the mass balance of the diluate solution.
The cellobiose concentration remained constant as well at 0.24 g L^{-1} in the feed / diluate solution during electrodialysis. The concentrate solution of 1 L initially contained about 10 g L^{-1} of ionic liquid to reduce the electrical resistance of the electrodialysis stack. After 9 hours of operation the concentration of ionic liquid had risen to 22 g L^{-1}. Due to the stack configuration the positively charged ionic liquid ions could enrich in the right electrode compartment (see Fig. 5.2). Hence, the ionic liquid could not completely be recovered into the concentrate stream. In an industrial process a multi-compartment electrodialysis stack would allow for a ionic liquid recovery with negligible losses in the electrode compartments.

5.3.4 Process synthesis

The experimental results were used to set up a basic process scheme for the production of glucose from cellulose. The process is divided into an upstream and a downstream section. In upstream processing the cellulose is converted to glucose via ionic liquid assisted enzymatic hydrolysis. In downstream processing the diverse compounds of the reaction mixture are separated. Aim is to recover a highly purified glucose solution and to simultaneously recycle enzymes, ionic liquid and cellulose residuals to the upstream processing. The direct conversion of cellulose to glucose is about 73% as experimentally determined in section 5.3.1. It is assumed that the residuals (intermediates) from the cellulose degradation can be recycled to the reactor for a full conversion of cellulose to glucose.
In downstream processing ultrafiltration is implemented to recycle enzymes into the hydrolysis reactor. For this unit operation a permeate yield of 80% is supposed to be reached. This value is slightly higher than determined in experimental investigations (see section 5.3.2), where a value of 60% was found to be reasonable. Nevertheless, a modified set-up (a cross flow membrane module for instance) would allow for higher permeate yields. In the subsequent nanofiltration process cellobiose is separated from the glucose solution. If the residual cellobiose in the glucose solution

has no negative impact on the subsequent fermentation, this membrane separation can be left out.
Electrodialysis is applied to remove the ionic liquid from the nanofiltrated hydrolysate. The electrical resistance of the solution is the higher, the lower the ionic liquid concentration in the diluate stream is. Thus, a minimum ionic liquid concentration of 0.25 g L^{-1} in the final product solution is not undercut to limit the electric power consumption of the electrodialysis. This concentration corresponds to a recovery rate of ionic liquid of 99.75%. Prior a recycle to the hydrolysis tank the ionic liquid has to be dried. The tolerable water content of the ionic liquid [MMIM][DMP] is assumed to not excess 1 wt.% in order to completely restore the ionic liquids dissolution strength regarding cellulose [21]. In the current process design water is stripped from the spent ionic liquid with dry air. Model calculations based on experimental results showed that a mass ratio of air to water of 135:1 had to be adjusted to fully dehydrate ionic liquid. All values concerning temperature, filtration pressure, electric current, mass balance or substance concentration were adopted from the experimental results presented in the previous sections, unless explicity stated to differ.

5.3.5 Assumptions for cost estimation

For the economic analysis the process is assumed to run for 10 years. The production of glucose is adapted to the nutrient consumption of an average itaconic acid plant with a capacity of about 5,000 tons per year. Assuming a conversion of glucose to itaconic acid of 50%, 100,000 tons of glucose have to be produced within 10 years. The average lifetime of the enzymes without loss of activity is supposed to be up to 100 hours. Thus, 1,000 tons of enzymes have to be provided within 10 years of production.
The price of cellulose is supposed to be 0.40 € per kg, while the standard selling price of glucose for fermentation purposes is assumed to be 0.53 € per kg [22, 23]. The price of ionic liquid is assumed to be 10 € per kg [24]. The recovery rate of ionic liquid is supposed to reach 99.75%. Hence, about 2,500 tons of ionic liquid have to be replaced within 10 years of plant operation. The investment costs for the membrane separation units include the membranes itself as well as cleaning,

maintenance and labor. The costs for housing and piping are included by adding 50% to the total investment costs. The investment costs for the pretreatment and hydrolysis reactors are calculated with the concept of Guthrie [25]. This method allows for an accuracy of cost estimation of 50%.

5.3.6 Cost estimation

In Table 5.1 the break-down of the production costs for glucose via ionic liquid pretreated cellulose hydrolysis is shown.

Table 5.1: Results for the total cost estimation of glucose production via ionic liquid assisted enzymatic hydrolysis of cellulose. Purification of the hydrolysate is performed with membrane techniques ultrafiltration, nanofiltration and electrodialysis.

Position	Investment costs [Mio. €]	Operating cost over 10 years [Mio. €]	Benefit over 10 years [Mio. €]
Glucose solution	-	-	302
Cellulose	-	-	-40
Ionic liquid	-	-	-25
Enzymes	-	-	-2
Water	-	-	-40
Pretreatment	-0.3	-1.6	-1.9
Enzyme reaction	-12.8	-6.9	-19.7
Ultrafiltration	-0.5	-0.4	-0.9
Nanofiltration	-1.6	-2.0	-3.6
Electrodialysis	-0.7	-1.0	-1.7
Stripping	-25.5	-34.5	-60.0
Total costs / benefit	-41.4	-46.4	107

The most expensive positions in the process are the drying and replacement of ionic liquid which account for 33% of the total costs. To calculate the minimum selling price for such produced glucose, the return of investment (ROI) before taxes is set to 30%. The ROI is defined as:

$$ROI = \frac{Net\ annual\ earnings}{Fixed\ capital\ +\ Working\ capital}$$

The working capital is set to 19.4% of the fixed capital which are the investment costs

[25]. In average, annual earnings of 14.9 Mio. € have to be achieved. The raw material costs including ionic liquid and enzyme replacement sum up to 10.7 Mio. € per year. Considering the plant operating costs of annual 4.6 Mio. € per year a profit of 30.2 Mio. € has to be earned annually (without taxes). Thus, the selling price of the glucose product solution has to be at least 2.75 € / kg. This is about 5 times higher than the current price for commercial glucose. To decrease the price of glucose the ionic liquid should be replaced by a cheaper solvent or protein with similar functionality [26]. Another possibility is to mix the ionic liquid with (cost-effective) co-solvents such as dimethylsulfoxide (DMSO) which do not affect its ability to decrystallize cellulose [19]. Furthermore, the input material should be changed from cellulose to cheaper wood to yield additional fractions, namely hemicellulose and lignin. These substances are supposed to be not chemically modified by the ionic liquid pretreatment which allows for the production of value-added products [27]. On the other hand, the production of glucose from wood would comprise a more sophisticated processing including the decomposition of the wooden material and separation of the cellulose fraction prior to a conversion to glucose.

5.3.7 Sensitivity analysis

A sensitivity analysis was performed to identify the most important process parameters which have to be adjusted to allow for a more economic process. The results of the analysis are shown in Fig. 5.5.

The most crucial process parameters are the price and recovery rate of the ionic liquid. A change of the recovery rate of +/- 0.15% already results in large differences of pronounced incomes. This result shows that the economy of the process relies on an optimal recovery strategy for the ionic liquid. In addition, the energy consumption for the ionic liquid dehydration has a strong influence on the process economics. One option to reduce production costs significantly is to increase the concentration of processed cellulose during hydrolysis. Increasing the cellulose concentration results in (1) a decreased water demand and (2) a lower energy consumption during dehydration of recycled ionic liquid. Hence, the employed ionic liquid has to provide a higher dissolution power regarding cellulose and a better compatibility for hydrolyzing enzymes.

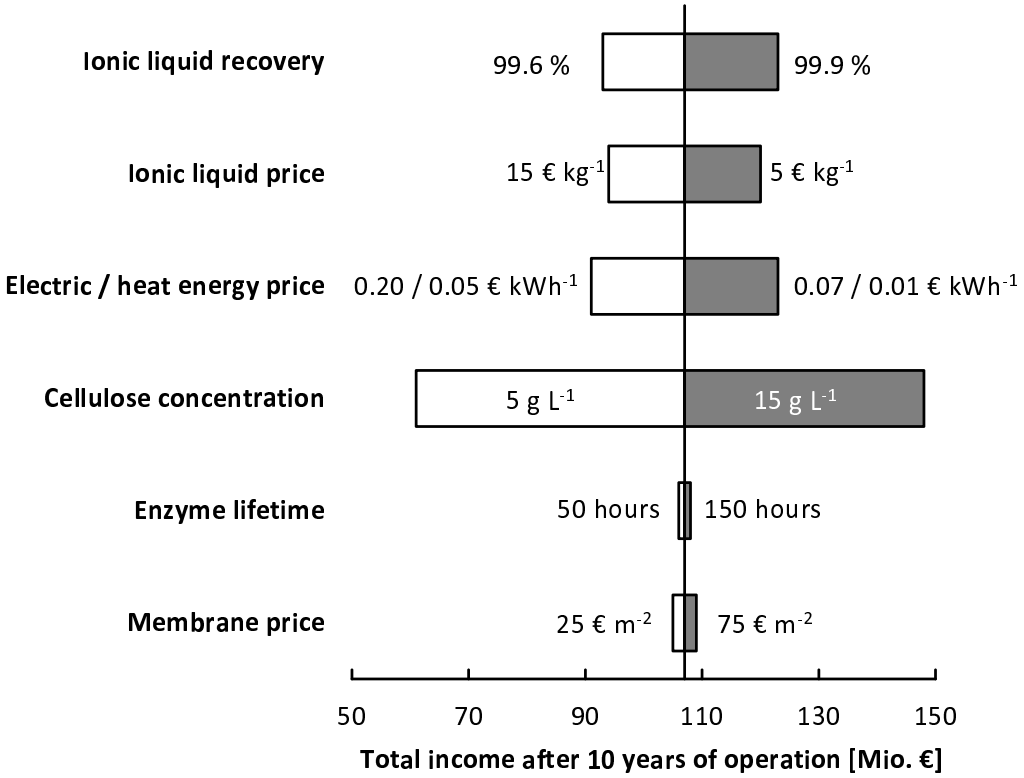

Figure 5.5: Results of the sensitivity analysis for the production of glucose via ionic liquid assisted enzymatic hydrolysis of cellulose. Purification of the hydrolysate is performed with membrane techniques ultrafiltration, nanofiltration and electrodialysis.

In contrast, the price of employed enzymes or membranes has a low impact on the process economics, because both are low price products.

5.4 Conclusions

In this work a process for cellulose conversion to glucose via ionic liquid assisted enzymatic hydrolysis is developed. The hydrolysate is purified with membrane techniques ultrafiltration, nanofiltration and electrodialysis.
Based on experimental results proving the feasibility of the process, a cost estimation is carried out. In the base case the produced glucose solution has to be sold at a price of 2.75 € per kg. Cost driver of the process is the ionic liquid which accounts for 33% of the total costs. Increasing the cellulose concentration during hydrolysis would significantly reduce the costs.

5.5 References

[1] R. Rinaldi, P. Engel, J. B□chs, A. C. Spiess and F. Schuth; *An Integrated Catalytic Approach to Fermentable Sugars from Cellulose*; ChemSusChem **3** (10) (2010) 1151--1153

[2] T. Klement, S. Milker, G. Jaeger, P. M. Grande, P. D. de Maria and J. Buechs; *Biomass pretreatment affects Ustilago maydis in producing itaconic acid*; Microbial Cell Factories **11** (43) (2012) 1--13

[3] C. Abels, F. Carstensen and M. Wessling; *Membrane processes in biorefinery applications*; Journal of Membrane Science **444** (2013) 285--317

[4] H. Joergensen, J. B. Kristensen and C. Felby; *Enzymatic conversion of lignocellulose into fermentable sugars: challenges and opportunities*; Biofuels, Bioprod. Bioref. **1** (2) (2007) 119--134

[5] R. M. F. Bezerra and A. A. Dias; *Enzymatic kinetic of cellulose hydrolysis - Inhibition by ethanol and cellobiose*; Applied Biochemistry and Biotechnology **126** (1) (2005) 49--59

[6] P. Andric, A. S. Meyer, P. A. Jensen and K. Dam-Johansen; *Reactor design for minimizing product inhibition during enzymatic lignocellulose hydrolysis: I. Significance and mechanism of cellobiose and glucose inhibition on cellulolytic enzymes*; Biotechnology Advances **28** (3) (2010) 308--324

[7] T. vom Stein, P. M. Grande, H. Kayser, F. Sibilla, W. Leitner and P. Dominguez de Maria; *From biomass to feedstock: one-step fractionation of lignocellulose components by the selective organic acid-catalyzed depolymerization of hemicellulose in a biphasic system*; Green Chemistry **13** (7) (2011) 1772--1777

[8] H. L. Chum, D. K. Johnson, S. Black, J. Baker, K. Grohmann, K. V. Sarkanen, K. Wallace and H. A. Schroeder; *Organosolv Pretreatment for Enzymatic-Hydrolysis of Poplars .1. Enzyme Hydrolysis of Cellulosic Residues*; Biotechnology and Bioengineering **31** (7) (1988) 643--649

[9] D. A. Fort, R. C. Remsing, R. P. Swatloski, P. Moyna, G. Moyna and R. D. Rogers; *Can ionic liquids dissolve wood? Processing and analysis of lignocellulosic materials with 1-n-butyl-3-methylimidazolium chloride*; Green Chemistry **9** (1) (2007) 63--69

[10] A. Brandt, J. Grasvik, J. P. Hallett and T. Welton; *Deconstruction of lignocellulosic biomass with ionic liquids*; Green Chemistry **15** (2013) 550--583

[11] R. P. Swatloski, S. K. Spear, J. D. Holbrey and R. D. Rogers; *Dissolution of Cellose with Ionic Liquids*; Journal of the American Chemical Society **124** (18) (2002) 4974--4975

[12] P. Engel, R. Mladenov, H. Wulfhorst, G. Jaeger and A. C. Spiess; *Point by point analysis: how ionic liquid affects the enzymatic hydrolysis of native and modified cellulose*; Green Chemistry **12** (11) (2010) 1959--1966

[13] B. D. Rabideau, A. Agarwal and A. E. Ismail; *Observed Mechanism for the Breakup of Small Bundles of Cellulose Iα and Iβ in Ionic Liquids from Molecular Dynamics Simulations*; J. Phys. Chem. B **117** (13) (2013) 3469--3479

[14] K. Belafi-Bako, A. Koutinas, N. Nemestothy, L. Gubicza and C. Webb; *Continuous enzymatic cellulose hydrolysis in a tubular membrane bioreactor*; Enzyme and Microbial Technology **38** (1-2) (2006) 155--161

[15] P. Andric, A. S. Meyer, P. A. Jensen and K. Dam-Johansen; *Reactor design for minimizing product inhibition during enzymatic lignocellulose hydrolysis II. Quantification of inhibition and suitability of membrane reactors*; Biotechnology Advances **28** (3) (2010) 407--425

[16] N. L. Mai, N. T. Nguyen, J. I. Kim, H. M. Park, S. K. Lee and Y. M. Koo; *Recovery of ionic liquid and sugars from hydrolyzed biomass using ion exclusion simulated moving bed chromatography*; Journal of Chromatography A **1227** (2012) 67--72

[17] D. X. Feng, L. Z. Li, F. Yang, W. Q. Tan, G. M. Zhao, H. B. Zou, M. Xian and Y. W. Zhang; *Separation of ionic liquid [Mmim][DMP] and glucose from enzymatic hydrolysis mixture of cellulose using alumina column chromatography*; Applied Microbiology and Biotechnology **91** (2) (2011) 399--405

[18] K. Shill, S. Padmanabhan, Q. Xin, J. M. Prausnitz, D. S. Clark and H. W. Blanch; *Ionic Liquid Pretreatment of Cellulosic Biomass: Enzymatic Hydrolysis and Ionic Liquid Recycle*; Biotechnology and Bioengineering **108** (3) (2011) 511--520

[19] L. Wu, S.-H. Lee and T. Endo; *Effect of dimethyl sulfoxide on ionic liquid 1-ethyl-3-methylimidazolium acetate pretreatment of eucalyptus wood for enzymatic hydrolysis*; Bioresource Technology **140** (2013) 90--96

[20] C. Abels, C. Redepenning, A. Moll, T. Melin and M. Wessling; *Simple purification of ionic liquid solvents by nanofiltration in biorefining of lignocellulosic substrates*; Journal of Membrane Science **405-406** (2012) 1--10

[21] M. Zavrel, D. Bross, M. Funke, J. Buchs and A. C. Spiess; *High-throughput screening for ionic liquids dissolving (ligno-)cellulose*; Bioresource Technology **100** (9) (2009) 2580--2587

[22] E. R. P. Keijsers, G. Yilmaz and J. E. G. van Dam; *The cellulose resource matrix*; Carbohydrate Polymers **93** (1) (2012) 9--21

[23] A. A. Koutinas, R. Wang and C. Webb; *Evaluation of wheat as generic feedstock for chemical production*; Industrial Crops and Products **20** (1) (2004) 75--88

[24] S. M. Sen, J. B. Binder, R. T. Raines and C. T. Maravelias; *Conversion of biomass to sugars via ionic liquid hydrolysis: process synthesis and economic evaluation*; Biofuels Bioproducts & Biorefining-Biofpr **6** (4) (2012) 444--452

[25] J. M. J. M. Douglas; *Conceptual design of chemical processes / James M. Douglas* (1988); McGraw-Hill

[26] K. Gourlay, J. Hu, V. Arantes, M. Andberg, M. Saloheimo, M. Penttilae and J. Saddler; *Swollenin aids in the amorphogenesis step during the enzymatic hydrolysis of pretreated biomass*; Bioresource Technology **142** (2013) 498 -- 503

[27] T.-Q. Yuan, T.-T. You, W. Wang, F. Xu and R.-C. Sun; *Synergistic benefits of ionic liquid and alkaline pretreatments of poplar wood. Part 2: Characterization of lignin and hemicelluloses*; Bioresource Technology **136** (2013) 345 -- 350

5.6 Appendix

5.6.1 Cost estimation results

Table 5.2: Assumptions for raw material and energy costs.

Raw material / Energy source	Value	Unit
Cellulose price	0.40	€ kg^{-1}
Glucose price	0.53	€ kg^{-1}
Ionic liquid price	10.00	€ kg^{-1}
Water price	0.004	€ kg^{-1}
Itaconic acid price	2.0	€ kg^{-1}
Electric energy price	0.13	€ kWh^{-1}
Heat energy price	0.03	€ kWh^{-1}
Enzyme price	2.0	€ kg^{-1}
Enzyme concentration	0.5	g L^{-1}
Enzyme lifetime	100	hour
Membrane price	50	€ kg^{-1}
Operating time	10	years
Cleaning costs	50	€ m^{-2}
Maintenance costs	5% of invest.	-
Installation	1.5 x invest.	-
Itaconic acid production	5000	tons $year^{-1}$
Operating time	8000	hours $year^{-1}$
Itaconic acid concentration	45	g L^{-1}
Glucose concentration	100	g L^{-1}
Cellulose conversion	95	%
Cellulose solubility in IL	10	wt.%
IL concentration in final product	0.25	g L^{-1}

Table 5.3: Raw material cost balance

Raw materials	Price [€ kg^{-1}]	Consumption within 10 years [t]	Costs [Mio. €]
Cellulose	0.40	100,000	-40
Ionic liquid	10.00	2,500	-25
Enzymes	2.00	1,000	-2
Water	0.004	10,000,000	-40
Glucose	2.75	110,000	303
Benefit			196

Table 5.4: Costs for pretreatment of cellulose with ionic liquid.

Type of costs	Parameter	Value	Unit
Investment	Cellulose feed	1.25	tons h^{-1}
	Reaction time	1.0	hours
	Ionic liquid content	12.50	tons
	Ionic liquid price	10.00	€ kg^{-1}
	Ionic liquid costs at startup	0.13	Mio. €
	Reactor volume	22.0	m^3
	Length	7.65	m
	Diameter	1.91	m
	Base length	1.20	m
	Base diameter	1.0	m
	Exponential factor α	0.81	-
	Exponential factor β	1.05	-
	Base costs vessel	1000	$
	Costs of base case	8863	$
	Material and pressure factor	1	-
	Module factor	4.23	-
	Update factor	5	-
	Reactor costs	0.14	Mio. €
	Total investment	0.27	Mio. €
Operating	Heat capacity ionic liquid	2.0	kJ kg^{-1} K^{-1}
[10 years]	Heat capacity cellulose	2.0	kJ kg^{-1} K^{-1}
	Temperature difference	80	K
	Amount of ionic liquid	$1.12 \cdot 10^9$	kg
	Energy demand of ionic liquid	$1.79 \cdot 10^{11}$	kJ
	Amount cellulose	$1.00 \cdot 10^8$	kg
	Energy demand cellulose	$1.60 \cdot 10^8$	kJ
	Heat energy costs	$8.33 \cdot 10^{-6}$	€ kJ^{-1}
	Total operating costs	1.6	Mio. €
	Total costs	1.9	Mio. €

Table 5.5: Costs for enzymatic hydrolysis of cellulose in aqueous solution.

Type of costs	Parameter	Value	Unit
Investment	Cellulose feed	1.25	tons h^{-1}
	Reaction time	10	hours
	Ionic liquid content	125	tons
	Water content	1125	tons
	Water price	0.004	€ kg^{-1}
	Water costs at startup	4500	€
	Reactor volume	2500	m^3
	Number of reactors	30	-
	Single reactor volume	83	m^3
	Length	11.9	m
	Diameter	3.0	m
	Base length	1.20	m
	Base diameter	1.0	m
	Exponential factor α	0.81	-
	Exponential factor β	1.05	-
	Base costs vessel	1000	$
	Costs of base case	20240	$
	Material and pressure factor	1	-
	Module factor	4.23	-
	Update factor	5	-
	Reactor costs	12.84	Mio. €
Operating	Heat capacity water	4.19	kJ kg^{-1} K^{-1}
[10 years]	Temperature difference	20	K
	Amount of water	$9.90 \cdot 10^9$	kg
	Energy demand of water	$8.30 \cdot 10^{11}$	kJ
	Heat energy costs	$8.33 \cdot 10^{-6}$	€ kJ^{-1}
	Total operating costs	6.9	Mio. €
	Total costs	19.80	Mio. €

Table 5.6: Costs for ultrafiltration plant set-up and operating.

Type of costs	Parameter	Value	Unit
Investment	Membrane permeability	20.0	kg m^{-2} h^{-1} bar^{-1}
	Permeate flow	140,000	kg h^{-1}
	Applied pressure	1.12	bar
	Membrane area	6,300	m^2
	Factor for installations	1.50	-
	Membrane plant	0.47	Mio. €
Operating	Feed flow	175,000	kg h^{-1}
[10 years]	Feed volume flow	0.049	m^3 sec^{-1}
	Operation time	80.000	h in 10 years
	Applied pressure	1.12	bar
	Pump efficiency	0.7	-
	Electric energy	8.37	Mio. €
	Electric energy consumption	$6.70 \cdot 10^5$	kWh
	Energy costs	0.09	Mio. €
	Membrane cleaning costs	0.31	Mio. €
	Maintenance & labor costs	0.02	Mio. €
	Total operating costs	0.42	Mio. €
	Total costs	0.9	Mio. €

Table 5.7: Costs for nanofiltration plant set-up and operating.

Type of costs	Parameter	Value	Unit
Investment	Membrane permeability	0.2	kg m^{-2} h^{-1} bar^{-1}
	Permeate flow	126,000	kg h^{-1}
	Applied pressure	30	bar
	Membrane area	21,000	m^2
	Factor for installations	1.50	-
	Membrane plant	1.58	Mio. €
Operating	Feed flow	140,000	kg h^{-1}
[10 years]	Feed volume flow	0.04	m^3 sec^{-1}
	Operation time	80.000	h in 10 years
	Applied pressure	30	bar
	Pump efficiency	0.7	-
	Electric energy	179.5	kW
	Electric energy consumption	$1.44 \cdot 10^7$	kWh
	Energy costs	2.01	Mio. €
	Total operating costs	2.01	Mio. €
	Total costs	3.59	Mio. €

Table 5.8: Costs for electrodialysis plant set-up and operating.

Type of costs	Parameter	Value	Unit
Investment	Feed flow	12,500	kg h^{-1}
	Operation time	80,000	h in 10 years
	Transferred IL	$5.68 \cdot 10^4$	mole h^{-1}
	Current density	200	A m^{-2}
	Current efficiency	0.8	-
	Membrane area	$9.93 \cdot 10^3$	m^2
	Factor for installations	1.50	-
	Investment costs	0.74	Mio. €
Operating	Diluate conductivity IL	0.05	mS cm^{-1}
[10 years]	Channel width	0.05	cm
	Membrane resistance	4	Ohm cm^{-2}
	Membrane thickness	$1 \cdot 10^{-2}$	cm
	Effective membrane area	0.4	m^2
	Cell pair resistance	0.252	Ohm
	Number of cell pairs in stack	1000	-
	Membrane area per stack	400	m^2
	Number of stacks	25	-
	Serial stacks	1	-
	Parallel stacks	25	-
	Channel height	1	m
	Crossflow velocity	0.70	m sec^{-1}
	Applied current	80	A
	Stack resistance	6.23	Ohm
	Electric energy	39.87	kW
	Energy consumption in 10 years	$3.19 \cdot 10^6$	kWh
	Energy costs	0.41	Mio. €
	Membrane cleaning costs	0.49	Mio. €
	Maintenance and labor costs	0.04	Mio. €
	Total operating costs	0.95	Mio. €
	Total costs	1.7	Mio. €

Table 5.9: Costs for stripping columns set-up and operating.

Type of costs	Parameter	Value	Unit
Investment	Number of columns	4	-
	Diameter of a column	15	m
	Height of a column	60	m
	Vapor velocity	0.89	m sec^{-1}
	F-Factor	0.97	m sec^{-1} (kg m^{-3})$^{1/2}$
	Pressure loss	0.04	bar
	Base length	1.20	m
	Base diameter	1.00	m
	Exponential factor α	0.81	-
	Exponential factor β	1.05	-
	Costs of base case	1000	$
	Material and pressure factor	1	-
	Module factor	4.06	-
	Update factor	5	-
	Investment costs	25.5	Mio. €
Operating	Feed flow water	20,000	kg h^{-1}
[10 years]	Feed flow ionic liquid	14,000	kg h^{-1}
	Ratio air / water	134	kg/kg
	Feed flow air	2,680,000	kg/h
	Inlet pressure	1.04	bar
	Outlet pressure	1.00	bar
	Temperature	20	◦C
	Specific gas constant air	287	J kg^{-1} K^{-1}
	Outlet density air	1.19	-
	Volume flow air	2,253,639	m^3 h^{-1}
	Pump efficiency	0.8	-
	Electric energy	3320.4	kW
	Energy consumption in 10 years	$2.66 \cdot 10^8$	kWh
	Total operating costs	34.53	Mio. €
	Total costs	60.04	Mio. €

CHAPTER 6

Discussion & Outlook

6.1 Processing of lignocellulosic biomass with ionic liquids - challenges & opportunities

Within this thesis the potential of membrane separation techniques in the field of ionic liquid (IL) assisted processing of lignocellulosic biomass was explored. Initially nanofiltration was investigated for its separation performance regarding ionic liquid solutions containing macro- and low-molecular lignocellulosic compounds as well as water. Hence, diverse hydrophobic and hydrophilic nanofiltration membranes were tested on their separation performance regarding low-molecular saccharides in IL / water solutions [1]. At first the solvent flux of pure IL / water mixtures through the nanofiltration membranes was experimentaly determined. A very strong solvent flux decrease was found by adding the ionic liquid 1,3-dimethylimidazolium dimethylphosphate ([MMIM][DMP]) to aqueous solutions, especially in the range of 0 wt.% - 40 wt.%. Concurrently, the initial rejection of IL diminished while increasing the ionic liquid content in the feed solution. The Maxwell-Stefan model was applied to explain the experimental findings. The theoretical results - which were in good agreement with the experiments - showed that the IL was partially retained by all tested membranes. In result, high osmotic pressures emerged reducing the effective pressure and with it the permeate flux. As soon as the osmotic pressure in the feed solution caused by the IL separation reached the range of the applied pressures - up to 40 bar were applied - the separation performance decreased. Hence, solvent mixtures containing about 30 wt.% of IL or more were not separated by nanofiltration.

Then the purification of IL / water mixtures from low-molecular saccharides glucose and cellobiose was investigated. The separation of saccharides by the nanofiltration membranes was found to be strongly dependent on the IL content in the feed mixture. For hydrophilic membranes a decline in rejection performance was found with increasing ionic liquid content. In contrast, hydrophobic membranes allowed for a better separation of saccharides with increasing ionic liquid content in the feed solution. The Maxwell-Stefan model was applied to explain these results. It could be concluded that the presence of ionic liquid in the solvent mixture decreased both the solvent flux - in this case the IL / water mixture - and the solute flux. Depending on the ratio of flux decreases the saccharides were either better or less rejected by

the membrane.

Nevertheless, the employed nanofiltration membranes were not able to purify IL / water mixtures from all lignocellulosic residuals effectively. Therefore, the separation of glucose - which is a target compound in the entire project - from other lignocellulosic compounds in IL / water solutions was investigated. In a series of nanofiltration batch experiments the separation of glucose from cellobiose in IL / water mixtures was performed. The influence of operating pressure and initial saccharide feed concentration was determined. It was found that the separation performance increased with increasing pressures. On the other hand the recovery of glucose diminished by increasing the pressure. The saccharide feed concentration did not noticably affect the separation performance in the range of 1 g L^{-1} to 10 g L^{-1}.

In result, glucose could be separated from other low-molecular lignocellulosic compounds cellobiose or cellotriose - in the experiments raffinose was used as substrate - via nanofiltration. A separation of glucose from IL in aqueous solution could not be performed via nanofiltration due to the very similar sizes of the molecules. Therefore, electrodialysis was chosen to separate these molecules not via size exclusion but by charge exclusion. Experimental results showed that the IL, which is a salt, could be simply removed from an aqueous stream via conventional electrodialysis utilizing cation- and anion- exchange membranes. The glucose as neutral molecule remained in the feed solution.

On base of these experimental results a process was designed allowing for the production of glucose from cellulose. It was assumed that the cellulose was pretreated with ionic liquid, which is the case after a wood dissolution process with subsequent precipitation of cellulose with water. An enzymatic hydrolysis of cellulose to glucose in presence of 100 g L^{-1} of ionic liquid was carried out. At this IL concentration the enzymatic activity was still sufficient [2]. The hydrolysate was purified using ultrafiltration, nanofiltration and electrodialysis. Hence, all residuals stemming from the hydrolysis reaction as well as the IL solvent were consecutively removed from the hydrolysate. To complement the process design the dehydration of spent ionic liquid via vacuum distillation [3, 4] and stripping with nitrogen was experimentally investigated. The experimental results - which were in good agreement with thermodynamical calculations - showed that the vacuum distillation consumed much more energy than the water stripping with nitrogen - a substitute for dry air. Then the

process was economically evaluated to assess its crucial parameters. The economic analysis gave the result that especially the costs for ionic liquid application and purification determine the economics of the process. Calculation results showed that a recovery of IL of more than 99% had to be achieved to allow for an almost competitive production of glucose.

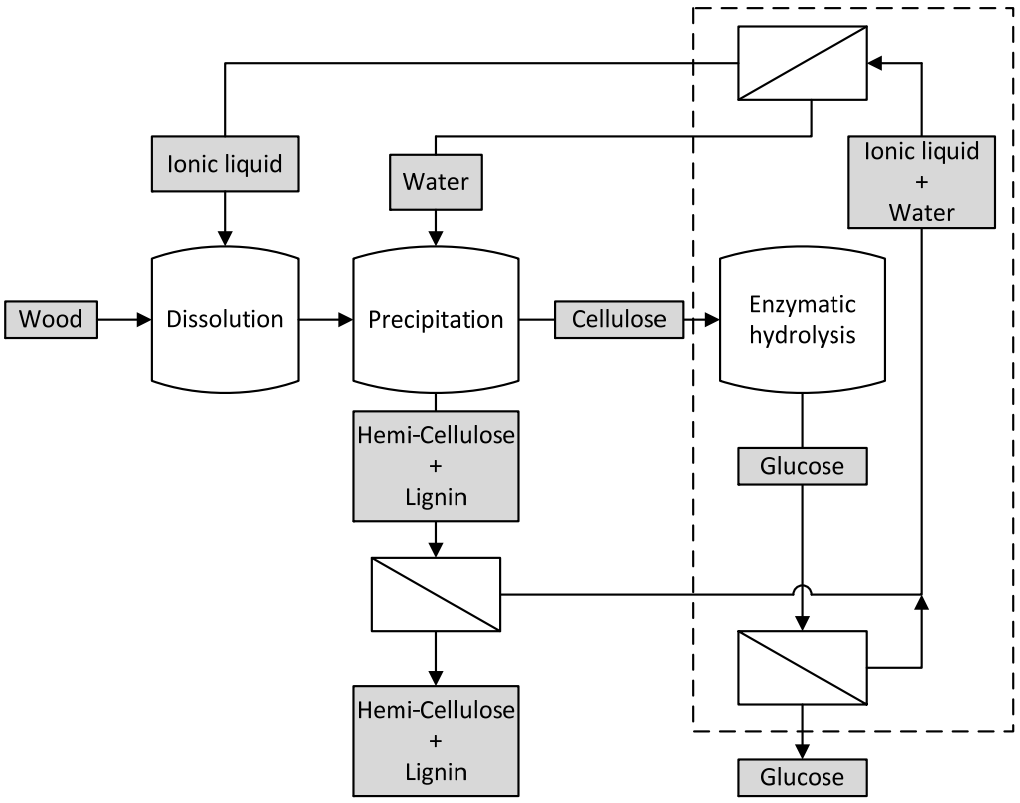

Figure 6.1: Process scheme for the dissolution and fractionation of wood via ionic liquid. Scheme adapted from [5]. Dashed line encloses the sub-process which was investigated within this thesis.

In Fig. 6.1 an entire process scheme for wood dissolution in ionic liquid with subsequent fractionation of its major constituents cellulose, hemi-cellulose and lignin is shown as proposed by Sun et al. [5]. The intermediate educt for this sub-process is IL pretreated and precipitated cellulose which is enzymatically converted to glucose. The glucose is than obtained in aqueous solution and can be fed to a fermentation broth producing itaconic acid for instance [6].

Within the first phase (2007-2012) the TMFB cluster focused on the utilization of cellulose, because it was an intermediate for the synthesis of the biofuel 2-MTHF. For economical and ecological reasons the cluster recently increased its research capacities regarding the utilization of the hemi-cellulose and lignin fraction. As shown in

Fig. 6.1, additional separations have to be performed to allow for a complete utilization of the wooden material. Most crucial point is the separation of hemi-cellulose and lignin from ionic liquid after the precipitation of cellulose. In contrast to cellulose these compounds remain mostly in dissolution [7]. Hence, a downstream process has to be set up which allows for (1) the recovery of hemi-cellulose and lignin from IL / water solutions with high ionic liquid contents and (2) the purification of spent IL from all residuals beside the target compounds, for instance phenols, salts and large amounts of water.

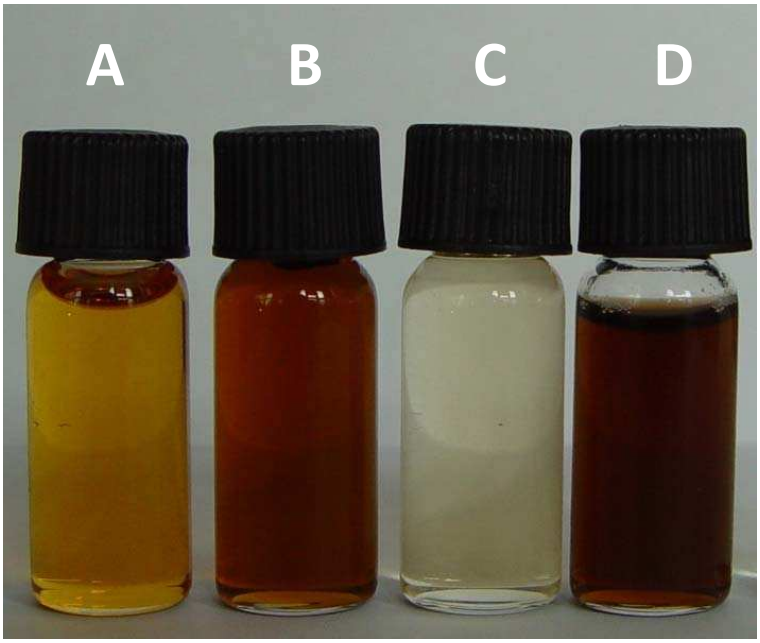

Figure 6.2: Samples of ionic liquid [EMIM][AC] prior biomass processing, after biomass processing and after filtration. Sample A: Fresh [EMIM][AC]; water content: 5 wt.%. Sample B: [EMIM][AC] after wood dissolution and precipitation; water content: 50 wt.%. Sample C: Permeate after filtration with Desal DK membrane at 30 bar; water content: 50 wt.%. Sample D: Retentate after filtration with Desal DK membrane 30 bar; water content: 50 wt.%.

Nanofiltration was tested on its performance regarding the purification of ionic liquid directly after the precipitation process (see Fig. 6.2). For the experiment milled beech wood powder was dissolved in hot ionic liquid ethyl-methyl-imidazolium acetate ([EMIM][AC]). After dissolution a solid fraction - preferably cellulose - was precipitated from the solution by adding the same amount of water. The spent ionic liquid (containing lignin and hemi-cellulose) was than nanofiltered with the Desal DK membrane at a feed pressure of 30 bar at ambient temperature. The results presented in Fig. 6.2 show that it was possible to purify the IL by nanofiltration. A

Karl-Fischer titration gave the result that the water content of the solution of 50 wt.% did not change during nanofiltration. Nevertheless, a thoroughly analysis of the permeate was not performed due to following problems which occurred during the experiment: (1) The permeate fluxes during nanofiltration were very low due to high osmotic pressures as described before [1], (2) the water content could not be reduced and - most striking - (3) the ionic liquid could not be recovered completely, because the impurities were just removed from the permeate but not from the retentate. Hence, nanofiltration as single unit operation did not enable for a complete recovery of spent ionic liquid. As the recovery of ionic liquid may not undercut a value of 99% to establish an economic process, alternative separation techniques or even combinations of several unit operations have to be applied to allow for a complete recovery of ionic liquid at this stage (nanofiltration + electrodialysis for instance).

6.2 Alternatives to ionic liquid pretreatment of lignocellulosic biomass

Within this thesis pretreatment of lignocellulosic biomass with ionic liquid was explored in terms of ionic liquid recovery and product discharge. The investigations revealed that especially the recovery of ionic liquid is crucial for process economics. Hereby it has to be considered that the performance of recovered ionic liquid has to be stable regarding its ability to dissolve wood. Nevertheless, several yet not specified impurities will enrich in the ionic liquid during repeated biomass dissolution and recycle. Depending on the starting material phenols or inorganic salts for instance may reduce the long-term performance of the ionic liquid. Hence, a purge stream for not re-usable ionic liquid has to be included in process design. In general, the drawbacks of ionic liquids in biomass processing are as follows:

- High costs of the ionic liquid. The ionic liquid itself is a high-value chemical product.
- High complexity of ionic liquid recovery and purification. The properties of ionic liquid such as high viscosity and strong hygroscopy make it difficult to purify the ionic liquid from biomass residuals and water.
- Low solubility of biomass in ionic liquid. In average just about 5 wt.% of lignocellulosic biomass can be dissolved in ionic liquid.

To evaluate the risks and chances for ionic liquid employment in biomass processing it has to be compared with alternative pretreatment processes which are in this case (1) the Organosolv process in which ethanol / water is used to dissolve biomass [8] and (2) an organic acid catalyzed process in which a biphasic system of oxalic acid / 2-MTHF (2-methyltetrahydrofuran) is used to dissolve and fractionate lignocellulosic biomass [9, 10]. A rough calculation of the process economics for these three variants is presented in Table 6.1. In the calculations only the raw material costs and product benefit were taken into account. The products were assumed to comprise glucose (obtained from the cellulose fraction), xylose (from the hemi-cellulose fraction) and lignin. These products were assumed to be sold at a price of in average 0.6 € per kg. The starting material was assumed to be wood which was considered

to cost 0.4 € per kg. The costs for the diverse solvents varied between 0.6 € per kg for ethanol and 10 € per kg for ionic liquid. The costs for process equipment and energy consumption were neglected.

Table 6.1: Comparison of minimal solvent recovery rates for establishing cost efficient wood pretreatment processes.

Pretreatment process	Pretreatment solvent	Ratio of wood/solvent [g/g]	Minimum solvent recovery [%]
Ionosolv [7]	Ionic liquid	25/1	99.89
Organosolv [8]	Ethanol/Water	4/1	91.04
Organic acid catalyzed [10]	Oxalic acid/ 2-MTHF	10/1	97.31

Table 6.1 shows that all pretreatment processes strongly depend on efficient solvent recovery. In none of these processes a solvent recovery of 90% may be undercut to allow for a cost-neutral production of glucose/xylose/lignin from wood. In general, two parameters can be changed to reduce the dependence on a very good recovery strategy: (1) reduction of the solvent price and (2) increase of the biomass solubility in the respective solvent. Here, ionic liquids may outperform the competitive solvents in future if their potential as designer solvent is capitalized by increasing the dissolution power regarding lignocellulosic biomass.

Within the TMFB cluster a route for lignocellulosic biomass pretreatment was developed utilizing a biphasic system comprising oxalic acid and 2-MTHF [9, 10]. A scheme of the process is shown in Fig. 6.3. The lignocellulosic raw material is separated within the biphasic reaction media as follows: the cellulose fraction remains mostly solid. A low conversion of cellulose to glucose which dissolves in the oxalic acid was observed. The hemi-cellulose fraction is mostly decomposed to xylose which remains in the oxalic acid as well. The lignin fraction is dissolved in the 2-MTHF solvent. In this process scheme the products - in this case cellulose, xylose and lignin - have to be separated from the reaction media, namely oxalic acid and 2-MTHF. Hydrophilic nanofiltration can be performed to separate the oxalic acid solvent from the products xylose and glucose. A simple process scheme of the unit operation is shown in Fig. 6.4. The oxalic acid which is a small molecule (90 g mol^{-1}) permeates through the nanofiltration membrane whereas the glucose and xylose with higher molecular weights (180 g mol^{-1}, respectively 150 g mol^{-1}) are preferably rejected by the membrane. The oxalic acid can than be recycled into the pretreatment reac-

tor, while the saccharides can be processed to a fermentation for instance.

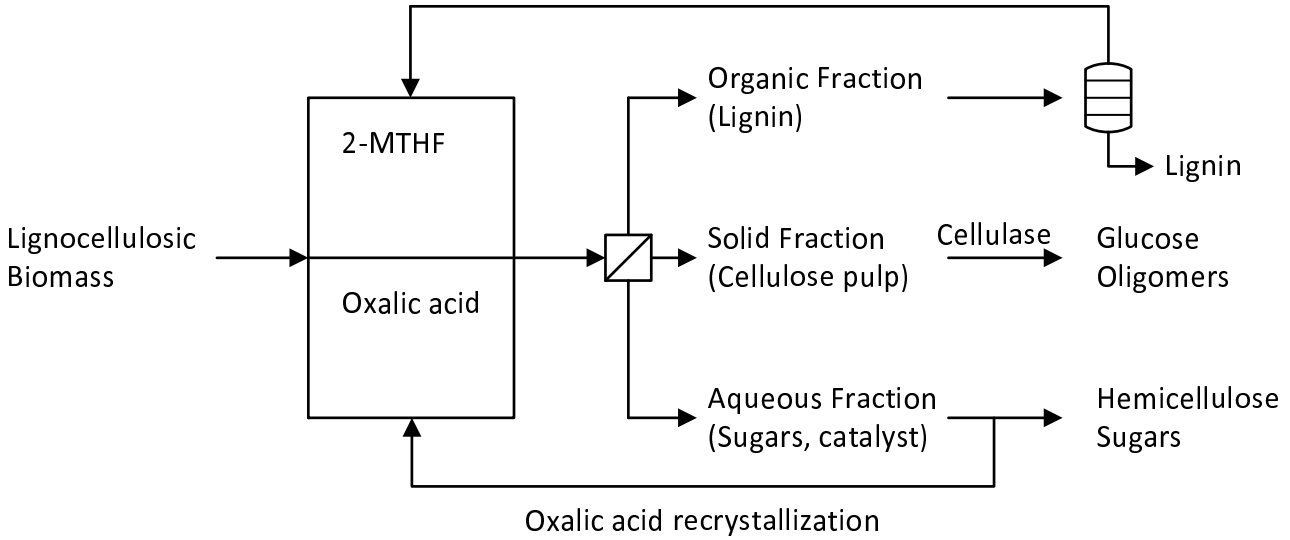

Figure 6.3: Process scheme for the fractionation of lignocellulosic biomass with a biphasic system consisting of oxalic acid and 2-MTHF. Scheme adapted from [10].

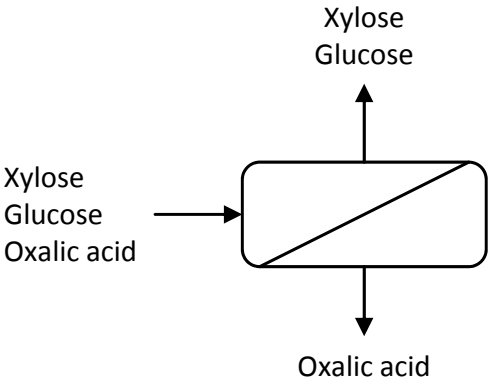

Figure 6.4: Scheme of the nanofiltration process to separate oxalic acid from the products glucose and xylose.

A first experiment regarding the separation of oxalic acid from glucose via nanofiltration was carried out in a batch filtration test cell. The tested membrane was the Desal DK, the pressure was set to 10 bar. The glucose and oxalic acid concentrations in the feed were set to 10 g L^{-1}, respectively 12 g L^{-1}. Results of this experiment are shown in Fig. 6.5 and Fig. 6.6. The current permeate concentrations of oxalic acid and glucose depending on the permeate yield are shown in Fig. 6.5.

The initial permeate concentration of oxalic acid was about 12 g L^{-1}. Hence, it was not separated by the membrane. Nevertheless, the marginal rejection of oxalic acid by the membrane resulted in concentration of oxalic acid in the batch filtration test cell. Therefore, the current permeate concentrations slightly increased with increasing permeate yield to values of up to 15 g L^{-1}. Finally, the acummulated permeate

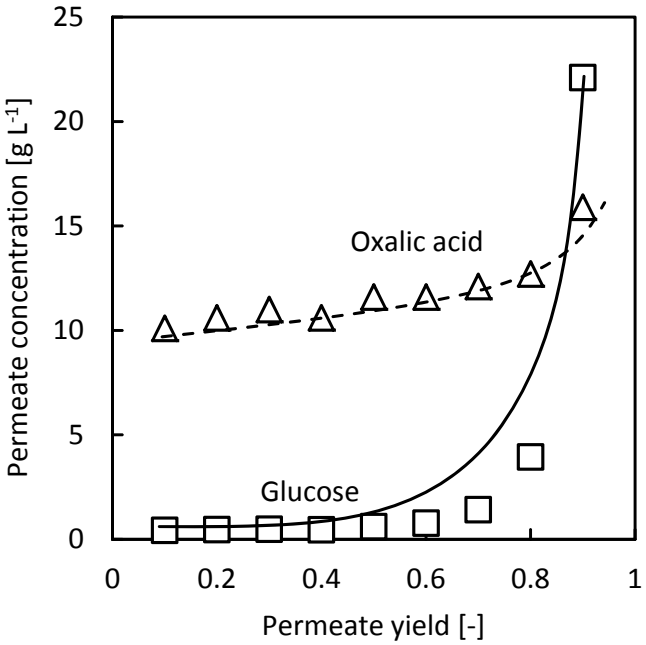

Figure 6.5: Current permeate concentration of oxalic acid and glucose depending on the permeate yield. The membrane was the Desal DK, the pressure was set to 10 bar. Experiments were carried out at ambient temperature. The initial feed concentration of oxalic acid and glucose was 12 g L^{-1}, respectively 10 g L^{-1}.

concentration of oxalic acid was 10.6 g L^{-1} at a permeate yield of 90%. In contrast, the glucose was nearly completely rejected by the membrane, especially at low permeate yields. At higher permeate yields the glucose feed solution was highly concentrated. Hence, it started to permeate through the membrane at a permeate yield of about 80%. In conclusion, it was demonstrated that oxalic acid can be effectively separated from glucose by hydrophilic nanofiltration. The permeate yield has to be limited to a certain value to ensure a complete rejection of the saccharide.

In Fig. 6.6 the corresponding evolution of the permeate flux is shown. It decreased continuously with increasing permeate yield and nearly diminished at a permeate yield of about 90%. It decreased due to increasing osmotic pressure of the feed solution, caused by the rejected glucose. Following the law of van't Hoff, each 10 g L^{-1} of glucose in the feed solution causes an osmotic pressure of about 1.4 bar. Hence, the osmotic pressure in the feed solution increased to about 10 bar at a permeate yield of about 90%. At this point the separation performance for glucose started to drop significantly, because the applied pressure did not longer overcome the chemical potential for mixture separation. It can be concluded that the permeate flux can be easily increased by increasing the filtration pressure. Increasing the filtration pressure will also result in a better separation performance of the membrane regarding

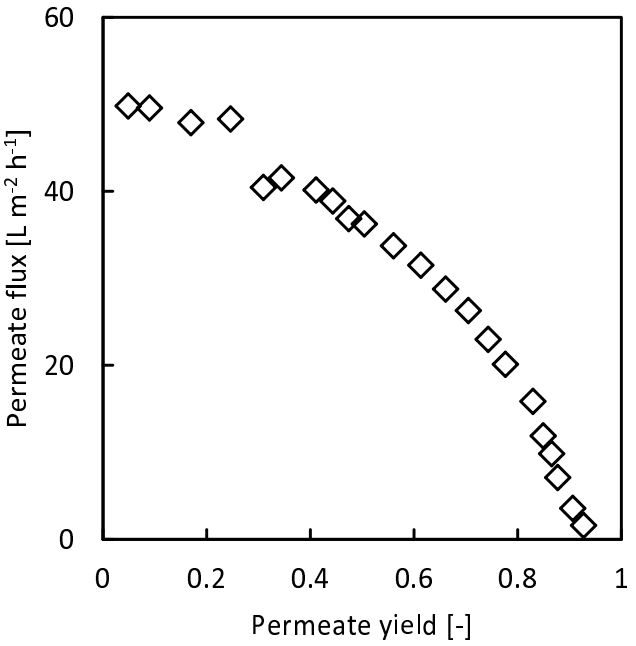

Figure 6.6: Total permeate flux depending on the permeate yield. The membrane was the Desal DK, the pressure was set to 10 bar. Experiments were carried out at ambient temperature. The initial feed concentration of oxalic acid and glucose were 12 g L^{-1}, respectively 10 g L^{-1}.

oxalic acid/glucose mixtures in aqueous solution.

Nanofiltration allows for the separation of a certain amount of oxalic acid from an oxalic acid/glucose mixture in aqueous solution. At the same time the glucose is concentrated in the feed solution. Nevertheless, a certain amount of oxalic acid remains in the retentate and causes problems in the downstream synthesis (chemical or bio-conversion). If the entire process depends on a complete recovery of oxalic acid (compare Table 6.1), the oxalic acid has to be removed utilizing an alternative unit operation. This thesis suggest earlier that electrodialysis is a viable technology to separate charged from uncharged species. A process scheme of this unit operation is presented in Fig. 6.7. Comparable to the electrodialysis of lactic acid [11] the oxalic acid is removed from the feed solution by applying an electric field while the neutral compound glucose (or xylose) remains in the retentate and causes problems. Hence, the oxalic acid can be completely removed from the product stream and fully recycled into the reaction tank.

Another option to efficiently separate oxalic acid from saccharides is to set up a nanofiltration cascade as shown in Fig. 6.8. In such a cascade an exchange solvent is added to the solution prior the last nanofiltration module (in this case pure water). The permeate of each nanofiltration module is handed over to the previous mod-

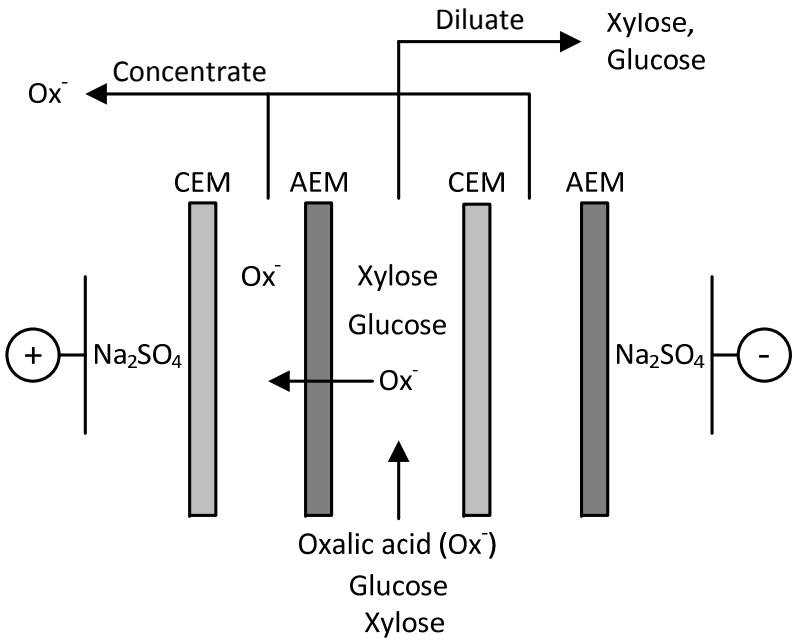

Figure 6.7: Scheme of conventional electrodialysis for separation of oxalic acid from glucose.

ule. Hence, the oxalic acid is recycled and concentrated successively until it can be removed from the permeate of the first stage.

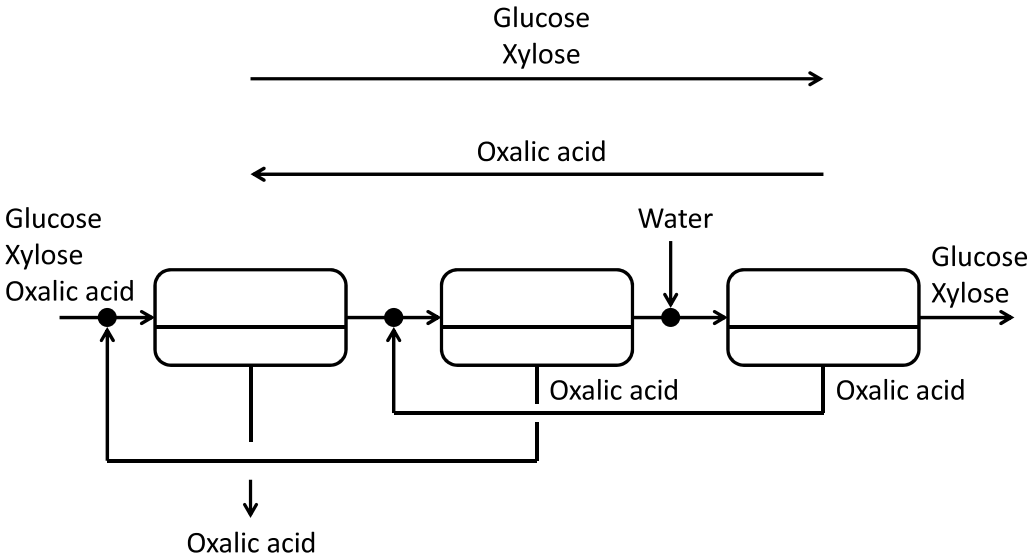

Figure 6.8: Scheme of a nanofiltration cascade for the recovery of oxalic acid from aqueous solution.

In Table 6.2 calculation results for diverse membrane cascades are presented. Following assumptions were made: Initial feed concentration of saccharides: 10 g L^{-1}. Initial feed concentration of oxalic acid: 10 g L^{-1}. Rejection of saccharides by the membrane R=85%. Rejection of oxalic acid by the membrane R=5%. Permeate yield was adapted to the ratio of exchange solvent water / feed stream to ensure a constant outlet stream.

Table 6.2: Results for the recovery of oxalic acid from aqueous solution depending on the number of cascade elements and the amount of exchange solvent.

Oxalic acid recovery [%] / Saccharides in outlet stream [g L^{-1}]	2-Stage	3-stage	4-stage	5-stage
Ratio of water / feed : 1:1	63 / 9.00	71 / 8.81	76 / 8.79	79 / 8.62
Ratio of water / feed : 2:1	83 / 8.70	91 / 8.59	95 / 8.46	97 / 8.51
Ratio of water / feed : 3:1	90 / 8.58	96 / 8.52	98 / 8.43	99 / 8.40

By increasing the number of elements in the cascade the recovery of oxalic acid can be considerably increased. An increase of exchange solvent amount also results in a better recovery of oxalic acid. Nevertheless, the valuable saccharides may also concentrate in the permeate if they are not completely rejected by the nanofiltration membrane. For the calculations a rejection of saccharides of 85% was assumed. As presented in Table 6.2 the final saccharide concentration decreases continuosly with increasing cascade elements and amounts of exchange solvent.

6.3 References

[1] C. Abels, C. Redepenning, A. Moll, T. Melin and M. Wessling; *Simple purification of ionic liquid solvents by nanofiltration in biorefining of lignocellulosic substrates*; Journal of Membrane Science **405** (2012) 1--10

[2] P. Engel, R. Mladenov, H. Wulfhorst, G. Jager and A. C. Spiess; *Point by point analysis: how ionic liquid affects the enzymatic hydrolysis of native and modified cellulose*; Green Chemistry **12** (11) (2010) 1959--1966

[3] M. J. Earle, J. M. S. S. Esperanca, M. A. Gilea, J. N. C. Lopes, L. P. N. Rebelo, J. W. Magee, K. R. Seddon and J. A. Widegren; *The distillation and volatility of ionic liquids*; Nature **439** (2006) 831--834

[4] A. W. Taylor, K. R. J. Lovelock, A. Deyko, P. Licence and R. G. Jones; *High vacuum distillation of ionic liquids and separation of ionic liquid mixtures*; Physical Chemistry Chemical Physics **12** (8) (2010) 1772--1783

[5] N. Sun, M. Rahman, Y. Qin, M. L. Maxim, H. Rodriguez and R. D. Rogers; *Complete dissolution and partial delignification of wood in the ionic liquid 1-ethyl-3-methylimidazolium acetate*; Green Chemistry **11** (2009) 646--655

[6] T. Klement, S. Milker, G. Jaeger, P. M. Grande, P. D. de Maria and J. Buechs; *Biomass pretreatment affects Ustilago maydis in producing itaconic acid*; Microbial Cell Factories **11** (43) (2012) 1--13

[7] A. Brandt, M. J. Ray, T. Q. To, D. J. Leak, R. J. Murphy and T. Welton; *Ionic liquid pretreatment of lignocellulosic biomass with ionic liquid-water mixtures*; Green Chem. **13** (2011) 2489--2499

[8] H. L. Chum, D. K. Johnson, S. Black, J. Baker, K. Grohmann, K. V. Sarkanen, K. Wallace and H. A. Schroeder; *Organosolv Pretreatment for Enzymatic-Hydrolysis of Poplars .1. Enzyme Hydrolysis of Cellulosic Residues*; Biotechnology and Bioengineering **31** (7) (1988) 643--649

[9] T. vom Stein, P. Grande, F. Sibilla, U. Commandeur, R. Fischer, W. Leitner and P. Dominguez de Maria; *Salt-assisted organic-acid-catalyzed depolymerization of cellulose*; Green Chemistry **12** (10) (2010) 1844--1849

[10] T. vom Stein, P. M. Grande, H. Kayser, F. Sibilla, W. Leitner and P. Dominguez de Maria; *From biomass to feedstock: one-step fractionation of lignocellulose components by the selective organic acid-catalyzed depoly-*

merization of hemicellulose in a biphasic system; Green Chemistry **13** (2011) 1772--1777

[11] C. Abels, F. Carstensen and M. Wessling; *Membrane processes in biorefinery applications*; Journal of Membrane Science **444** (2013) 285--317

Curriculum Vitae

Name:	Christian Abels
Date of birth:	January 01, 1981
Place of birth:	Cologne, Germany

School & Civil service

1992 - 2000	Hildegard-von-Bingen Gymnasium, Cologne, Germany
2000 - 2001	Civil service in *evang. Kirchengemeinde Köln-Sülz*

Academic education

2001 - 2007	Mechanical engineering studies (major chemical engineering) RWTH Aachen University, Germany
2007	Diploma Thesis, Chair for Thermal Process Engineering: "*Optimierung einer Dampf-Wasser-Apparatur zur gleichmässigen Befeuchtung von Faserstoffbahnen*"
2008 - 2013	Ph.D. Student in Chemical Process Engineering RWTH Aachen University, Germany

List of publications

C. Niewersch, S. Petzet, **C. Abels**, R. Li, T. Wintgens, T. Melin, P. Cornel; *Mass transport modelling to estimate the efficiency of nanofiltration application for the recovery of phosphorus from sewage sludge*; Desalination and Water Treatment (6) (2009) 86–93

C. Abels, C. Redepenning, A. Moll, T. Melin, M. Wessling; *Simple purification of ionic liquid solvents by nanofiltration in biorefining of lignocellulosic substrates*; Journal of Membrane Science 405–406 (2012) 1–10

C. Abels, F. Carstensen, M. Wessling; *Membrane processes in biorefinery applications*; Journal of Membrane Science 444 (2013) 285–317

C. Abels, K. Thimm, H. Wulfhorst, A.C. Spiess, M. Wessling; *Membrane-based recovery of glucose from enzymatic hydrolysis of ionic liquid pretreated cellulose*; Bioresource Technology 149 (2013) 58–64